Max-Planck-Institute für Biochemie
Abteilung Strukturforschung
Biologische NMR-Arbeitsgruppe

Biochemical and biophysical characterization of the retinoblastoma protein and its interacting partners

Narasimharao Nalabothula

Vollständiger Abdruck der von der Fakultät für Chemie der Technischen Universität München zur Erlangung des akademischen Grades eines

Doktors der Naturwissenschaften

genehmigten Dissertation.

Vorsitzender: Univ. Prof. Dr. W. Hiller
Prüfer der Dissertation: 1. apl. Prof. Dr. Dr. h. c. R. Huber
2. Univ. Prof. Dr. Johannes Buchner

Die Dissertation wurde am 18.03.2004 bei der Technischen Universität München eingereicht und durch die Fakultät für Chemie am 04.05.2004 angenommen.

ACKNOWLEDGEMENTS

This work was carried out at the Department of Strukturforschung, Max Planck Institute for Biochemistry, Martinsried. It is a great pleasure and privilege to express my deep sense of gratitude to Prof. Dr. Robert Huber for giving the opportunity to work in his department and for considering me as his PhD student.

I am indebted to my guide and supervisor Dr. Tad A Holak for his constant encouragement and financial support during all these years. It was only with his supervision, creative criticism, help and inspiration that this thesis was possible.

All former and present members of our laboratory are thanked for offering friendly and scientific atmosphere in the laboratory. I wish to thank Ms. Renate Rüller for her kind help in administrative work throughout my stay at the department. I thank Mr. Snezan Marinkovic for excellent technical assistance during this work. I would like to thank Mr. Reinhard Mentele for sequencing proteins. I thank Ms. Weyher-Stingl Elisabeth for extending her help to measure CD spectrum.

It is my pleasure to thank Dr. Till Rehm for friendly and scientific discussions and for his constant moral support. I would like to thank Mr. Marcin Krajewski for scientific and spiritual discussions. I would like to thank all friends, both in and outside the department for sharing time, knowledge, and for encouragement.

Last, but not least, I thank my parents and other family members for their support during all these years.

PUBLICATIONS

Part of this thesis will be published in due course:

Narasimharao Nalabothula, Loyola DSilva, Madhumita Ghosh, Shirley Gil-Parrado, Werner Machleidt, and Holak T.A. Identification of cleavage sites of calpain in the G_1 cyclin-dependent kinase inhibitor $p19^{INK4d}$, submitted to Biochemistry, 2004.

Pawel Smialowski, Mahavir Singh, Aleksandra Mikolajka, Narasimharao Nalabothula, Sudipta Majumdar and Holak T.A. The human HLH proteins MyoD and Id-2 do not interact directly with either pRb or CDK6, submitted to FEBS letters, 2004.

Madhumita Ghosh, Sreejesh Shanker, Igor Siwanowicz, Karlheinz Mann, Narasimharao Nalabothula, Werner Machleidt and Holak T.A. Pattern of proteolytic cleavage of insulin-like growth factor binding proteins (IGFBPs) by calpain, submitted to Biological Chemistry, 2004.

Table of Contents

1 Overexpression and large-scale purification of the retinoblastoma tumor suppressor protein for structural investigation 1
1.1 Introduction 1
1.1.1 The mammalian cell cycle 1
1.1.2 The retinoblastoma protein pathway and cancer 3
1.1.3 Organization of functional domains of pRb and its related proteins 7
1.1.3.1 Functional domains of pRb 7
1.1.3.2 The retinoblastoma family 9
1.1.4 pRb binding proteins 11
1.1.4.1 DNA methyl transferase 1 (DNMT 1) 12
1.1.4.2 E2F transcription factors 12
1.1.4.3 HDACs 13
1.1.4.4 NF-kB p50 14
1.1.4.5 PHox, B4, Pax3, Chx10 paired-like homeodomain transcription factors 15
1.1.4.6 D-type cyclins 15
1.1.4.7 Viral oncoproteins: (adenovirus E1A, HPV 16-E7, SV40 large T-antigen) 16
1.1.4.8 PML 17
1.1.4.9 Cyclin dependent kinase inhibitors ($p21^{CIP1/WAF1}$ and $p57^{KIP2}$) 18
1.1.4.10 c-Jun & c-Fos 18
1.1.4.11 UBF 19
1.1.4.12 ATF2 transcription factor and JNK/p38 kinases 19
1.1.4.13 Trip230 20
1.1.4.14 RbAp46 and RbAp48 20
1.1.4.15 hBRM and hBRG1 proteins 21
1.1.4.16 C/EBP and NF-IL6 proteins 22
1.1.4.17 HBP1 22
1.1.4.18 p202 23
1.1.4.19 Rak/Frk 24
1.1.4.20 MyoD 24
1.1.5 Nuclear magnetic resonance (NMR) spectroscopy 25
1.1.6 Aim of the project 27

1.2 Materials and Methods 29
1.2.1 Materials 29
1.2.1.1 Chromatography equipments, columns and media 30
1.2.1.2 Consumables 30
1.2.1.3 Miscellaneous 30
1.2.1.4 Media, buffers and stock solutions 31
1.2.1.5 Antibodies, proteases, nucleases and other proteins used for this study 34
1.2.1.6 Plasmids and experimental organisms 35
1.2.2 Methods 37
1.2.2.1 Amplification of plasmids in *E. coli* 37
1.2.2.2 Molecular cloning 39
1.2.2.3 Site directed mutagenesis 41
1.2.2.4 Deletion mutagenesis 42
1.2.2.5 Overexpression of proteins in *E. coli* and purification 44
1.2.2.6 Methods to express pRb in insect cells 47
1.2.2.7 Western blotting 49
1.2.2.8 EKMax digestion 50
1.2.2.9 N-terminal amino acid sequence analysis 50
1.2.2.10 CD spectroscopy 50
1.2.2.11 1D-^{1}H and 2D-^{15}N HSQC experiments 50
1.2.2.12 In vitro binding assays 50
1.3 Results and Discussion 52
1.3.1 Results 52
1.3.1.1 Pilot expressions of full-length pRb 52
1.3.1.2 Expression and purification of the large pocket region of pRb 52
1.3.1.3 Expression and purification of pRb (large pocket) from baculovirus 56
1.3.1.4 Expression and purification of the small pocket of pRb from 4 liter *E. coli* cultures 56
1.3.1.5 Expression and purification of the A/B pocket of pRb 58
1.3.1.6 pRb and MyoD binding studies 67
1.3.2 Discussion 69
2 Identification of cleavage sites of calpain in the G_1 cyclin dependent kinase inhibitor p19^{INK4d} 71
2.1 Introduction 71

2.1.1 Aim of the project 72
2.2 Materials and Methods 72
2.2.1 Materials 72
2.2.2 Methods 72
2.2.2.1 Proteolytic cleavage of p19 by µ-calpain 72
2.2.2.2 Calpain mediated proteolytic assays of p19 in the presence or absence of calcium and calpastatin 73
2.2.2.3 N-Terminal amino acid analysis of fragments generated by calpain 73
2.3 Results and Discussion 74
2.3.1 Results 74
2.3.2 Discussion 77
3 Zusammenfassung 80
4 Summary 82
5 References 84
6 Appendix 104
6.1 Amino acid sequences of different constructs of pRb 104
6.1.1 Amino acid sequence of full-length of pRb 104
6.1.2 Amino acid sequence of large-pocket region of pRb 104
6.1.3 Amino acid sequence of small-pocket region of pRb 105
6.1.4 Amino acid sequence of A/B-pocket region of pRb 105
6.1.5 Amino acid sequence of A/B pocket of *E. coli* purified recombinant pRb. 105
6.1.6 Amino acid sequence of A/B pocket of *E. coli* purified pRb after Entirokinase digestion. 106
6.2 Abreviations 106

1 Overexpression and large-scale purification of the retinoblastoma tumor suppressor protein for structural investigation

1.1 Introduction

1.1.1 The mammalian cell cycle

The mammalian cell division cycle is divided into two basic parts: mitosis and interphase. Mitosis corresponds to the separation of daughter chromosomes, consists of four steps (prophase, metaphase, anaphase and telophase), usually ending with cell division (cytokinensis). Interphase is the time during which replication and cell proliferation occur in an orderly manner in preparation for cell division and the cell spends approximately 95% of the cycle in interphase and 5% in mitosis. While the cells double in size between each mitotic step, the DNA is synthesized only during a portion of interphase. The timing of DNA synthesis thus conventionally divides the cell cycle into four discrete phases. The M phase followed by G_1 phase (gap 1), corresponds to the interval between mitosis and initiation of DNA replication. During G_1 phase, the histones necessary for the formation of new chromatin are synthesized, and the cell is metabolically active and continuously grows but does not replicate its DNA. G_1 phase is followed by S phase (synthesis), during which chromosomes are faithfully duplicated. The completion of chromosome duplication is followed by the G_2 phase (gap 2), during which the cell growth continues and proteins are synthesized in preparation for mitosis. In vertebrates, the cell cycle exits the G_1 phase under unfavourable environments and enters the quiescent G_0 phase. From there, it can return to the cycle through the G_1 phase when environmental cues permit and this reentry is regulated, thereby providing control of cell proliferation (Grana and Reddy, 1995; Nurse, 2000; Oft et al., 1996; Pardee, 1989; Sherr, 1993).

Regulated phosphorylation and degradation of proteins through three classes of cyclin-cyclin dependent kinase (cdk) complexes, controls the passage through the cell cycle. These three classes are: the G_1, S-phase and mitotic cdk complexes (Carnero, 2002; Evans et al., 1983; Minshull et al., 1989). In higher organisms, control of the cell cycle is achieved primarily by regulating the synthesis and activation of G_1 cdk complexes. While the cyclins C, D, and E are essential for the progression of the cycle

into S phase, and synthesized during G_1, cyclins A and B, are synthesized during S and G_2 phases, which are essential for entry into mitosis. The activity of cyclin-dependent kinases is regulated by temporal synthesis and binding of cyclins, by the association and dissociation of cdk inhibitors (CDKI's), and by inhibitory and activating phosphorylation events (Sherr, 1996).

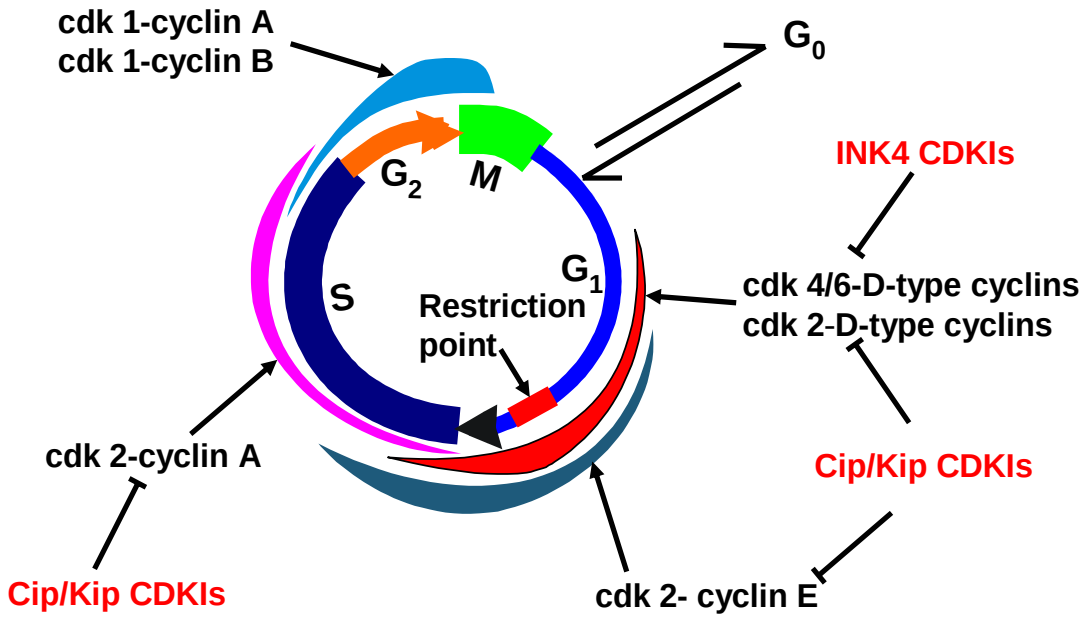

Figure 1. *A schematic depiction of the mammalian cell cycle. G_1, S, G_2, and M denote different phases of the mammalian somatic cell division cycle. G_0-phase is a quiescent stage when the cell experiences unfavourable conditions and stops the cycle. Upon mitogenic stimulation cells enters the cycle and goes through the G_1-, S-, G_2-, and M-phase of a cycle to replicate itself and divide into two daughter cells. Decision to pass through an entire cycle is made at the G_1-S restriction point in late G_1 phase. Cell cycle progression through different phases of the cycle accomplish in part by different cdk-cyclin complexes, indicated here and described in the text. Cyclin dependent kinase inhibitors (CDKIs) exert negative regulatory effects on cell cycle progression and are represented in red.*

1.1.2 The retinoblastoma protein pathway and cancer

The principle task of the cell division cycle is to ensure that DNA is replicated once during S phase without errors and to segregate chromosomal copies equally to two daughter cells during mitosis. Molecular regulators that drive these processes and a monitoring circuitry ensure that the interphase is completed before mitosis begins and vice versa (Grana and Reddy, 1995; Nurse, 2000). Therefore, accumulating genetic and functional evidence now shows that uncontrolled cell proliferation, which is the hallmark of cancer, results from common occurrence of tumorigenic aberrations among cell cycle regulators, in particular, those governing G_1 progression and G_1/S restriction point. The point in late G_1 phase where passage through the cell cycle becomes irreversible and independent of mitogens is called the restriction point. Passage through the restriction point and entry into S phase is mainly controlled by the key regulatory mechanism that has become known as the “Rb/E2F pathway”. The central element of the pathway, the retinoblastoma protein (pRb) is a tumor suppressor and cell cycle regulator, which prevents premature G_1/S transition via physical interaction with a plethora of cellular proteins.

Mitogenic growth factors induce the sequential activation of genes encoding D-type cyclins, which assemble with their catalytic partners to form active cdk4/6-cyclin D complexes (Mittnacht, 1998; Sherr, 1993; Sherr, 1996). Active cdks trigger the phosphorylation of pRb thereby releasing the pRb bound E2Fs. Then, the free E2F activates transcription of genes involved in cell cycle progression, which thereafter allows cells to traverse the G_1 phase. pRb represses the transcription of genes whose products are needed for cell cycle progression by two distinct ways. First, by direct binding to the transactivation domain of E2F’s thereby exterminating the E2F transactivational activity (Flemington et al., 1993; Helin et al., 1993). Second, by recruiting repressors such as histone deacetylases and chromosomal remodeling SWI/SNF complexes to E2F responsive promoters on DNA (Bremner et al., 1995; Ogawa et al., 2002; Rayman et al., 2002; Sellers et al., 1995; Weintraub et al., 1995). Apart from the battery of genes that regulate DNA metabolism (e.g., thymidine kinase, DHFR, DNA pol α, thymidylate synthase (TS), PCNA, ribonucleotide reductase), E2F also induces cell cycle regulatory proteins such as cyclin A, E, and D1, p107, E2F-1,4, and 5, and cdk2 (Dyson, 1998; Nevins, 1998). Cyclin E then enters into a complex with

its catalytic partner cdk2 and facilitates progressive pRb phosphorylation. Since cyclin E and E2F itself are E2F responsive, a positive cross regulation of E2F and cyclin E produces a rapid rise of both activities, contributing to the irreversibility of the restriction point transition thereby making the cell cycle mitogen independent (Botz et al., 1996; Degregori et al., 1995; Duronio and Ofarrell, 1995; Geng et al., 1996; Johnson et al., 1994; Leone et al., 1998; Neuman et al., 1994; Ohtani et al., 1995; Schulze et al., 1995; Weinberg, 1995). In addition, cyclin E-cdk2 complexes phosphorylate regulatory sites in the proteins that form DNA pre-replication initiation complexes, which are assembled on replication origins during G_1 phase (Heichman and Roberts, 1994; Stillman, 1996; Wuarin and Nurse, 1996). Phosphorylation of these proteins by S-phase cdk complexes not only activates initiation of DNA replication but also prevents re-assembly of new replication initiation complexes which ensures that each chromosome is replicated only once during passage through the cell cycle. Once cells enter S phase, cyclin E undergoes phosphorylation by cdk2 and subsequent proteosome mediated degradation (Clurman et al., 1996; Won and Reed, 1996). Cyclin A-cdk2 phosphorylates one of E2F's heterodimeric components (DP-1), thereby precluding the transactivational activity of E2F (Dynlacht et al., 1994; Krek et al., 1994). The timely inactivation of cyclin E and E2F activities by the above processes drive the cell cycle irreversibly and cyclin A and cyclin B dependent kinases probably maintain Rb in its hyperphosphorylated form, and pRb is not dephosphorylated until it reenters the G_1 phase.

cdk's are negatively regulated by two distinct families of polypeptide inhibitors which include the Cip/Kip family, consisting of $p21^{Cip1}$, $p27^{Kip1}$, and $p57^{Kip2}$ (Sherr and Roberts, 1995), and the INK4 family, including $p15^{INK4b}$, $p16^{INK4a}$, $p18^{INK4c}$ and $p19^{INK4d}$ (Ruas and Peters, 1998; Sherr and Roberts, 1995). $P27^{KIP1}$ inhibits the activity of cyclin E/A-cdk2 and stabilizes cyclin D-cdk 4/6 complexes (Kato et al., 1994; Nourse et al., 1994; Polyak et al., 1994a; Polyak et al., 1994b), whereas INK4 inhibitors block cyclin D-cdk4/6 activation. In quiescent cells, the levels of $p27^{KIP1}$ are generally high. However, as cells enter the cell cycle, the $p27^{KIP1}$ are sequestered into complexes with cyclin D-cdk4/6, thereby facilitating cyclin E-cdk2 activation. This complements the Rb-E2F transcriptional programme and helps make the appearance of cyclin E-cdk2 activity contingent upon accumulation of cyclin D-cdk4/6-Cip/Kip complexes. Cyclin E-cdk2 phosphorylates unbound $p27^{KIP1}$ to a form that undergoes proteosome-mediated degradation. However, absence of free $p27^{KIP1}$ drives the cell cycle passage through the

restriction point irreversibly. INK4 proteins sequester cdk4/6 into binary cdk-INK4 complexes, liberating bound Cip/Kip proteins, thereby indirectly inhibiting cyclin E-cdk2 to ensure cell cycle arrest (Sherr and Roberts, 1999). The ability of INK4 proteins to arrest the cell cycle in G_1 phase depends upon the presence of a functional Rb protein, implying that Rb remains hypophosphorylated and represses transcription of S phase genes by inhibiting cyclin D-dependent kinases. Disruption of cyclin D-cdk4/6-Cip/Kip complexes and release of bound Cip/Kip proteins is insufficient to inhibit cyclin E-cdk2 activity in Rb negative cells. Moreover, Rb negative cells exhibit greatly elevated cyclin E-cdk2 activity which attributes to the fact that cyclin E-cdk2 activity is under Rb-E2F control and enables a conceptually simplified view of the "Rb/E2F pathway"; CDKIs — cyclin D-cdk 4/6 — Rb — E2Fs→ S phase entry. (see Fig 2).

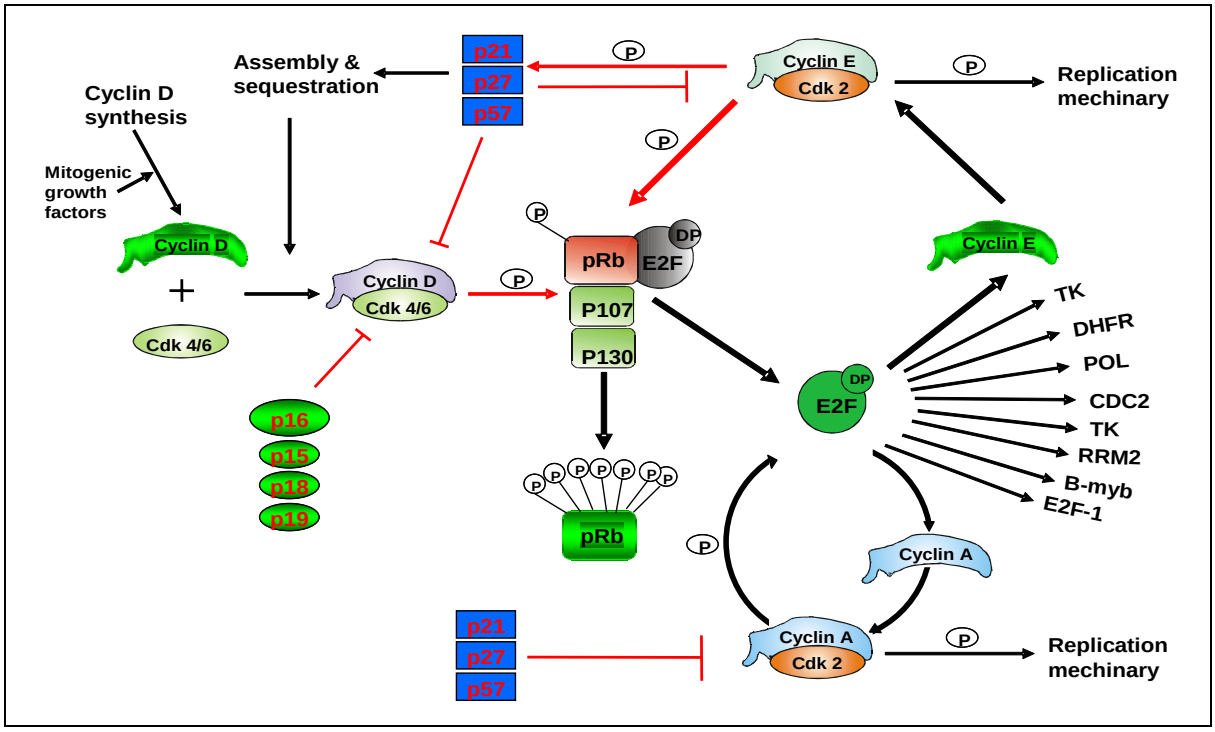

Figure 2. *Rb/E2F pathway and restriction point control. In quiescent G_0-phase and early G_1-phase, pRb stays in active hypophosphorylated form, which inhibits E2F induced transcription. As a cell enters the cycle in response to mitogenic signals, accumulated cyclin D-dependent kinases assemble into an active holoenzyme complexes in sequestration with Cip/Kip proteins. The active cyclin D-cdks mediated Rb phosphorylation releases E2F from negative constraints and which activate genes, the products of which involve in S-phase entry and cell cycle progression. Initiation of self-reinforcing E2F transcriptional programme together with $p27^{Kip}$ degradation and cyclin*

A-cdk2 mediated E2F inactivation drive the cell cycle from mitogen dependent to mitogen independent (see the text for details). INK4 CDKIs inhibit cyclin D-cdk activity; where as Cip/Kip CDKIs inactivate cyclin E-cdk2 and cyclin A-cdk2. The proteins involve in human cancers through Rb/E2F pathway are highlighted. Activation and inactivation steps are represented with black and red arrows respectively.

A diverse body of evidence indicates that the cell cycle regulatory genes most often altered in tumors are those involved in controlling G_1-S transition through the regulation of the Rb-E2F pathway. This suggests that disabling "the Rb-E2F pathway" may be essential for tumorigenesis (Hahn and Weinberg, 2002; Nevins, 2001; Ortega et al., 2002; Sellers and Kaelin, 1997; Sherr and Roberts, 1999). Loss of pRb function through mutations has been implicated in adult cancers, particularly in retinoblastoma's, in small cell lung carcinomas, and in many sarcomas and bladder carcinomas (Horowitz et al., 1990). In cervical carcinomas, loss of pRb function is achieved through the actions of the human papilloma virus E7 oncoprotein (Dyson et al., 1989; Hausen, 1991). Overexpression of cyclins is one among the predominant gain-of-function (proto-oncogene) mutations involved in disrupting the Rb-E2F pathway. Amplification of cyclin D gene and aberrant overexpression of cyclin D1 have also been found in many adult human cancers, including esophageal carcinomas, squamous cell carcinomas of the head and neck, small-cell lung tumors, hepatocellular carcinomas, primary breast cancer, bladder cancer, melanomas, sarcomas, and colorectal tumors (Hall and Peters, 1996). Furthermore, overexpression of cyclin E has been implicated in breast, stomach and colon cancers, and in some adult acute lymphocytic leukaemia's (Akama et al., 1995; Keyomarsi et al., 1995; Keyomarsi et al., 1994; Kitahara et al., 1995; Li et al., 1996; Scuderi et al., 1996; Tahara, 1995). Mutations in $p16^{INK4a}$ gene that inactivates its cyclin-dependent kinase inhibitory function are associated with familial melanomas, esophageal and biliary tract carcinomas, (Hall and Peters, 1996; Morgan, 1995; Nigg, 1995; Norbury and Nurse, 1992; Reed, 1992). Also, deletion of INK4a, INK4b or both occur in many esophageal squamous carcinomas, glioblastomas, lung, bladder, and pancreatic carcinomas (Hall and Peters, 1996; Morgan, 1995; Nigg, 1995; Norbury and Nurse, 1992; Reed, 1992). CDK4 gene amplification and a mutation in CDK4 gene have been found in many glioblastomas and melanomas (He et al., 1994; Schmidt et al., 1994). The various changes mentioned above interrupt the Rb/E2F pathway through a common scheme: functional inactivation (through sequestration or deregulated

phosphorylation) or genetic inactivation of pRb (via chromosomal mutation) liberates E2F thereby the progression of cells from G_1 into S phase become uncontrolled.

1.1.3 Organization of functional domains of pRb and its related proteins

1.1.3.1 Functional domains of pRb

The retinoblastoma protein is a ubiquitously expressed 105-kDa nuclear phospho-protein consisting of 928 amino acids. In vitro binding studies, using both artificially produced and naturally occurring pRb mutations, have defined three major and distinct functional domains: The N-terminal domain, followed by the A/B pocket and the C pocket (Fig 3).

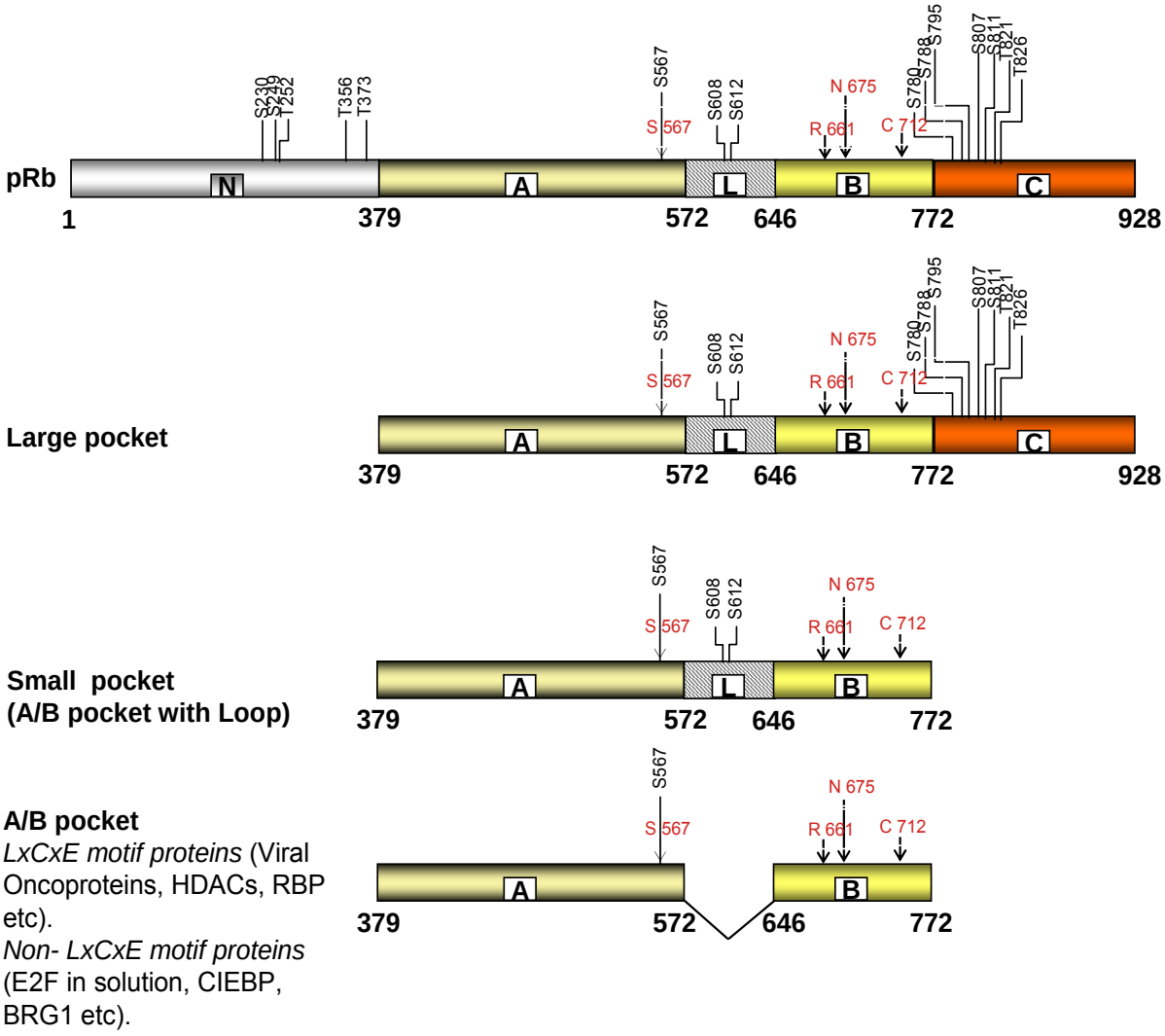

Figure 3. *Domain structure, phosphorylation sites and binding proteins of the retinoblastoma protein (pRb). The functional domains of pRb from N to C terminus*

include the N-terminal domain, A/B pocket and the C-terminal domain and different functional domains are depicted in different colours. The Large pocket region, which is needed for pRb to perform growth suppressor activity, and A/B pocket, which is conserved among all pocket proteins, and chiefly involve in binding of pRb to numerous cellular and viral oncoproteins are depicted. Cancer causing point mutations are marked in red.

N terminal domain

The N terminal domain comprises 378 amino acids (1-378). Internal deletions in the N-terminal domain of pRb have been reported in inactivation of its tumor suppressor activity (Qian et al., 1992). Further, deletion of 40 amino acids in the N-terminal domain of pRb has been reported in one of the retinoblastoma's (Dryja et al., 1993; Hogg et al., 1993). This region contains of consensus cdk phosphorylation sites, which may regulate pRb activity when they are phosphorylated during the cell cycle. Through protein–protein interactions using the N-terminal domain of pRb as a probe, nine nuclear proteins have been identified of which at least two are cell cycle regulated serine/threonine kinases that can phosphorylate histone H1 and pRb. The N-terminal region of pRb plays crucial role in the receptor-targeted chromatin remodeling, and apoptosis by enhancing the interactions between the receptor and hBRM containing SWI/SNF complex. It also interacts with several proteins, including MCM7 (Sterner et al., 1998), a novel G_2/M transition regulated kinase (Sterner et al., 1995) and several other proteins (Durfee et al., 1994). However, the functions of these interactions remain unresolved. The identification of proteins that bind to the N-terminal region of pRb indicates that there could be an "N pocket", which could play a crucial role in the regulation of pRb phosphorylation and apoptosis.

A/B pocket

The first protein-binding domain to be identified in pRb consist of domain A (379-577) and domain B (645-772) separated by a spacer region (573-645), which is highly conserved from humans to plants. Both domains (A and B) interact with each other along an extended interdomain interface to form the central "pocket" (Chow and Dean, 1996; Lee et al., 1998), which is essential for the tumor-suppressor activity of pRb (Qin et al., 1992). This pocket region was first defined as the binding site for two viral

oncoproteins, E1A and SV40 large T antigen, based on their ability to bind pRb deletion mutants in vitro (Hu et al., 1990; Huang et al., 1990; Kaelin et al., 1990). A number of naturally occurring point mutations of pRb found in cancer cells, result in disruptions of the integrity of A/B pocket (Hamel et al., 1993; Zacksenhaus et al., 1993).

Insertion domain

A stretch of 75 amino acids between A and B domains has been termed the insert domain (Hu et al., 1990; Huang et al., 1990). Point mutations and small deletions within the insert domain do not affect Rb activity (Hu et al., 1990; Huang et al., 1990; Qin et al., 1992), suggesting that the insert domain provides a physical separation necessary for the formation of the A/B pocket. So far topoisomerase-α has been found to interact with this region of pRb.

C pocket

The C pocket lies within pRb amino acids 768-928 although the actual size of this pocket is considerably smaller. The binding site formed by the A/B pocket and C terminal amino acids has been termed the “large A/B pocket”, which is necessary for the tumor suppressor activity of the retinoblastoma protein (Hiebert, 1993; Qin et al., 1992). The C terminal part also contains of a bipartite nuclear localization signal (860-876). The protein binding property of C pocket is independent of the A/B pocket as evident from the binding of C-Abl tyrosine kinase (a target protein of the C pocket), does not interfere with the binding of viral proteins (T antigen) to the A/B pocket (Welch and Wang, 1993). Since viral oncoproteins do not affect the C pocket but do disrupt the interactions mediated through the large A/B pocket, the C pocket and the C terminal part of the large A/B pocket may not overlap. Thus, the A/B and C pockets of pRb may interact with different proteins simultaneously.

1.1.3.2 The retinoblastoma family

One of the better-studied tumor suppressor families is the retinoblastoma family, which consists of three structurally and functionally similar tumor suppressor proteins named as pRb or p105, pRb2 or p130, and p107 (Fig 4).

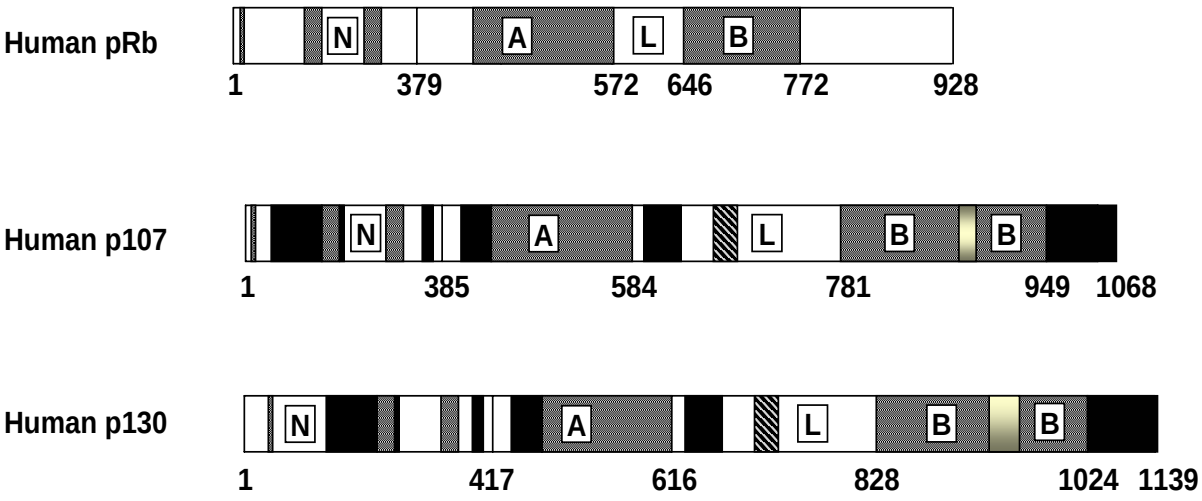

Figure 4. *Schematic representation of the retinoblastoma protein family. Borders of different structural domains are represented with respective amino acid numbers. Highly conserved regions among all three proteins are highlighted in gray. Regions conserved between p107 and p130 are highlighted in black.*

Genetic features

The three human genes, RB gene, p107 (RBL1) gene, and p130 (RBL2) gene, that encode members of the retinoblastoma protein family were mapped to 13q14, 20q11.2 and 16q12.2 chromosomes respectively. All three genes have common genetic features that are similar to the other housekeeping genes. They include the presence of (A) a GC-rich zone immediately surrounding the main transcription initiation site, (B) presence of multiple consensus sequences for binding the Sp1 transcription factor and (C) presence of transcription start sites and lack of canonical TATA or CAAT boxes found in the promoters of most differentially expressed genes. While the Rb transcript is encoded by 27 exons dispersed over about 200 kb of genomic DNA with the exons ranging from 31 to 1,889 bp and the introns from 80 bp to 60 bp; the p107 gene consists of 22 exons ranging in length from 50 to 840 bp spanning over 100 kb of genomic DNA. The p130 gene consists of 22 exons and spans over 50 kb of genomic DNA. Twenty-one introns vary in length from 82 bp to 9kb. The arrangement of each gene in the genomic DNA is similar to that of the other members of the family (Baldi et al., 1996; Ewen et al., 1991; Hong et al., 1989).

Structural features

An insight into the biochemical nature of adenovirus E1A protein in transforming primary rodent cells has led the discovery of two novel proteins, pRb2 or p130, and p107, related in structure and function to pRb. Primary sequence comparison studies allowed a structural relationship among pRb, p130, and p107. E1A/T binding region is been recognised as the most conserved region among all these three proteins. The E1A/T region is composed of conserved A and B domains separated by a spacer region of varying length and is named after its requirement for interactions with viral oncoproteins (Hu et al., 1990; Huang et al., 1990; Kaelin et al., 1990).

The three pocket proteins consist of an amino terminal domain, a pocket region and a carboxy-terminal domain. The conserved pocket region is responsible for interaction of all three-pocket proteins with viral oncoproteins, cyclins, transcription factor family, HDAC's and for its functional activity. The carboxy-terminal halves of all retinoblastoma family proteins comprise of similar structural domains and multiple sites for phosphorylation by cdk's. Unlike pRb, the other two proteins contain insertions within the "B half" of the pocket domain. In addition, the spacer sequences found in p107 and p130 are longer than the analogous region in pRb and share a conserved motif in the spacer region. This allows them to form stable complexes with cyclin A/cdk2 and cyclin E/cdk2 (Ewen et al., 1992; Faha et al., 1992; Hannon et al., 1993; Lees et al., 1992; Li et al., 1993). In addition to subtle changes in the spacer region, p107 and p130 also contain an extended region of homology near their amino-terminus that is missing in pRb. It has been suggested that these sequences enable p130 and p107 to act as cdk inhibitors (Castano et al., 1998; Woo et al., 1997).

1.1.4 pRb binding proteins

Protein/protein and protein/DNA interaction studies provide clues about physiological significance of a protein under investigation. Coimmunoprecipitation studies of endogenous proteins, affinity binding assays, targeted mutations that eliminate protein/protein interactions, and tissue specific knockout studies demonstrated that pRb interact with three classes of proteins that are involved in cell cycle regulation, cell differentiation and apoptosis. Most of these studies suggested that the pocket region of pRb is essential for tumorigenesis and interaction with most of its binding partners.

Some of the pRb binding proteins, associations of which with pRb were characterized *in vitro* and *in vivo*, are summarized below.

1.1.4.1 DNA methyl transferase 1 (DNMT 1)

Methylation of cytosine residues in CpG dinucleotides is one of the general mechanisms involved in the regulation of transcription in vertebrates. DNMT 1, 3a and 3b are three methyl transferases show distinct specificities in *De Novo* methylation (Li et al., 1992; Okano et al., 1999). Biochemical fractionation studies with HeLa cell nuclear extracts resulted in cofractionation of DNMT1 predominantly with pRb, E2F and HDAC1 (Li et al., 1992). *In vitro* GST pull-down experiments with GST-Rb (A/B) and a series of DNMT1 deletion mutants demonstrated that the small pocket of pRb and an N-terminal portion (aa 416-923) of DNMT1 participate in the formation of pRb/DNMT1 complex (Robertson et al., 2000). Transcriptional studies using reporter gene assays have been shown that the DNMT1 interact with both pRb and HDAC1, which allowed to hypothesize that DNMT1 mediated methylation, might further potentiate the HDAC induced transcriptional repression state.

1.1.4.2 E2F transcription factors

E2F transcription factors play an important role in the cell cycle and growth arrest by regulating the expression of a number of genes required for DNA synthesis and cell cycle progression (Chellappan et al., 1991; Weintraub and Dean, 1992). They appear to be a major target of pRb, p130 and p107(Nevins, 1992). In mammalian cells E2Fs exist as heterodimers composed of E2F and DP. Six E2Fs (E2F-1 to E2F-6) and two DP (DP-1 to DP-2) family members form different combinations of E2F/DP complexes (Dyson, 1998). Based on sequence homology, the E2F family is further divided into three subgroups. E2F-1, E2F-2 and E2F-3 share basic nuclear localization signal and an N-terminal cyclin A/cdk binding domain, both of which are absent in E2F-4 and E2F-5, which instead possesses a nuclear export signal (Gaubatz et al., 2001). E2F-6 represents a third group and act through pocket protein independent manner (Morkel et al., 1997). E2F-4 and E2F-5 are uniformly express in quiescent (G_0) cells and interact with p107 and p130, whereas E2F-1, E2F-2 and E2F-3 are under cell cycle control with levels peaking as cells approach the G_1/S boundary and exhibit high affinity binding to hypophosphorylated pRb (Dyson, 1998). pRb-E2F complexes are found in several mammalian cell lines, and inhibition of E2F activity appears to be regulated at least in

part by phosphorylation of pRb by cdk's (Buchkovich et al., 1989; Chen et al., 1989; Decaprio et al., 1989; Mihara et al., 1989). *In vitro* transcriptional and DNase foot printing assays have shown that pRb blocks E2F mediated transcription by integrating with transactivation domain of E2F, thereby hindering the assembly of the basal transcription machinery (Morkel et al., 1997). Multiple *in vitro* and *in vivo* studies had demonstrated that E2F transcription factors interact with low affinity to small pocket and high affinity to large pockets of pRb through a conserved domain embodied in the transactivation domain (Hiebert, 1993; Huang et al., 1992; Qian et al., 1992; Qin et al., 1992). E2Fs have been reported to regulate the expressions of genes involved in apoptosis. All these studies allow to hypothesize that pRb negatively regulates cell proliferation and apoptosis by inhibiting E2F transactivational activity through association with its transactivation domain.

1.1.4.3 HDACs

Eukaryotic DNA is complexed with histones in nucleosomes and nuclesomes are basic components of eukaryotic chromosomes. The activation domains (AD) in transcription factors attract activating protein complexes that contain histone acetyltransferase enzymes (HAT). Histone acetyltransferase mediated acetylation of the histone core generally disrupts the nuclesome structure and makes promoters accessible to the transcription factors. Protein complexes containing histone deacetylases are recruited to the promoters by repression domains (RD) in transcription factors. Deacetylation of histone core by HDACs promotes chromatin assembly and blocks promoter accessibility to the transcriptional machinery. Such HAT and HDAC mediated acetylation and deacetylation events play potential role in regulation of eukaryotic gene expression. The HDACs are a family of seven different enzymes divided into two groups. Group I includes HDAC 1, 2, 3 and group II includes HDAC 4, 5, 6, and 7. Various cell culture studies demonstrated that HDACs perform their function as two different repressor complexes: Sin3a/HDAC complex (Zhang et al., 1997) and the NuRD/HDAC complex (Zhang et al., 1999). Association of pRb with components of both complexes have been reported which suggests that pRb might be involved in chromatin remodelling as a multisubunit regulatory net work. Earlier studies showed that pRb represses transcription of E2F responsive genes by recruiting chromatin remodeling complexes such as HDAC's to the E2F promoters. Mutations in pRb that abolish its function to recruit HDACs to chromatin were implicated in cancers.

Immunoprecipitation of endogenous pRb from cell extracts and co expression by transient transfection of mammalian cells, followed by western blot analysis revealed direct interaction between pRb and HDACs *in vivo*. Pull-down assays with GST-Rb (A/B) and a mutant HDAC1 in which IxCxE sequence was deleted shown weak interaction. *In vitro* and *in vivo* binding studies with tumor-derived mutations of pRb, *in vitro* peptide competitive binding studies and coimmunoprecipitation studies in the presence and absence of viral oncoproteins suggested HDAC 1 and HDAC 2 interact with small pocket region of Rb through their IxCxE motifs (Brehm et al., 1998; Luo et al., 1998; Magnaghi-Jaulin et al., 1998). Though HDAC3 interact with pRb small pocket region, its mechanism of interaction is uncertain as it lacks IxCxE motif. Provided experimental evidence and existed literature suggests pRb role in eukaryotic gene expression through HDACs.

1.1.4.4 NF-kB p50

Nuclear factor-kB (NF-kB) p50 is a cellular transcription factor, which regulates expression of viral and several cellular genes. NF-kB p50 belongs to a family of transcription factors called NF-kB/Rel family, which share an N-terminal Rel homology domain spanning about 300 amino acids. *In vitro* transcriptional studies with HIV-1 LTR showed increased rate of transcription in the presence of NF-kB p50 and repression of NF-kB mediated transcription was observed in the presence of small pocket of pRb, which suggested pRb mediated repression of NF-kB transactivational activity (Tamami et al., 1996). Binding of pRb to NF-kB induces a transcriptional repressive conformational change in NF-kB, which is susceptible to chymotrypsin digestion and hence chymotripsin treated pRb/NF-kB complexes showed a shift in electrophoretic gel mobility shift assays, which provided further evidence of pRb-NF-kB interactions. *In vitro* binding studies with GST-Rb (A/B) and *in vitro* translated NF-kB, *in vivo* coimmunoprecipitation experiments with whole cell extracts prepared from jurkat cell lines demonstrated specific interactions between the pRb small pocket region and Rel homology domain of NF-kB (Tamami et al., 1996). E2F-1 has been implicated in inducing cell death by blocking NF-kB activity as well as by inactivating NF-kB activity through inhibition of IKK (Phillips et al., 1997). Both pRb and NF-kB have been reported to inhibit E2F induced apoptosis (Phillips et al., 1997; Phillips et al., 1999); on the other hand, E2F and pRb have been reported to have antagonistic effects on apoptosis. Thus, physiological functions of pRb/NF-kB interactions remain controversial.

1.1.4.5 PHox, B4, Pax3, Chx10 paired-like homeodomain transcription factors

In vitro binding studies performed with *E. coli* purified paired-like homeodomain transcription factors (GST-Chx10, GST-B4 and His-Pox3) and nuclear extracts prepared from pRb deficient C33A cells and Maurine T cell lymphoma (3T7) cells containing endogenously expressed Rb revealed that the small pocket region of pRb interacts with high affinity to Chx10 and B4, whereas it interacts with low affinity to Pax3 transcription factor. *In vitro* binding studies of the *E. coli* purified GST-Chx10, GST-PHox and nuclear lysates of γ-phasphatase treated and untreated CHO cells suggested that PHox and Chx10 interact with active hypophosphoralated pRb. *In vitro* binding studies with various mutants demonstrated that helix I and II in the paired like homeodomain interact with the small pocket region of pRb to form pRb/Pox3, pRb/PHox, pRb/Chx10, pRb/B4 complexes (Wiggan et al., 1998). Sequence comparison studies showed striking similarities between helix I and helix II of paired-like homeodomain and pRb binding region of E2F-1, E2F-2, E2F-3, E2F-4 and E2F-5. This suggests that paired like homeodomain transcription factors might bind to pRb in a similar way to that of E2F. Later, GST pull-down experiments were carried out with different *E. coli* purified pRb fragments and nuclear lysates of C33A cells containing stably expressed Pax-3 or PHox showed that paired-like homeodomain transcription factors interact with the N-terminal domain of pRb in addition to the small pocket region. However, conclusions have been also made that the paired-like homeodomain transcription factors interact with pRb in a distinct way from E2F (Wiggan et al., 1998). Transient co-transfection assays revealed pRb mediated repression of Pox3 transcriptional activation, which potentiates the role of pRb in cell fate determination. Several earlier studies showed Pox3 to regulate expression of genes involved in cell fate determination (Daston et al., 1996; Epstein et al., 1996; Yang et al., 1996). These evidence allowed for speculation on the role of pRb in cell fate determination by interacting with and modifying the activity of paired-like homeodomain transcription factors.

1.1.4.6 D-type cyclins

Growth factors stimulate differential expression of various D-type cyclins in different cell types during G_0 to G_1/S interval of the mammalian cell cycle (Ajchenbaum et al., 1993; Decaprio et al., 1992; Matsushime et al., 1991; Won et al., 1992). Thereafter, the cdk/cyclin-D mediated phosphorylation of pRb results in dissociation of pRb/E2F

complex and subsequent cell cycle progression. Sequence alignment studies found that the N-termini of the three D-type cyclins contain an LxCxE sequence motif that has sequence homology with the Rb binding motif of DNA-tumor virus transforming proteins. Competitive binding studies with E1A protein and peptides containing mutated LxCxE motif sequences showed that D-type cyclins associate with pRb through LxCxE motif sequence (Dowdy et al., 1993; Ewen et al., 1993). *In Vitro* binding studies with various pRb pocket mutants and three different murine D-type cyclins demonstrated that D-type cyclins interact with the small pocket region of pRb, binding to the same region that is targeted by viral oncoproteins. Studies have also shown the requirement of the C-terminal domain of pRb for high affinity binding to D-type cyclins. Kato et al. (Kato et al., 1993) have found ternary complexes composed of pRb, cyclin-D2/D3 and catalytically inactive cdk-4 *in vivo*. Ewen et al. (Ewen et al., 1993) demonstrated a decreased amount of pRb/E2F complex in the presence of overexpressed cyclin-D1. All these findings together with existed literature suggest that D-type cyclins may recruit cdk/cyclin-D complexes to the Rb/E2F complexes to promote cdk mediated pRb phosphorylation and cell cycle progression.

1.1.4.7 Viral oncoproteins: (adenovirus E1A, HPV 16-E7, SV40 large T-antigen)

Human papillomavirus (HPVs), adenovirus and polyomaviruses such as simian virus 40 (SV40) are small DNA viruses infection of which contribute to the development of cancers in humans (Vousden and Farrell, 1994). They accomplish this cellular transformation activity through their oncoproteins such as E1A of adenovirus, E7 of HPV16 or SV40 large T-antigen (SV40LT). Studies of the transforming properties of viral oncoproteins have revealed that the viral oncoproteins share three conserved regions termed CR1, CR2, and CR3, and all of them directly interact with the small pocket region of retinoblastoma family proteins through LxCxE sequence motif of CR2 region (Dyson et al., 1992; Ewen et al., 1989; Helt and Galloway, 2003; Imai et al., 1991; Nevins, 1992; Patrick et al., 1994). Mutations in oncoproteins that inactivate their ability to bind the small pocket also abolished their ability to stimulate cell proliferation, which suggest that the viral oncoprotein-mediated cellular transformation needs an intact A/B pocket region of pRb. Binding of viral oncoproteins with pRb dissociate pRb/E2F complex. Thereafter, the derepressed E2F activate the expression of genes products of which drive the cell cycle in uncontrolled manner. Several mutational analysis have shown that the adenoviral E1A protein needs CR1 region besides CR2

region containing LxCxE motif sequence to induce cell cycle progression and cellular transformation (Egan et al., 1989; Egan et al., 1988; Jelsma et al., 1989; Moran and Zerler, 1988; Moran and Mathews, 1987; Whyte et al., 1989). Even though HPV16 E7 interacts with pRb through CR2 region, reports showed that it also needs CR1 and C-terminal regions to elicit complete cellular transformation (Chellappan et al., 1992; Helt and Galloway, 2001; Patrick et al., 1994; Wu et al., 1993). In addition to the LxCxE motif, it has been suggested that the integrity of SV40LT CR1, which lies within the J-domain of SV40LT, is required for its complete cellular transformation activity (Chen and Paucha, 1990; Srinivasan et al., 1997). All these studies suggest that viral oncoproteins may have more than one pRb binding regions. The detailed mechanism of viral oncoprotein mediated cellular transformation yet to be explored and which may provide therapeutic insights into viral induced human malignancies.

1.1.4.8 PML

PML is a nuclear localized and ubiquitously expressed phosphoprotein belongs to a family of proteins that consist of a common N-terminal region that has a RING motif, two Cys/His rich regions called B-boxes and an α-helical coiled coil region. PML forms homodimers through N-terminal coiled-coil region and its overexpression induces growth suppression. (Borden et al., 1995; Borden et al., 1996; Kastner et al., 1992; Lovering et al., 1993; Perez et al., 1993; Reddy et al., 1992). The retinoic acid receptor-α (RARα) is involved in normal hematopoietic differentiation (Kastner et al., 1992). A chromosomal translocation results in the PML/RARα fusion gene that encodes PML/RARα fusion protein (Grignani et al., 1994; Warrell et al., 1993), and which heterodimerizes through an N-terminal coiled-coil region and involve in the pathogenesis of acute promyelocytic leukaemia (Alcalay et al., 1992). Transient transfection and subsequent coimmnoprecipitation experiments performed with lysates of U937 and C33A cells showed coprecipitation of PML with fastest migrating form of pRb, which has been identified as a hypophosphorylated form (Lee et al., 1987). *In vitro* binding studies of *in vitro* translated pRb (large pocket) and PML3 also supported these *in vivo* results. *In vivo* association of the pRb small pocket and PML3 were demonstrated by cotransfection and coimmunoprecipitation of various deletion mutants of pRb and wild type PML3. *In vitro* binding studies with *E. coli* purified GST-Rb mutants and PML3 suggested the B domain of pRb is involved in PML binding. *In vivo* studies performed with various PML deletion mutants indicated that the N-terminal tripartite

motif (RING region, B1-B2 boxes and a coiled-coil region) conserved in all isoforms of PML, is indispensable for pRb/PML complex formation (Alcalay et al., 1998; Labbaye et al., 1999). Differential association of various PML isoforms through their C-terminal region has also been demonstrated experimentally. The PML-RARα/pRb small pocket complex has been identified *in vivo* but unsuccessful reconstitution experiments of PML-RARα-pRb complex have been reported. All these experimental evidence suggests PML interaction with pRb and proposed that the PML/pRb complex might have a role in normal hematopoiesis.

1.1.4.9 Cyclin dependent kinase inhibitors ($p21^{CIP1/WAF1}$ and $p57^{KIP2}$)

Cyclin dependent kinase (cdk) mediated phosphorylation and inactivation of retinoblastoma protein permit cell cycle progression through G_1/S phase of the mammalian cell division cycle. $p21^{CIP1/WAF1}$ and $p57^{KIP2}$ are negative regulators of cyclin dependent kinases and they belong to the Cip/Kip family of CKIs. *In vivo* (coimmunoprecipitation) experiments with MJ-90 cell extracts and *in vitro* (GST pull-down) studies with *E. coli* purified p21, p57, p27 and *in vitro* translated pRb deletion mutants, demonstrated that the N-terminal (1-71) region of p21 directly interacts with the small pocket region of pRb (Nakanishi et al., 1999). Interactions of p57 with the large pocket region of pRb have been observed. However, the exact regions required for binding to each other were not mapped (Nakanishi et al., 1999). CKIs thus interact with pRb *in vitro* and *in vivo*; nevertheless, the physiological function and biochemical activities of these interactions remain unknown.

1.1.4.10 c-Jun & c-Fos

C-Fos and c-Jun are oncogenes, which belong to the AP-1 family of transcriptional activators. AP-1 transcription factors bind to the TPA response elements (TRE) in promoters of target genes, and are involved in many cellular processes including proliferation, differentiation, and stress responses (Angel and Karin, 1991; Briata et al., 1993; Pfarr et al., 1994). Several coimmunoprecipitation studies performed with various mammalian cell lysates, transient transfection assays and GST pull-down experiments showed that c-Jun binds independently to two regions of Rb, one in the small pocket and the other in the C-terminal domain, through its leucine zipper domain spanning amino acids 224 to 331. Association of c-Fos with the large pocket of pRb was also reported but the exact region of pRb that is involved in association with c-Fos have not

yet been mapped (Angel and Karin, 1991; Briata et al., 1993; Nead et al., 1998; Pfarr et al., 1994). pRb modulated c-Jun activity and down-regulation of c-Jun mediated transcription in the presence of HPV-16 E7 was shown by reporter gene assays. All above investigations suggest that the pRb-c-Jun complex up-regulates c-Jun mediated transcription, which may play a role in cell differentiation.

1.1.4.11 UBF

UBF (upstream binding factor) is an auxiliary transcription factor which stimulates the expression of ribosomal DNA genes by dimerization and subsequent association with upstream promoter element (UPE) and the basal rDNA transcription initiation factor SL1 (Hannan et al., 2000). *In vivo* and *in vitro* studies performed with pRb (A/B) pocket and an inactive pocket mutant showed that UBF binds to the pRb (A/B) pocket. Competitive binding studies in the presence of E7 peptide containing LxCxE motif allowed mapping A/B pocket of pRb as a binding region of UBF (Hannan et al., 2000). *In vitro* transcriptional assays, foot printing experiments and immunoprecipitation studies with cell lysates suggest that pRb represses UBF-dependent rDNA transcription by binding directly to UBF, and that the UBF-pRb complex can no longer interact with SL1 and activate RNA polymerase 1 mediated rDNA transcription. Available experimental evidence supports pRb role as a negative regulator of RNA polymerase 1 mediated transcription through interaction with UBF.

1.1.4.12 ATF2 transcription factor and JNK/p38 kinases

Activating transcription factor 2 (ATF2) is a member of the bZip family of transcriptional activators, which play an important role in the cellular stress response (Livingstone et al., 1995; Vandam et al., 1995). The Jun-N-terminal kinase (JNK) and p38 mitogen-activated protein kinase are stress-activated protein kinases (SAPK) that are members of MAP kinase family, which involve in stress responsive signal transduction. In response to cellular stress, the N-terminus of ATF2 undergoes JNK/p38 mediated phosphorylation that relives intramolecular inhibition and enhances transcriptional activation of ATF2 (Abdelhafiz et al., 1992; Raingeaud et al., 1996; Tsai et al., 1996; Vandam et al., 1995). Transcriptionally active ATF2 target ATF/cAMP-response element motif promoter genes which include tumor necrosis factor (TNFα), transforming growth factor β (Kim et al., 1992), cyclin A (Shimizu et al., 1998), E-selectin (Read et al., 1997), DNA polymerase β (Narayan et al., 1994), and c-Jun

(Vandam et al., 1993). These genes are known to play important roles in the stress response, cell growth and differentiation, and immune response. *In vivo* and *in vitro* studies demonstrated that AFT2 and JNK/p38 interact with the small pocket and the C-terminal region of pRb subsequently (Chauhan et al., 1999; Li and Wicks, 2001). Li et al, (Li and Wicks, 2001) found pRb-ATF2-JNK/p38 ternary complexes *in vivo*. These studies suggest pRb function in stress responsive signal transduction by facilitating stress responsive kinase mediated ATF2 transcriptional activation.

1.1.4.13 Trip230

Thyroid hormone receptors are hormone-activated transcription factors that bind to short repeated sequences of DNA called thyroid or T3 response elements (TREs), thereby act by modulating gene expression. Trip230 is a coactivator of the thyroid hormone receptor identified in yeast two-hybrid screens as pRb interactor (Durfee et al., 1993). Coimmunoprecipitation studies performed with WR2E3 cell lysates in the presence and absence of T3 (thyroid hormone) exhibited T3 dependent and independent interactions of Trip230/TR and Trip230/pRb subsequently (Chang et al., 1997). *In vitro* binding studies of *E. coli* purified GST fusion proteins containing different regions of Trip230 and pRb (p56) indicated that Trip230 interacts with pRb through a region spanning amino acids 1099 to 1382. Yeast two-hybrid assays carried out with various pRb deletion mutants and pRb binding region of Trip230 demonstrated direct interaction between the Rb small pocket region and Trip230. Cotransfection experiments carried out with WERI-pRb-27 cells showed the down-regulation of Trip 320 cooperative thyroid hormone receptor mediated transcription. These findings suggest pRb function in the repression of nuclear hormone receptor mediated gene expression through Trip320.

1.1.4.14 RbAp46 and RbAp48

RbAp46 and RbAp48 are widely expressed nuclear proteins, identified as major polypeptides from HeLa cell extracts that specifically bound to an Rb affinity column (Qian et al., 1993). Immunoprecipitation studies performed with HeLa (RbAp46) and Molt 4 (RbAp48) cell lysates demonstrated RbAp46/pRb and RbAp48/pRb complexes *in vivo*. RbAp46/pRb and RbAp48/pRb complexes were also confirmed *in vitro* by separating different combinations of *E. coli* purified RbAp46, RbAp48 and pRb (large pocket) proteins on native polyacrylamide gel electrophoresis and subsequent silver

staining (Qian and Lee, 1995; Qian et al., 1993). Although neither possesses LxCxE motifs, abolished RbAp46/48-pRb complexes in the presence of T-antigen peptide containing LxCxE motif suggested that the T-antigen binding region of pRb might be involved in the binding. The exact regions involved in complex formation have not yet been mapped. RbAp48 and RbAp46 are components of several chromatin-remodelling complexes. Since they can directly interact with histone H4, they are thought to target chromatin-remodelling complexes to nucleosomes (Parthun et al., 1996; Verreault et al., 1996; Verreault et al., 1997). Transient transfection and immunoprecipitation studies suggest that the HDAC1 can mediate the interaction between pRb and RbAp48, leading to the formation of a pRb/HDAC1/RbAp48 ternary complex *in vivo*. Competitive binding studies performed with HDAC1 peptide containing LxCxE motif reported a decreased interaction between pRb and RbAp48 in dose-dependent manner (Nicolas et al.). It has been shown that pRb interacts with E2F1 and HDAC1, and mediates transcriptional repression (Brehm et al., 1998; Magnaghi-Jaulin et al., 1998). E2F1/RbAp48/pRb ternary complex was also confirmed *in vivo* (Nicolas et al., 2000). These data suggest that HDAC1 recruits RbAp46 and RbAp48 to pRb and forms a repressor complex (E2F1/RbAp48/pRb/DCAC1) which represses E2F mediated transcription.

1.1.4.15 hBRM and hBRG1 proteins

hBRM (SNF2α) and hBRG1 (SNF2β) proteins are mutually exclusive DNA-dependent ATPase/helicase subunits of human homologues of yeast SWI/SNF complex, which belongs to the SWI2/SNF2 ATP-dependent chromatin-remodeling complex (Wang et al., 1996a; Wang et al., 1996b). hBRG1 have been shown to play a role in cell cycle progression (Khavari et al., 1993), while knockout mice studies revealed BRM role in cell proliferation (Reyes et al., 1998). *In vivo* studies done with several human cell lines showed that hBRG1 and hBRM physically interact with pRb and that the formation of this complex accounts for the cooperative coactivation of glucocorticoid receptor signalling (Singh et al., 1995). Furthermore, these studies showed that hBRG1/hBRM could function as tumor suppressor genes and induce the formation of growth-arrested cells in an pRb-dependent manner (Dunaief et al., 1994; Singh et al., 1995; Strober et al., 1996). hBRM/pRb/E2F ternary complexes have also been identified both *in vitro* and *in vivo*, on the other hand BRG1/pRb/HDAC1 trimolecular complexes were found in transiently-transfected C33A cells (Trouche et al., 1997; Zhang et al., 2000). Central role of pRb in the regulation of fundamental cellular

processes such as proliferation and differentiation have been addressed. Therefore, these studies suggest that the ATPase subunits of hSWI/SNF complexes cooperate with pRb to regulate cell fate.

1.1.4.16 C/EBP and NF-IL6 proteins

C/EBPα, C/EBPβ and C/EBPδ are the CCAAT/enhancer-binding proteins (C/EBP), which belong to the basic-leucine zipper (bZIP) class of DNA-binding proteins. The C/EBPs function primarily as transcriptional activators in establishing the terminally differentiated phenotypes of many cells, most notably liver, adipocytes and monocytes (Darlington et al., 1998; Diehl, 1998; Lekstrom-Himes and Xanthopoulos, 1998; Poli, 1998; Wu et al., 1995). NF-IL6, an interleukin-6 (IL-6)-regulated human nuclear factor, is a homologue of C/EBPβ. NF-IL6 has been implicated in the regulation of IL6 gene and other genes involved in acute-phase reaction, inflammation and hemopoiesis (Akira et al., 1990). pRb has been reported in the positive regulation of C/EBPα mediated adipocyte differentiation as well as NF-IL6 mediated monocyte differentiation (Akira et al., 1990; Chen et al., 1996a; Chen et al., 1996b). Immunoprecipitation studies with different cell lysates and electrophoretic mobility shift assays demonstrated that pRb interact with C/EBPα, C/EBPβ, C/EBPδ and NF-IL6, and that pRb-C/EBP complexes associate with DNA containing C/EBP binding sites. *E. coli* purified C/EBP proteins, NF-IL6 and *E. coli* cell lysates containing exogenously expressed Rb deletion mutants were used for *in vitro* binding studies. Those binding studies suggested that all C/EBP proteins interact with the small pocket region of pRb through a similar “Y(X7-37) D/E(X3) DLF” motif which is also found in Rb binding region of the E2F family of transcription factors (Charles et al., 2001; Chen et al., 1996b). The enhanced rate of transcription by NF-IL6, as well as C/EBPs in the presence of pRb, have been observed in transient transfection assays (Charles et al., 2001; Shan et al., 1992). Available experimental evidence allowed for speculation that pRb may facilitate cell differentiation by acting cooperatively with both C/EBPs and NF-IL6.

1.1.4.17 HBP1

HBP1, an HMG-box transcription factor, belongs to the HMG family of proteins; with LEF1, being the closest homologue (Travis et al., 1991) and it was initially identified in yeast two hybrid screens (Lesage et al., 1994). Several recent studies have reported the ability of HBP1 to interact with proteins of the retinoblastoma family, to induce

morphological transformation of cells in culture and to act as a transcriptional repressor of the cyclin D1, p21 and N-myc genes (Gartel et al., 1998; Lavender et al., 1997; Shih et al., 1998; Tevosian et al., 1997; Yee et al., 1999). MyoD transcription factor family proteins (MyoD, myogenin, Myf5, and Mrf4) are critical regulators of muscle cell differentiation (Olson and Klein, 1994). However, Shih et al. (1998) have shown that HBP1-mediates inhibition of MyoD family transcriptional activation and differentiation, and pRb can reverse the HBP1 inhibition of muscle cell differentiation (Shih et al., 1998). pRb/HBP1 complexes were identified *in vivo* by performing coimmunoprecipitation studies with different cell lysates. *In vitro* binding studies carried out with *E. coli* expressed different deletion mutants of HBP1 and *in vitro* translated pRb suggests two Rb (small pocket) binding sites in HBP1; a high affinity binding site spanning amino acids 11-63, which consist of LxCxE motif and an another low affinity binding site spanning amino acids 37-120. pRb binding and transcriptional activation, characteristics of HBP1, have been shown to resemble those of viral E1A protein (Lavender et al., 1997; Tevosian et al., 1997). HBP1 mediated cell cycle arrest under optimal growth conditions and induction of cell differentiation in the presence of pRb-HBP1 suggests pRb/HBP1 role in cell differentiation.

1.1.4.18 p202

p202 is an interferon inducible transcription factor that was identified as a murine 52 kDa protein. Through pull-down (*in vitro*) experiments and immunoprecipitation (*in vivo*) studies, Choubey et al. (Choubey and Lengyel, 1995) mapped two p202 binding sites (one spans amino acids 1-254 and the other amino acids 379-928) in pRb, as well as, two pRb binding sites (one in the N-terminal region (58-291) and the other in the C-terminal region (285-445) in p202. pRb association through an N-terminal segment of p202 was within the limit of experimental artifacts and no pRb was detected in immunoprecipitation experiments performed with the lysates of human osteosarcoma cell line Saos-2 which expresses a C-terminal truncated (amino acids 713-928) pRb. Pull-down experiments showed that pRb interact with p202 through its large pocket region. However, a pocket mutant of pRb (706.C to F) exhibited poor interaction. This evidence allowed concluding that pRb interacts with the C-terminal domain of p202, which consist of the LxCxE motif through its viral oncoprotein-binding pocket. p202 have been implicated in cell cycle arrest and inhibition of E2F mediated transcription (Choubey et al., 1996; Datta et al., 1998). These data, together with experimental

evidence, suggest that p202 could inhibit Rb/E2F pathway, but the biological significance of pRb/p202 yet to be revealed.

1.1.4.19 Rak/Frk

Rak and Frk are identical nuclear tyrosine kinases, independently identified in human breast tumors and human hepatoma cell lines subsequently (Cance et al., 1994; Chandrasekharan et al., 2002; Lee et al., 1994). Rak/Frk kinases show similarities to Src related kinases, possessing an N-terminal SH2 and SH3 domains and autoregulatory tyrosine residues in their catalytic domains. However, they differ in certain structural features such as presence of bipartite nuclear localization signal in the SH2 domain, absence of the critical glycine residue in the consensus myristoylation motif MGXXXS/T that is necessary for the conjugation of myristate and plasma membrane targeting and replacement of the conserved serine residue (S) at position 6 with a glutamine (Q). Furthermore, the consensus motif required for palmitylation (CXXC or CXC) is only partially retained. pRb/Rak complexes were identified in different *in vivo* and *in vitro* studies (Craven et al., 1995). GST pull-down experiments performed with the *E. coli* expressed Rak deletion mutants and *in vitro* translated pRb, demonstrated that Rak binds by its SH3 domain (from amino acids 46 to 110) to sequences within the small pocket region of pRb. Competitive peptide binding studies suggested the SH3 domain of Rak is essential for pRb interaction and its N-terminal LxCxxxE motif does not involve in association with pRb. pRb has no proline-rich SH3 binding site and thus, Rak SH3 domain may have a unique binding specificity.

Frk/rak was found to associate with hyper, as well as hypophosphorylated forms of pRb during the G_1 and S phases of the cell cycle *in vitro*. Cell cycle analysis studies indicate that activated Frk/rak suppresses cell growth by inducing a G_1 arrest, possibly by preventing entry into the S phase of the cell cycle (Anneren and Welsh, 2000; Oberg-Welsh et al., 1998). These observations, in conjunction with the epithelial expression pattern of Rak, suggest that in association with pRb, Rak may function as a novel tumor suppressor gene.

1.1.4.20 MyoD

The MyoD protein is one of the muscle determination factors (MDFs) belonging to a group of muscle-specific basic helix-loop-helix (bHLH) transcription factors. MyoD has

been reported to promote muscle cell differentiation in cooperation with pRb (Gu et al., 1993). Moreover, it induces pRb expression, which is required for proper muscle gene expression and to maintain muscle cells in quiescent stage that is a pre-requisite for cell differentiation (Martelli et al., 1994; Novitch et al., 1996; Schneider et al., 1994). Analysis of muscle differentiation in pRb knockout mice revealed defects in skeletal muscle differentiation (Zacksenhaus et al., 1996). All these evidence suggest pRb role in muscle cell differentiation.

pRb/MyoD complexes were identified both in vitro and in vivo. Moreover, in vitro binding studies demonstrated that the C-terminal region (aa 605-928) of pRb associates with the basic helix-loop-helix (bHLH) region of MyoD (Gu et al., 1993). Competitive binding studies performed in the presence of T-antigen peptide containing LxCxE motif suggested that MyoD might interact with the T-antigen binding region (A/B pocket) of pRb (Gu et al., 1993). However, three different studies failed to reproduce pRb/MyoD interactions in vivo reported by Gu at al (Halevy et al., 1995; Li et al., 2000). Thus, further investigation of pRb/MyoD interactions using NMR should provide conclusive evidence about these contradictory results.

1.1.5 Nuclear magnetic resonance (NMR) spectroscopy

NMR is a powerful spectroscopic technique that provides information about the structural and chemical properties of molecules. The phenomenon of magnetic resonance results from the interaction of the magnetic moment of atomic nuclei (μ) with an external magnetic field. The cause of this magnetic moment is the quantum mechanical angular momentum (spin angular momentum) of nuclei, which poses a non-zero spin. Nuclei that are significant in protein NMR are mainly ^{1}H, ^{2}H, ^{15}N, ^{13}C, ^{19}F and ^{31}P. ^{1}H, ^{19}F and ^{31}P are highly abundant isotopes whilst ^{15}N, ^{13}C, ^{2}H are present at only low levels (<1.5%). When a protein sample is placed in a static external magnetic field B0, the magnetic moment (μ) of nuclei experiences a torque tending to turn it parallel to the direction of external magnetic field. This results in macroscopic magnetization of the sample parallel to B0, whose direction defines Z-axis. When a strong exciting radio frequency (RF) pulse is applied to the sample at right angle to that of the static external magnetic field B0, the net magnetization M (average magnetization among many atoms) is tilted away from the z-axis and precesses around the z-axis at its resonance

(Larmore) frequency. By Faraday's law of electromagnetic induction, the precessing magnetization of the nuclei will generate an electromotive force (voltage) in the coil of the NMR probe at the larmore frequency, which defines the transverse plane (xy-plane). This signal, which contains the larmore frequencies of all the nuclei of a given element, is recorded as function of time over a period of few seconds. The signal decays exponentially due to dephasing of the spin pockets. This signal is called free induction decay (FID). Fourier transformation (a mathematical process which convert time domain into frequency domain) of the data will produce the frequency dependent NMR spectrum.

Four parameters can be measured from a typical NMR spectrum; 1) the chemical shifts; the electrons surrounding the magnetic nucleus generate a small local magnetic field that opposes the applied magnetic field. The degree of such shielding depends on the surrounding electron density. Consequently, nuclei in different environments will precess with slightly different frequencies, which are termed chemical shifts. The chemical shifts of a perturbed sample are expressed in functional units δ (parts per million or ppm) relative to the shifts of a standard sample. 2) The half-height peak width, which reflects the degree of motion in solution of the absorbing species; 3) The intensity of the peak or integrated area, which is proportional to the total number of absorbing nuclei; 4) The coupling constant, which measures the extent of direct interaction or influence of neighbouring nuclei on the absorbing nuclei. These four measurements enable the determination of the identity and number of nearest-neighbour groups that affect the response of absorbing species through bonded interactions. Recent developments in two-dimensional and three-dimensional NMR spectroscopy made assignment of bonded and nonbonded interactions easy, and enhanced application of NMR in determination of protein three-dimensional structures and drug discovery. We applied NMR to understand different aspects of proteins such as protein conformations, protein-peptide interactions and protein-protein interactions.

Chemical shifts in one-dimensional proton spectra reveal information about protein conformation, protein aggregation and its stability. Backbone amides in random-coil configuration exhibit intense chemical shifts at ~8.3 ppm and hence appearance of a large and broad signal near ~8.3 ppm is a characteristic feature of unfolded proteins. Folded proteins give dispersed signals between 8.5 -11 ppm because of different chemical environments. Structured proteins can also be differentiated from unstructured

proteins based on signal dispersion versus a steep flank of the dominant peaks at aliphatic region (between +1.0 and -1.0 ppm) respectively. Extent of folding in partially structured proteins can be quantitatively estimated by observing the signal dispersion pattern near 8.3 ppm. The Line width of the signals gives information about protein aggregation. As larger molecules relax faster than smaller ones, they will produce broader lines. In addition to the all above applications, one-dimensional proton spectra also provide information on α-helical or β pleated-sheets in proteins. The Cα protons in a helix display few resonances in the region between 5 and 6 ppm, whereas those in a β pleated-sheet resonate in this region. Since frequencies in the region between 5 and 6 ppm is often disturbed by water suppression frequencies, this feature can be seen only in 100% D_2O. Appearance of prominent signals from the small peptide fragments around 1 ppm indicates the degradation of protein with time. The ^{15}N HSQC spectrum shows exactly one signal per amino acid residue, except proline. Positioning of peaks indicates structural status of the protein. In the spectrum of an unfolded protein, all signals cluster in a characteristic “blob” around a ^{1}H frequency of 8.3 ppm, with minor signal dispersion in both dimensions. The spectrum of a folded protein show large signal dispersion. Thus, if the peaks are assigned their respective sequential positions in the polypeptide chain, disordered regions may be identified. Since the number of signals in the HSQC spectrum approximately corresponds to the number of residues in the protein under investigation, conformational changes upon ligand binding, residues involve in binding with substrates under study can be easily detected by a shift in the position of existed peaks and/or appearance of new peaks.

1.1.6 Aim of the project

The goal of the project was to purify sufficient quantities of isotopically labelled and unlabelled retinoblastoma protein for NMR spectroscopy and X-Ray crystallographic studies. Through immunological and biochemical studies, pRb has been shown to interact with viral oncoproteins and a plethora of cellular proteins involved in cell cycle regulation, apoptosis and cell differentiation. The exact regions through which all these proteins interact with pRb have not yet been mapped. In this context, NMR based binding studies with isotopically labelled pRb should help to test the validity of pRb interactions with its binding proteins and to map the exact binding sites on pRb and in

pRb docking proteins. By solving the crystal structures of complexes of pRb and its binding proteins, one can address the mechanism of action of pRb in all three major biological processes such as cell cycle, cell differentiation and apoptosis. This project was also aimed at investigation of physical associations between pRb and MyoD.

1.2 Materials and Methods

1.2.1 Materials

All chemicals were of analytical grade and were purchased from Sigma-Aldrich (Deisenhofen, Germany), Fluka (Buchs, Switzerland), and Merck (Dramstadt, Germany) if not stated otherwise.

- New England Biolabs (NEB, Frankfurt, Germany): EcoRI, BamHI, HindIII and Nde1 restriction endonuleases. NEB buffers, T4-DNA ligase, Quick Ligation Kit.
- Stratagene (La Jolla, CA, USA): Quick change site-directed mutagenesis Kit, pfu turbo DNA polymerase, 10x cloned pfu buffer, Quick change XL-site-directed mutagenesis kit, ExSite PCR-based site-directed mutagenesis kit.
- Roche (Mannheim, Germany): Complete, EDTA-free protease inhibitor cocktail tablets, Rapid DNA ligation kit.
- Novagen (Schwalbach, Germany): Benzonase nuclease
- Bio Rad (München, Germany): Bio-Rad protein dye reagent
- Invitrogen (Karlsruhe, Germany): EKMax entirokinase, Novex tris-glycine gels.
- MBI Fermentas (St,Leon-Rot, Germany): Restriction endonucleases, 6x mass loading dye.
- Peq Labs (Erlangen, Germany): IPTG, dATP, dGTP, dTTP, dCTP, Taq-DNA-polymerase, PWO-DNA-polymerase, 1 kb DNA ladder, 100 bp DNA ladder.
- Qiagen (Valencia, USA; Hilden, Germany): Ni-NTA superflow resin, Plasmid midi kit, QIAprep spin mini prep kit, QIAquick PCR purification and gel extraction kit.
- Campro Scientific (Berlin, Germany): Deuterium oxide (D_2O) 99%, ^{15}N-Ammonium chloride (NH4Cl) 99.9%.
- Gibco (Karlsruhe, Germany): Spodoptera frugiperda (*Sf9*) cells, Sf-900 II SFM media, Antibiotic-antimycotic (100x), liquid, Fetal bovine serum.
- Pharmingen (San Diego, CA92121, USA): pVL1392-XylE control vector, Transfection buffer A and B.

<u>Antibiotics</u>

- Ampicillin
- Chloramphenicol
- Kanamycin

1.2.1.1 Chromatography equipments, columns and media

- Amersham Pharmacia (Freiburg, Germany): ÄKTA explorer 10, Peristaltic pump P-1, Fraction collector RediFrac, Recorder REC-1, UV flow through detector UV-1, HiLoad 16/60 Superdex S30pg, S200pg, HiLoad 26/60 Superdex S75pg, HiLoad 10/30 Superdex S75pg, Mono Q HR 5/5, 10/10, Mono S HR 5/5, 10/10, Butyl sepharose 4 FF, Q-sepharose FF, SP-sepharose FF, Glutathione sepharose.

1.2.1.2 Consumables

- Millipore (Eschborn, Germany): YM3, YM10 amicon centriprep concentrators
- Roth (Kleinfeld, Hanover, Germany): Dialysis tubing spectra/por MW 3,500, 10,000
- Becton Dickinson (Heidelberg, Germany): 15 and 50 ml Falcon tubes
- Gilson (Villiers-le Bel, France): Pipette tips 10 µl, 200 µl, 1000 µl
- Bio Rad (München, Germany): BioLogic LP system biorad, Gene pulsar electroporation cuvettes, Mini-PROTEAN 2 electrophoresis cell
- Invitrogen: Xcell SureLock Mini-cell electrophoresis apparatus, Novex tris-glycine precast gels
- Millipore (Molsheim, Germany): Sterile filters millex 0.22 µm, 0.45 µm sterile filters, Nitrocellulose membranes
- Falcon (FRG): Sterile 10 ml, 25 ml and 50 ml pipettes, 15 cm and 60 mm tissue culture plates, 12-well tissue culture plates
- Techne (Cambridge, UK): Spinner flasks

1.2.1.3 Miscellaneous

- Autoclave Bachofer, Reutlingen, Germany
- Balances PE 1600, AE 163 Mettler, Germany
- Centrifuge Avanti J-30I Beckman, USA
- Centrifuge Microfuge R Beckman, USA
- Centrifuge 3K15 Sigma, Germany
- Centrifuge 5414 Eppendorf, Germany
- Chambers for SDS PAGE and Western blotting MPI für Biochemie, Germany
- Ice machine Scotsman AF 30 Frimont, Bettolino di Pogliano, Italy
- MAR research image plates, mar345 MAR research, Hamburg, Germany

- Magnetic stirrer Heidolph M2000 Bachofer, Reutlingen, Germany
- NMR-spectrometer Bruker DRX500, Bruker DRX600, Bruker AV-900, Rheinstetten, Germany
- pH-meter pHM83 Radiometer, Copenhagen, Denmark
- Pipettes 2.5 µl, 10 µl, 20 µl, 200 µl, 1000 µl Eppendorf, FRG
- Quartz cuvettes QS Hellma, Germany
- Shaker Adolf-Kühner AG, Switzerland
- Spectrophotometer Amersham Pharmacia, Freiburg, Germany
- Ultra filtration cells, 10 ml, 50 ml, 200 ml Amicon, Witten, Germany
- Vortex Cenco, Germany

1.2.1.4 Media, buffers and stock solutions

1.2.1.4.1 Media

- **Luria-Bertani (LB) medium** 10 g/l Bacto-tryptone
  5 g/l Bacto-yeast extract
  10 g/l NaCl

pH of the medium was adjusted to 7.0 with 5 N NaOH and then made up the final volume to 1 litre with ddH_2O. Later medium was sterilized by autoclaving.
(For plates, medium was supplemented with 15 g/l agar and recommended amount of appropriate antibiotics).

- **Terrific Broth (TB) medium** 12 g/l Bacto-tryptone
  23.9 g/l Bacto-yeast extract
  8 ml/l glycerol
  2.2 g/l KH_2PO_4
  9.4 g/l K_2HPO_4

- **Minimal medium (MM) for uniform labelling of proteins with ^{15}N isotope**

Stock solutions

1) 1% thiamine (filter sterilized)
2) Antibiotics (filter sterilized)
3) 1M $MgSO_4$, (filter sterilized)
4) Zn-EDTA solution

EDTA 5 mg/ml

$Zn(Ac)_2$ 8.4 mg/ml

(Each component was dissolved separately in water and then mixed together).

5) trace elements solution

H_3BO_3 2.5 g/l

$CoCl_2*H_2O$ 2.0 g/l

$CuCl_2*H_2O$ 1.13 g/l

$MnCl_2*2H_2O$ 9.8 g/l

$Na_2MoO_4*2H_2O$ 2.0 g/l

(The mixture was dissolved completely by lowering pH with citric acid or conc. HCl).

6) 20% glucose (filter sterilized)

Procedure to prepare minimal medium (1liter)

To 900 ml of ddH_2O, added

NaCl	0.5 g
Trace elements solution	1.3 ml
Citric acid monohydrate	1 g
Ferric citrate	36 mg*
KH_2PO_4	4.02 g
$K_2HPO_4*3H_2O$	7.82 g
Zn-EDTA solution	1 ml
NH_4Cl or $^{15}NH_4Cl$	1 g

(*: 36mg of ferric citrate was dissolved separately by adding 120 µl conc. HCl and subsequent heating at 95°C for couple of minutes, and then added to the medium).

pH of the solution was adjusted to 7.0 with 5 N NaOH and then made up the final volume to 975 ml with ddH_2O. The solution was sterilized by autoclaving for 20 min at 15 lb/sq liquid cycle. After cooling down the medium to room temperature, Filter sterilized 25 ml of 20% glucose, 2 ml of 1 M $MgSO_4$, 560 µl of 1% thiamine and half of the recommended amounts of appropriate antibiotics were added.

1.2.1.4.2 Buffers and stock solutions

- Phosphate-buffered saline (PBS) buffer

  $Na_2HPO_4*2H_2O$ (10 mM), pH 7.3 1.78 g/l

KH_2PO_4 (1.8 mM)	1.36 g/l
NaCl (140 mM)	8.18 g/l
KCl (2.7 mM)	0.2 g/l
NaN_3 (0.05%)	0.5 g/l

- Transformation buffer I

KOAc	30 mM
RbCl	100 mM
$CaCl_2$	10 mM
$MnCl_2$	50 mM
Glycerol	15%

Adjusted pH to 5.8 with acetic acid and then filter sterilized.

- Transformation buffer II

$CaCl_2$	75 mM
RbCl	10 mM
Glycerol	15%
MOPS or PIPES	10 mM

Adjusted pH with KOH to 6.5 and filter sterilized.

- Lysis buffer: 50 mM KH_2PO_4 pH 8.0, 500 mM NaCl, 10 mM β-mercaptoethanol, 10 mM imidazole, EDTA-free protease inhibitor cocktail.
- Ni-NTA wash buffer A: 50 mM KH_2PO_4, 300 mM NaCl, 10 mM β-mercaptoethanol, 20 mM imidazole, pH 8.0.
- Ni-NTA wash buffer B: 50 mM KH_2PO_4, 300 mM NaCl, 10 mM β-mercaptoethanol, 50 mM imidazole, pH 8.0.
- Ni-NTA elution buffer: 50 mM KH_2PO_4, 300 mM NaCl, 10 mM β-mercaptoethanol, 200 mM imidazole, pH 8.0.
- MES buffer (EQ): 25 mM MES, 10 mM β-mercaptoethanol, pH 6.0.
- MES buffer (Elution) : 25 mM MES, 10 mM β-mercaptoethanol, 1 M NaCl, pH 6.0.
- EKMax dgst buffer: 50 mM Tris base pH 7.6, 150 mM NaCl, 3 mM DTT, 3 mM $CaCl_2$.
- Phosphate buffer for NMR: 50 mM KH_2PO_4, 150 mM NaCl, 3 mM DTT, pH 7.2.
- TBE (10x stock): 890 mM tris base, 890 mM boric acid, 20 mM EDTA.

- IPTG stock solution (1.0 M): 2.4 g of IPTG was dissolved in 8 ml of ddH_2O. The final volume of the solution was adjusted to 10 ml with ddH_2O. Filter sterilized (0.22 μm filter) stock solution was stored in 1 ml aliquots at -20°C.
- Kanamycin stock solution (50 mg/ml): 0.5 g of kanamycin was dissolved in 10 ml of ddH_2O. Filter sterilized (by 0.22 μm filter) stock solution was aliquoted and stored at –20°C until used.
- Ampicillin stock solution (100 mg/ml): 1.0 g of ampicillin was dissolved in 9 ml of ddH_2O. Thereafter the final volume of the solution was adjusted to 10 ml with ddH_2O. After filtering through 0.22 μm filter, stock solution was stored in aliquots at -20°C until used.
- Chloramphenicol stock solution (34 mg/ml): 680 mg of chloramphenicol was dissolved in 20 ml of ethanol and then stored at –20°C until used.

1.2.1.5 Antibodies, proteases, nucleases and other proteins used for this study

1.2.1.5.1 Antibodies

Epitope	Name	Catalogue number.	Type of anti Body	Supplier
Rbp100	Rb (IF8)	Sc-102	Primary	Santa Cruz Biotechnology, Inc., USA
Mouse IgG	Goat anti – mouse IgG	Sc-2047	Secondary	Santa Cruz Biotechnology, Inc., USA
Human p19	P19 (N-20)	Sc-1075	Primary	Santa Cruz Biotechnology, Inc., USA
Goat IgG	Donkey anti – goat IgG	Sc-2033	Secondary	Santa Cruz Biotechnology, Inc., USA

1.2.1.5.2 Proteases

Entirokinase (Invitrogen, Germany)

Thrombin

1.2.1.5.3 Nucleases

DNase1

RNaseA

Benzonase (Novagen)

1.2.1.5.4 Other proteins

Hen Egg White Lysozyme

Bovin Serum Albumin (Bio Rad)

Prestained Protein Marker, Broad Range (6-175 kDa) used for SDS-PAGE analysis (NEB, Germany).

#	Name of the protein	Source	Apparent MW (Da)
1	MBP-β galactosidase	*E coli*	175.000
2	MBP-paramyosin	*E coli*	83,000
3	Glutamate dehydrogenase	Bovin liver	62,000
4	Aldolase	Rabbit muscle	47,500
5	Triosephosphate isomerase	Rabbit muscle	32,500
6	B-Lactoglobulin A	Bovine milk	25,000
7	Lysozyme	Chicken egg white	16,500
8	Aprotinin	Bovin lung	6,500

1.2.1.6 Plasmids and experimental organisms

1.2.1.6.1 Plasmids

The following constructs have been used for the expression of proteins in *E. coli* (Table 1).

Table 1. Constructs used for the expression of proteins in *E. coli.*

#	Construct	Vector	Restriction sites	Reference
1	28a_nlabc*	pET28a	XhoI/EcoRI	
2	pTB_albc**	pTrc/His	EcoRI/HindIII	Brosius, J. et al.1984
3	pBB_albc**	pBAD/His	EcoRI/HindIII	Guzman, L.M. et al. 1995
4	28a_albc**	pET28a	EcoRI/HindIII	
5	Sb_aΔlbc***	pRSETb	EcoRI/HindIII	
6	pTB_aΔlbm****	pTrc/His	EcoRI/HindIII	Brosius, J. et al.1984
7	pBB_ aΔlbm****	pBAD/His	EcoRI/HindIII	Guzman, L.M. et al. 1995
8	4T2_ aΔlbm§	pGEX4T2	BamHI	
9	Sb_aΔlbm****	pRSETb	EcoRI/HindIII	
10	28a_aΔlbm****	pET28a	EcoRI/HindIII	

11	42a_ aΔlbm§	pET42a	EcoRI/HindIII	Smith, D.B. et all. 1988
12	Sb_aΔlb (785)&	pRSETb	EcoRI/HindIII	
13	Sb_aΔlb(793)&&	pRSETb	EcoRI/HindIII	
14	Sb_aΔlbW*****	pRSETb	EcoRI/HindIII	
15	15b_p19§§	pET15b	NdeI/BamHI	

*: The full-length RB gene cloned inframe to the 6x-His affinity tag.

**: The large pocket region (ALBC) of RB gene cloned inframe to the 6x-His affinity tag.

***: The large pocket region of RB gene without loop (AΔLBC) cloned inframe to the 6x-His affinity tag.

****: I716V Mutant of the small pocket region of RB gene (from M379 to ?772) without loop cloned inframe to the 6x-His affinity tag.

*****: The small pocket region of RB gene (from M379 to ?772) without loop cloned inframe to the 6x-His affinity tag.

§: I716V Mutant of the small pocket region of RB gene (from M379 to ?772) without loop fused inframe to the GST affinity tag.

&: The small pocket region of RB gene (from M379 to ?785) without loop fused inframe to the GST affinity tag.

&&: The small pocket region of RB gene (from M379 to ?793) without loop fused inframe to the GST affinity tag.

§§: p19 ^{INK4D} gene fused to 6X-His tag.

The following constructs have been used for the expression of retinoblastoma protein in *Sf9* cells after transfection in to Baculovirus (Table 2).

Table 2. Constructs used for over expression of pRb in Insect cells.

#	Construct	Vector	Restriction sites	Reference
16	pBBH2a_nlabc*	pBlue Bac His 2A	XhoI/BamHI	
17	pBB4.5_nalbc§	pBlue Bac 4.5	XhoI/BamHI	
18	pBBH2_albc**	pBlue Bac His 2A	XhoI/HindIII	

*: The full-length RB gene cloned inframe to the 6x-His tag.

**: The full-length RB gene cloned in to an expression vector, which does not have an affinity tag.

§: The large pocket region of RB (ALBC) cloned under His tag.

1.2.1.6.2 Experimental organisms

The following experimental organisms have been used for expression of p19 and Rb proteins.

1.2.1.6.2.1 Bacterial strains

Table 3. ***Escherichia coli*** strains used for this study.			
#	Strain type	Product provider	Reference
1	BL21(DE3)	Invitrogen	Philips, T.A. et al. 1989
2	BL21(DE3)pLysE	Invitrogen	Philips, T.A. et al. 1989
3	BL21(DE3)pLysS	Invitrogen	Philips, T.A. et al. 1989
4	One Shot BL21-AI	Invitrogen	Philips, T.A. et al. 1989
5	BL21 Star (DE3) One Shot	Invitrogen	Makrirides S.C. et al. 1995 Lopez, P.J. et al. 1999
6	BL21 Star (DE3)pLysS One Shot	Invitrogen	Makrirides S.C. et al. 1995 Lopez, P.J. et al. 1999
7	BL21 Star (DE3)pLysE One Shot	Invitrogen	Makrirides S.C. et al. 1995 Lopez, P.J. et al. 1999
8	LMG 194	Invitrogen	

1.2.1.6.2.2 Insect cell line used for baculovirus mediated overexpression of the retinoblastoma protein: ***Spodoptera frugiperda*** (*Sf9*) cells.

1.2.2 Methods

1.2.2.1 Amplification of plasmids in *E. coli*

Chemically and electrocompetent DH5-α *E. coli* cells were used to amplify all plasmid constructs used in this study. For overexpression of heterologous proteins, various chemically competent *E. coli* expression strains were used.

1.2.2.1.1 Preparation of chemically competent cells (*RbCl method*)

1) Desired bacterial strain from frozen stocks was plated onto LB-agar plates and incubated overnight at 37°C.

2) 5 ml of 2% LB medium supplemented with 20 mM $MgSO_4$ was inoculated with a single fresh colony from a plate and cells were grown overnight at 37°C with shaking at 200 rpm.

3) Saturated overnight culture was diluted with fresh LB medium containing 20 mM $MgSO_4$ in 1:100 (v/v) ratio and grown at 37°C until the OD_{600} reaches 0.45-0.55.

4) Cells were placed on ice for 10 min and then pelleted by centrifugation in autoclaved centrifuge tubes at 3000 rpm, 4°C for 10 min.

5) Pellet was gently resuspended in 1/2.5th the culture volume of the prechilled transformation buffer I (TFB I), then incubated on ice for 5 min. Thereafter, centrifugation was followed like before.

6) The pellet was resuspended in 1/25th the culture volume of transformation buffer II (TFB II). After incubation on ice for 15 to 20 min, cells were aliquoted in 100 μl volumes into prechilled sterile 1.5 ml eppendorfs.

7) Tubes containing cells were frozen in liquid nitrogen and stored immediately at -80°C.

1.2.2.1.2 Transformation (heat shock method)

1) Frozen chemically competent cells were thawed by placing on ice for 5 to 10 min. After addition of 50-100 ng of plasmid DNA, cells were mixed by tapping gently and then incubated on ice for 30 min.

2) Cells were heat pulsed at 42°C for 45 sec, then placed on ice for 2-3 min. 0.9 ml of prewarmed LB medium to each transformation reaction was added and then incubated at 37°C for 1 hr with shaking at 300 rpm.

3) 100 μl to 150 μl cells were plated on a single LB agar plate that contained the appropriate antibiotic to select transformants and then incubated at 37°C overnight.

1.2.2.1.3 Preparation of electrocompetent cells

1) Overnight culture was prepared by inoculating 50 ml LB medium with a single fresh colony of desired strain followed by growing cells overnight at 37°C with vigorous shaking.

2) Saturated culture was added to one-liter fresh LB medium and grown at 37°C, 200 rpm, until the OD_{600} reaches to 0.5 to 0.6. Later, cells were transferred to sterile prechilled centrifuge bottles and incubated on ice for 30 min.

3) Following centrifugation at 2000 xg for 15 min at 4°C, pelleted cells were resuspended in equal the culture volume of sterile prechilled water and then pelleted by spinning like earlier.

4) Pelleted cells were washed again by resuspending in ½ the culture volume of sterile prechilled water followed by centrifugation.

5) Pelletes were resuspended in 1/25th the culture volume of sterile chilled 10% glycerol. Thereafter, cells were spun at 4000 xg, 4°C, for 15 min.

6) After resuspending the pellet in 1/500th the culture volume of sterile 10% glycerol, cell suspension was aliquoted in 40 μl volumes into sterile prechilled 1.5 ml eppendorfs. After freezing in liquid nitrogen immediately, cells were stored at -80°C for further use.

1.2.2.1.4 Transformation of electrocompetent cells

1) Electrocompetent cells were thawed on ice, then added >1 μl of water containing 20 to 30 ng of plasmid DNA. Thereafter, the mixture was put between the electrodes of a 0.1 cm prechilled electroporation cuvette (Biorad, Germany).

2) Later the cuvette was placed into the electroporator (Stratagene, Germany) followed by a 1660 V electric pulse was applied. The transformation efficiency was monitored based on the time constant observed (usually 3.5-5.4 ms).

3) Electrophoresed cells were resuspended in 1 ml prewarmed LB medium and then incubated at 37°C for one hour with shaking. 50 to 100 μl of cells was plated on LB agar plate containing the appropriate antibiotic. Plates were incubated at 37°C overnight.

1.2.2.2 Molecular cloning

Plasmid constructs produced during this study were cloned with the aid of polymerase chain reaction (PCR), followed by restriction digestion and ligation. The standard PCR protocol followed is summarized in Table 4.

Table 4. Standard protocol for polymerase chain reaction.

Reaction composition	Thermal cycling parameters			
	Segment	Cycles	Temperature	Time
5.0 μl 10x pfu reaction buffer	1	1	95°C	1.0 min
150 ng sense primer				
150 ng antisense primer	2	28	95°C	1.0 min
200 μM dNTPs			54°C to 56°C	30 sec
100 ng template DNA			72°C	1 min/kb
1.0 μl pfu DNA polymerase (2.5U)				
sterile ddH_2O up to 50 μl.	3	1	72°C	10 min

4	1	4°C	hold

The reaction mixtures of appropriate reaction samples were prepared in sterile thin-wall PCR tubes and overlaid with 20 μl of sterile mineral oil. PCR was performed using the robocycler temperature cycler. The amplified PCR products were analyzed by agarose gel electrophoresis [1% agarose dissolved in TBE buffer containing ethidium bromide (10 μg/ml)]. Desired PCR amplified products were purified by QIAquick PCR purification kit (anion exchange chromatography) following the manufacturers instructions. The restriction digestion of purified PCR products and the target vector were performed overnight at 37°C in a 50 μl reaction containing the recommended amount of each restriction enzyme and appropriate 10x reaction buffer (NEB). The restriction digested vectors were dephosphorylated by treating with 5 units of intestinal phosphatase at 37°C for one hour whenever needed. All reactions were stopped by heating at 65°C for 20 min. Digested target vectors and inserts were separated from other components of the digestion reaction by agarose gel electrophoresis. Desired DNA fragments were purified from agarose gel slices using QIAquick gel extraction kit (anion exchange chromatography) following the manufacturers instructions. Ligation reactions composed of 5μl of vector and insert DNAs, molar ratio of vector DNA and insert DNA was 1:2 subsequently, and 2 μl of 5x DNA dilution buffer, 10 μl of T4 DNA ligation buffer, 1 μl of T4 DNA ligase (5u) and 3 μl of sterile ddH_2O were incubated at 21°C for 5 min. Later 2 to 4 μl of the ligation reactions were transformed into chemically competent *E. coli* TOP 10 cells. After addition of ligation reaction, cells were mixed gently by tapping and incubated on ice for 30 min, followed by a 30 sec heat shock was given at 42°C. Transformed cells were incubated on ice for 2 to 3 min and then resuspended in 250 μl of pre-warmed LB medium. Cells were incubated at 37°C for one hour at 300 rpm. 25 to 100 μl of cell suspensions were plated on LB-Agar plates containing appropriate antibiotics for selection of transformants. After incubation of plates for 18 to 20 hrs at 37°C, overnight cultures were prepared by inoculating a single colony into 8 ml LB medium supplemented with appropriate antibiotic, followed by growing the cultures at 37°C overnight. Cells were harvested and used for plasmid isolation with the aid of “QIAprep miniprep kit” (anion exchange chromatography), following manufacturers instructions. Clones were analysed by colony PCR, restriction digestion and DNA sequencing (Medigenomix, Munich, Germany).

1.2.2.3 Site directed mutagenesis

Quick-Change® Site-Directed Mutagenesis Kit was used to introduce single amino acid substitutions and stop codons at desired sites in the gene encoding retinoblastoma protein. A supercoiled double stranded DNA carrying a gene of interest was used as a template to PCR amplify the complementary oligonucleotide primers carrying desired mutations with the aid of pfu turbo DNA polymerase. The extension of mutagenic primers generated mutated covalently closed and nicked plasmids. Following PCR, the product was treated with 1 μl of Dpn I at 37°C for two hours. The Dpn I endonuclease was used to digest non-mutated, methylated and hemimethylated parental DNA and select mutated DNA. β-ME treated XL10 ultracompetent cells were mixed with 2 μl of Dpn I treated DNA sample and incubated on ice for 30 min. Following a 30 sec heat shock at 42°C, cells were incubated on ice for 2 to 3 min. Cells were resuspended in 0.5 ml of pre-warmed LB medium and incubated at 37°C for one hour with shaking at 300 rpm. 100 to 200 μl cells were plated on LB-Agar plate containing appropriate antibiotic to select transformants. 5 ml overnight cultures were prepared by growing a single colony in 5 ml LB medium supplemented with appropriate antibiotic. Plasmids were isolated from pellets as described earlier and the desired mutation was confirmed by DNA sequencing. PCR protocol used for site directed mutagenesis is summarised in Table 5.

Table 5. PCR protocol followed to create site directed mutagenesis.

Reaction composition	Thermal cycling parameters			
	Segment	Cycles	Temperature	Time
5.0 μl 10x reaction buffer	1	1	95°C	1.0 min
150 ng sense primer				
150 ng antisense primer	2	15	95°C	30 sec
1.0 μl dNTPs			54°C to 57°C	1.0 min
20 ng template DNA			68°C	1.0 n/kb
1.0 μl pfu Turbo DNA polymerase (2.5U)				
sterile ddH_2O up to 50 μl.	3	1	68°C	10.0 min
	4	1	4°C	hold

1.2.2.4 Deletion mutagenesis

Deletion of a 201 bp region, which encodes the loop situated between A and B domains of retinoblastoma protein, was performed by oligonucleotide assisted polymerase chain reaction. Four primers designed to delete the loop (Table 6) were supplied by Metabion, Germany.

Table 6. Oligonucleotide primers used for deletion mutagenesis.

S.N	Primer name	oligo sequence
1	P60F	5’**CTTTATTTGATCTTATTAAACAATCAAAG***ACCTCTCTT TCACTGTTTTATAAAAAAGTG*-**3’**
2	P60R	5’-*CACTTTTTTATAAAACAGTGAAAGAGAGGT***CTTTGATT GTTTAATAAGATCAAATAAAGG**-3’
3	EcoF	5’-GGTACCATATGG**GAATTC**CATGAACACTATC-3’
4	HinR	5’-GCCAAAACAGCC**AAGCTT**TCATTTCTCTTC-3’

Shaded and shaded bold sequences of P60F primer represent upstream and downstream sequences to the loop respectively. P60R is a reverse complementary sequence of P60F. Restriction sites in forward (EcoF) and reverse (HinR) primers are underlined.

In stage one, two extension reactions were carried out in two separate tubes; first extension reaction was performed with primers EcoF and P60R, to amplify a region upstream to the loop and the second with primers HinR and P60F to amplify a region downstream to the loop. In stage two, products of the two reactions were mixed and then a third extension reaction was carried out with forward (EcoF) and reverse (HinR) primers. P60F and P60R primers are reverse complementary deletion primers designed against upstream and downstream boundaries of the loop. Products of PCR II and I anneal at their 5’ complementary sequences and a third PCR of these 5’ annealed products with forward and reverse primers, results in a complete gene with desired deletion. Strategy for deletion mutagenesis is depicted in Fig 3.

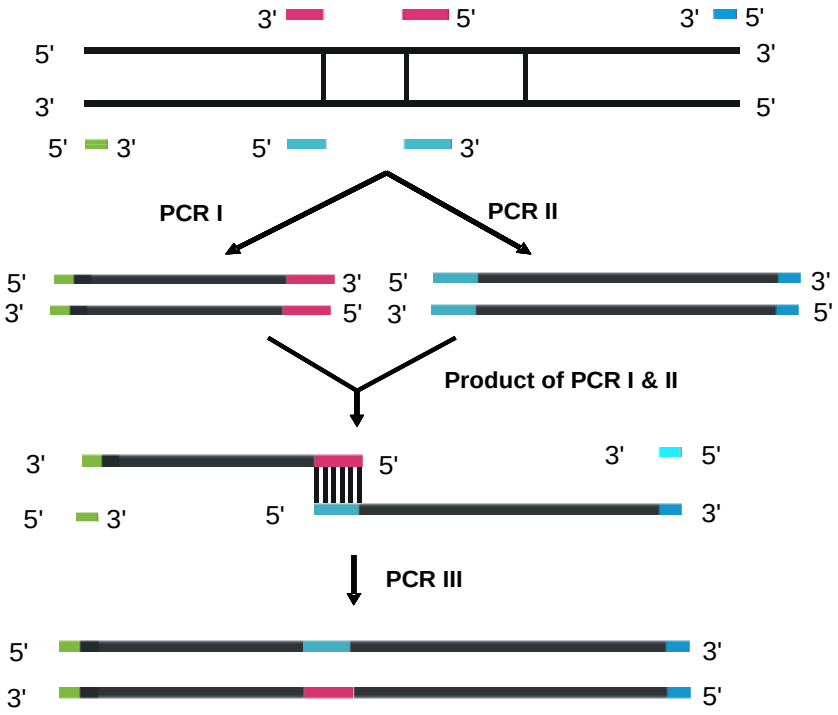

Figure 3. Strategy for deletion mutagenesis. *Step 1: Upstream sequence to the region to be deleted is PCR amplified with forward (EcoF) primer and reverse deletion (P60R) primer. Step 2: Downstream sequence to the region to be deleted amplified with the aid of PCR using reverse (HinR) primer and forward deletion (P60F) primer. Step 3: Products of PCRI and II are mixed and subjected to PCR using forward (EcoF) and reverse (HinR) primers. Different primers are marked in different colours and all steps are depicted schematically.*

PCR protocols standardised to carry out three extension reactions are summarized in Table 7.

Table 7. PCR protocol used for deletion mutagenesis.

Long template PCR for Reaction I and II

Reaction I composition

100 ng template DNA

25 pmol P60F

25 pmol HinR
25 mM dNTPs
5.0 μl 10x reaction buffer
sterile ddH_2O up to 50 μl
1.0 μl pfu Turbo DNA polymerase (2.5U)

Thermal cycling parameters

Segment	Cycles	Temperature	Time
1	1	95°C	30 sec
		48°C	30 sec
		68°C	30 sec

Reaction II composition

100 ng template DNA
25 pmol P60R
25 pmol EcoF
25 mM dNTPs
5.0 μl 10x reaction buffer
sterile ddH_2O up to 50 μl
1.0 μl pfu Turbo DNA polymerase (2.5U)

		95°C	30 sec
2	28	55°C	30 sec
		68°C	2.0 min
3	1	68°C	5.0 min
4	1	4°C	hold

Reaction III composition

2.0 μl of product of PCR I
2.0 μl of product of PCR II
25 mM dNTPs
25 pmol HinR
25 pmol EcoF
5.0 μl 10x reaction buffer
sterile ddH_2O up to 50 μl
1.0 μl pfu Turbo DNA polymerase (2.5U)

Thermal cycling parameters

Segment	Cycles	Temperature	Time
1	1	95°C	1.0 min
2	30	95°C	30 sec
		55°C	30 sec
		68°C	2.0 min
3	1	68°C	5.0 min

1.2.2.5 Overexpression of proteins in *E. coli* and purification

Recombinant plasmid constructs harbouring genes, which encode different fragments of pRb, were generated by PCR amplification followed by cloning into desired expression vectors (Table 1). *E. coli* transformants consist of desired recombinant plasmid were selected against appropriate antibiotics. Test expressions were performed at numerous conditions to identify the optimal condition where heterologous protein expression levels and their solubilities were reasonably high. Later, large-scale

production of recombinant proteins from *E. coli* were carried out by culturing cells at previously optimised conditions followed by purification using appropriate biochemical methods. Recombinant proteins were purified to homogeneity using various chromatographic techniques. Native proteins were obtained after removal of the affinity tag by proteolytic digestion and subsequent separation of an untagged protein from the affinity tag. *E. coli* expressed and purified native proteins were characterised by subjecting to immunoblotting and N-terminal amino acid analysis. Folding status and the secondary structural content of proteins were monitored by NMR and CD spectroscopy.

1.2.2.5.1 Affinity chromatography, gel filtration chromatography and ion exchange chromatography

We have used Ni-NTA affinity chromatography to fractionate His tagged recombinant proteins. Cellular lysates of one-litre *E. coli* cultures were incubated with 2 ml of 50% Ni-NTA slurry (Qiagen) equilibrated in Ni-NTA lysis buffer. Protein bound resin was washed with Ni-NTA wash buffer and then eluted with Ni-NTA elution buffer (see materials). Contaminant proteins that were copurified along with the recombinant protein were separated using gel filtration chromatography followed by ion exchange chromatography. Gel filtration chromatography separates molecules according to their size and shape. Superdex™75 prepgrade, Superdex™200 prepgrade columns (Pharmacia) were used for purifying proteins during this study. Ion exchange chromatography separates proteins according to their net charge. Mono S (cation exchange) as well as Mono Q (anion exchange) column purifications was performed during this study. Purification parameters for each column were chosen based on the extent of purity of protein to be fractionated and the isoelectric point of the protein to be purified from other contaminant proteins.

1.2.2.5.2 SDS-polyacrylamide gel electrophoresis

SDS-polyacrylamide gel electrophoresis under denaturing and reducing conditions can largely be used to separate proteins based on mass. Mass of desired proteins worked on during this study and the effectiveness of protein purification scheme were analyzed by this method. Protein samples to resolve on SDS-PAGE were prepared by addition of 5x sample buffer (10% SDS, 1.5 M β-mercaptoethanol, 250 mM tris-HCl pH 6.8, 50% glycerol and 0.5% bromophenol blue) to the final concentration of 1x followed by incubation for 5 min at 98°C. Denatured protein samples were loaded in the wells of

a slab. For the present study, separating gels were used with 10% or 12% polyacrylamide and staking gels containing 5% polyacrylamide (Sambrook et al, 1989). Electrophoretic separations were always performed by applying a constant current of 125 V in the tris-glycin (25 mM tris, 250 mM glycin (pH 8.3), 0.1% (w/v) SDS) electrophoresis buffer.

1.2.2.5.3 Staining methods to detect proteins in gels

All proteins purified during this study were separated on SDS-PAGE gels and detected by staining with coomassie blue. Proteins resolved on polyacrylamide gels were simultaneously fixed and stained in the coomassie staining solution (Sambrook et al, 1989). After rinsing the gel briefly in water, the gel was distained in the destaining solution, which eliminates the blue background while the proteins retain the blue colour. Gels were dried and/or photographed for further analysis.

Proteins of low quantity (0.2-0.6 ng) were detected by silver staining method, which is 50 to 100 times more sensitive than coomassie staining. The silver staining procedure described below is developed based on the method of Heukeshoven et al. 1985.

- 1 × 30 min — fixing solution
  - 40 ml ethanol
  - 10 ml acetic acid
  - dd H_2O to 100 ml
- 1 × 30 min — sensitising solution
  - 30 ml ethanol
  - 6.8 g sodium acetate
  - 0.2 g $Na_2S_2O_3.5H_2O$
  - 0.5 ml 25% glutaraldehyde
  - dd H_2O to 100 ml
- 3 × 10 min — dd H_2O
- 1 × 30 min — silver solution
  - 0.25 g silver nitrate
  - 40 µl of 37% formaldehyde
  - dd H_2O up to 100 ml
- 2 × 2 min — dd H_2O
- 1 × 3 min — developing solution

	2.5 g Na_2CO_3 (anhydrous)
	20 μl of 37% formaldehyde
	dd H_2O
• 1 × 10 min	stopping solution
	1.5 g Na_2EDTA (sodium salt of EDTA)
	dd H_2O to 100 ml
• 5 × 5 min	dd H_2O
• 1 × 30 min	preserving solution
	30% (v/v) ethanol
	4% (v/v) glycerol

1.2.2.6 Methods to express pRb in insect cells

1.2.2.6.1 Establishment of insect (*Sf9*) cell lines

The *Sf9* (Spodoptera frugiperda) cell lines, which double in every 18 – 24 h were grown in Sf-900 II SFM media supplemented with 1% antibiotic-antimycotic liquid and 5% fetal bovine serum. The cells were maintained in an incubator at 27°C. When the cells reached confluency healthy cultures of monolayer *Sf9* cells were maintained by sub culturing 1:3 ratio.

1.2.2.6.2 Cotransfection

Recombinant baculovirus was prepared by cotransfection followed by viral amplification. ~2 x 10^6 cells were seeded onto each 60 mm tissue culture plate with an initial cell density of 50 –70% confluency and allowed the cells to attach to the plate. 0.5 μg of BaculoGold DNA (Pharmingen) and 5 μg of a recombinant baculovirus transfer vector containing the insert were mixed well by vortexing and then the mixture was incubated for 5 min at 27°C. Thereafter, 1 ml of transfection buffer B was added to the mixture. A positive control for cotransfection was prepared as before using 2 μg of the pVL1392-XylE (Pharmingen) control plasmid instead of the recombinant baculovirus vector. Medium was aspirated off from cells that were previously allowed to attach the plate and replaced with 1 ml of the transfection buffer A. Two plates of cells in 1 ml each of the transfection buffer A were used as an experimental and a positive control cotransfection plate. *Sf9* monolayer cells were used as a negative control.

The previously prepared transfection buffer B/DNA mix was then added dropwise to the experimental cotransfection plate. After every 3-5 drops, the plate was gently rocked to mix the drops with the medium. A similar procedure was followed with the positive control. Later all plates were incubated at 27°C for 4 hrs. The medium was removed after 4 hrs from the experimental and positive control cotransfection plates and 3 ml fresh medium was added to each plate. All plates were incubated at 27°C for 4–5 days. After 4 days, the plates were checked for signs of infection. Infected cells appeared larger with enlarged nuclei than uninfected cells. After 5 days, the supernatant of the positive control and experimental cotransfection plates were collected and assayed for cotransfection efficiencies by the end-point dilution assay.

1.2.2.6.3 Endpoint dilution assay (EPDA)

1×10^5 *Sf9* cells per well were seeded and allowed to attach firmly on a 12-well EPDA plate. 100, 10, 1 and 0 µl of the recombinant virus supernatant (obtained five days after the start of transfection) were added to separate wells. This procedure was repeated for the positive control also. All plates were incubated at 27°C for three days. After incubation, infected cells were differentiated from uninfected once based on the enlargement of nucleus of infected cells.

1.2.2.6.4 Preparation of high titer viral stock

2×10^7 *Sf9* cells were seeded on a 15 cm plate and allowed to attach for 15 min. Later, cells were added with 100 µl of a low titer recombinant viral stock and then incubated at 27°C for 3 days. After 3 days of incubation, signs of infection were checked as before. Next, the supernatant from the plates were harvested by spinning down the cellular debris in a tabletop centrifuge at 10,000 xg. The virus supernatant was stored at 4°C in a sterile tube and covered with foil to protect against light. Later, large-scale virus amplification was carried out and the stocks were stored at 4°C for further applications. The presence of the gene in the amplified virus titer was checked by isolating DNA from baculovirus.

1.2.2.6.5 Isolation of DNA from Baculovirus

750 µl of an occlusion negative cell suspension was transferred to a micro centrifuge tube and centrifuged at 5,000 rpm for 3 min at room temperature. To the supernatant

750 μl of ice cold 20% PEG in 1 M NaCl was added, mixed and incubated on ice for 30 min. The viral particles were pelletted by centrifuging at maximum speed for 10 min at 4°C. Pelleted viral particles were centrifuged again at maximum speed for 2 min and the residual supernatant was aspirated off. Thereafter, the pellets of viral particles were resuspended in 100 μl of TE buffer. Plasmid DNA was isolated from viral particles using Easy-DNA kit (invitrogen) following the manufacturers instructions. Presence of the gene of interest was identified by PCR amplifying the isolated plasmid DNA with forward and reverse primers designed against up and downstream sequences of the gene of interest.

1.2.2.7 Western blotting

Crude extracts and purified proteins were heated in the SDS-PAGE sample buffer and then resolved on 10% and sometimes 12% SDS-PAGE. Protein samples resolved on SDS-PAGE were electroblotted onto nitrocellulose membrane (Amersham Pharmacia, Germany) according to the procedure described in Sambrook et al, 1989. The protein blotted membrane was blocked with 1% skim milk (1% milk powder dissolved in PBST buffer), and then incubated with primary antibodies (1/1000 dilution in 1% skim milk) either one hour at room temperature or 12 to 14 hrs at 4°C. Monoclonal antibodies raised against human native pRb were used to immunoprecipitate the Rb protein and its fragments, whereas polyclonal antibodies raised against human p19 were used to detect p19 and its cleavage products. Excessive primary antibodies were washed thoroughly in TBST buffer and then the antigen bound primary antibodies (IgG) were probed with alkaline phosphatase linked secondary antibodies for one hour at room temperature. Secondary antibodies were used at 1/2000 dilution in TBST buffer containing 1% milk powder. Excessive secondary antibodies were thoroughly washed with TBST. Thenceforth, the membrane was developed with a substrate solution of carbonate buffer (0.1 mol/l $NaHCO_3$, pH 9.8 and 1.0 mmol/l $MgCl_2$) containing 0.35 mmol/l 5-bromo-4-chloro-3-indolyl-phosphate and 0.37 mmol/l P-nitroblue tetrazolium chloride for about 20 min. Broad range molecular mass standards (NEB, Germany) were used to estimate the molecular mass of the immunoprecipitated protein bands.

1.2.2.8 EKMax digestion

The recombinant pRb was digested with entirokinase to remove hexahistidine-tag. 2 mg of the protein was digested with one unit of EKMax (invitrogen) in 50 mM tris buffer pH 7.6, supplemented with 150 mM NaCl, 3 mM DTT, and 3 mM $CaCl_2$. The reaction was carried out at 12°C for 10-12 hrs.

1.2.2.9 N-terminal amino acid sequence analysis

The N-terminal sequence of proteins purified during this work was obtained by Mr. Reinhard Mentele using Edman degradation method, with the aid of an automated protein sequencer (MPI for Biochemistry, Martinsried).

1.2.2.10 CD spectroscopy

Ms. Weyher-Stingl Elisabeth (Department of Bioorganic Chemistry, MPI for Biochemistry, Martinsried) was collected CD spectrum on a jasco J-715 spectropolarimeter using 0.1-cm path length cuvette. The protein concentration was estimated according to Beer-Lambert Law. The spectrum was converted to mean residue ellipticity after correcting with the corresponding buffer (50 mM Tris, 150 mM NaCl, 3 mM DTT, pH 7.6) spectrum obtained in the same way.

1.2.2.11 1D-^{1}H and 2D-^{15}N HSQC experiments

0.2 to 0.8 mM protein samples in 10% D_2O was used to measure 1D proton and 2D ^{1}H-^{15}NHSQC spectra. All 1D and 2D spectra were acquired at 300K on Bruker DRX-600 and Bruker AV-900 spectrometers. HSQC spectra were recorded with 128 increments in the indirect ^{15}N dimension with a number of scans varying from 128 to 1024 depending on the concentration of the sample. XWINNMR (Bruker) and Sparky (T.D Goddard and D.G Kneller) programmes were used for processing and analysis of spectra.

1.2.2.12 In vitro binding assays

Pull-down assays and binding studies using NMR were performed to confirm physical interactions between pRb and MyoD.

1.2.2.12.1 Pull-down assays

The “bait” protein (MyoD) with the His–tag was allowed to bind to the Ni-NTA column. Prey (pRb) with an enzymatically cleaved tag was applied over Ni-NTA column saturated with the bait. The complex was eluted with 250 mM imidazole after thorough washing. Fractions obtained were checked on SDS–PAGE.

1.2.2.12.2 NMR aided binding studies

Selectively labelled pRb was mixed with the E. coli purified MyoD or chemically synthesized E7 peptide containing LxCxE motif and then the ^{1}H-^{15}N NMR spectra were acquired in 10% D_2O on a Bruker 600 MHz spectrometer. Molecular interactions were monitored based on the changes in positioning of the ^{1}H-^{15}N resonances in the ^{1}H-^{15}N HSQC spectrum upon addition of the partner protein.

1.3 Results and Discussion

1.3.1 Results

1.3.1.1 Pilot expressions of full-length pRb

The Rb gene that encodes a full-length pRb was cloned under the T7 promoter using a standard PCR based cloning (see Methods). The recombinant plasmid with the Rb gene was transformed into different *E. coli* strains (see Materials), each of which has its own advantage for heterologous protein expression. Expression levels of the full-length pRb in *E. coli* were tested by performing pilot expressions at different conditions such as growing cells at numerous temperatures, in different nutrient media, inducing the expression of the recombinant protein with the varying concentrations of an inducer and so on. Western blots of these experiments showed multiple pRb bands of very low intensity.

1.3.1.2 Expression and purification of the large pocket region of pRb

1.3.1.2.1 Construction of recombinant vectors

The open reading frame (ORF) of the large pocket region of pRb (aa 379 to 910) was subcloned into pTrc, pBAD, and pET prokaryotic expression vectors. All clones were confirmed by sequencing (Medigenomix). The pTrc vector permits expression under the Trp/Lac promoter whereas the pBAD vector under the arabinose promoter. Both constructs introduce a hexahistidine tag at the N-terminus of the recombinant protein. The pGEX2T construct was a kind gift from Dr. Wen L. Dong, Angewandte Tumorvirologie, Deutsches Krebsforschungszentrum, D-69120, Heidelberg, Germany.

Optimal expression conditions were identified by performing a series of small-scale expression trials with each of the above constructs at various conditions after transforming into different *E. coli* strains (see Materials). pRb exhibited better expression under the Trp/Lac (pTrc) hybrid promoter at 23°C.

1.3.1.2.2 Maxi prep of pRb (large-pocket) from 10 liter *E. coli* cultures

Using a single colony of the BL21 (DE3) Star cells harbouring recombinant pTrc vector, a 100 ml of non-induced overnight cultures were grown at 37°C. Later 100 ml of non-induced overnight cultures were subcultured in 10 liter of fresh LB medium

supplemented with ampicillin (100µg/ml) at 23°C. Recombinant protein expression was induced with 1 mM IPTG when cells reached an OD_{600} of 0.6-0.8. After induction, cultures were grown for 4 hrs. Cells were harvested by spinning at 4200 xg for 30 min and then lysed by lysozyme treatment followed by sonication. Cell debris were removed after centrifugation at 40,000 xg for 1 hr. Clear lysate containing the His-tagged pRb was used for NI-NTA affinity purification.

Ni-NTA affinity purification

The Ni-NTA spin column (Invitrogen) was equilibrated with the lysis buffer. Thereafter, the bacterial lysate containing recombinant protein was allowed to bind to the resin by batch method. Non-specifically bound proteins were washed with the Ni-NTA washing buffer and then the His-tagged protein bound to the Ni-NTA resin was eluted with the Ni-NTA elution buffer. Presence of the protein of interest was confirmed by immunoprecipitation using human pRb antibodies (Figure. 1).

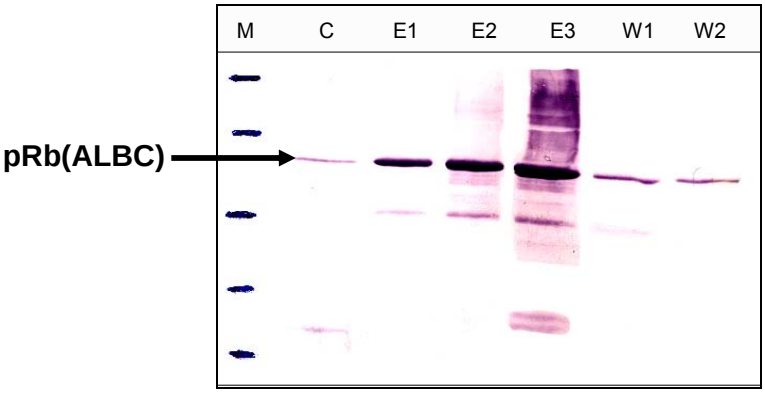

Figure. 1 Western blot analysis of Ni-NTA affinity column purified pRb (large-pocket). *15 µl samples from each step of the purification were transferred to a nitrocellulose membrane and the pRb antigens were probed with human pRb monoclonal antibodies. Immunoblot was developed with the NBT/BCIP alkaline phosphatase substrate. Lane M is molecular mass marker; Lane C, represents control pRb (received from ROCHE GmbH); Lanes E1-E3 are fractions eluted with 300 mM imidazole; Lane W1 and W2 are fractions eluted with 50 mM imidazole. The pRb (Large pocket) band is indicated with an arrow mark.*

No pRb was observed in the flowthrough, indicating that the His-tag was sufficiently exposed to allow complete binding of the recombinant pRb to the nickel–chelate matrix. Some of the pRb was seen in the non-specifically or weakly bound fraction (Figure. 1, lane 4 and 5) which suggests partial exposure of 6-histidine residue tag due to the aggregation of pRb with *E. coli* host proteins. Contaminants observed to elute at 300 mM imidazole concentration along with His-tagged pRb were proposed to possess surface exposed histidine residues, accounting for their affinity for the nickel-chelate matrix. The Protein sample eluted from the affinity column was further purified by Mono Q and then by a gel filtration column in order to eliminate impurities.

Anion exchange (Mono Q) chromatography

A mono Q (8 ml) column was equilibrated with tris buffer pH 7.5 and then allowed for the protein to bind to the resin. Non-specifically bound proteins were washed with an equilibration buffer and then resin bound protein was eluted using salt (1 M NaCl) gradient in tris buffer pH 7.5. SDS-PAGE analysis of Mono Q eluted protein samples (Figure. 2a, lanes 5-18) demonstrated copurification of contaminant proteins along with pRb, which was probably due to their similar net charge to the pRb.

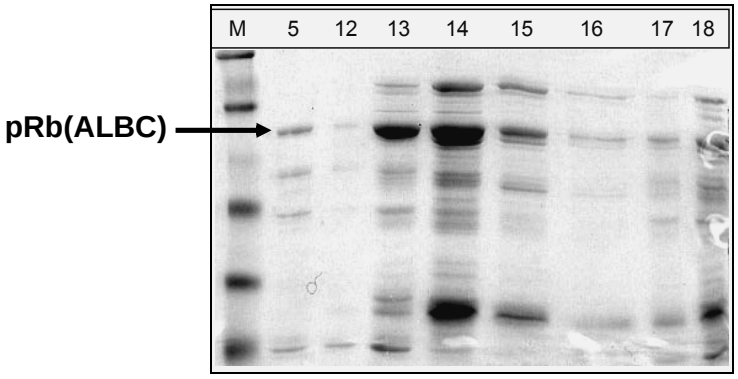

Figure. 2a 10% SDS-PAGE of Mono Q purified pRb (large pocket). *Lane M, molecular mass marker (NEB); Lanes 5, 12, 13, 14, 15, 16, 17 and 18 are fraction numbers collected during gradient elution. The Arrow mark indicates the pRb band.*

Western blot analysis of the mono Q purified protein with human pRb monoclonal antibodies showed multiple pRb bands, which suggests pRb degradation during purification and storage at 4°C (Figure. 2b). Immunoprecipitation studies with His-tag antibodies revealed that pRb degradation occurs from its C-terminus (Figure. 2c).

Figure. 2b Figure. 2c

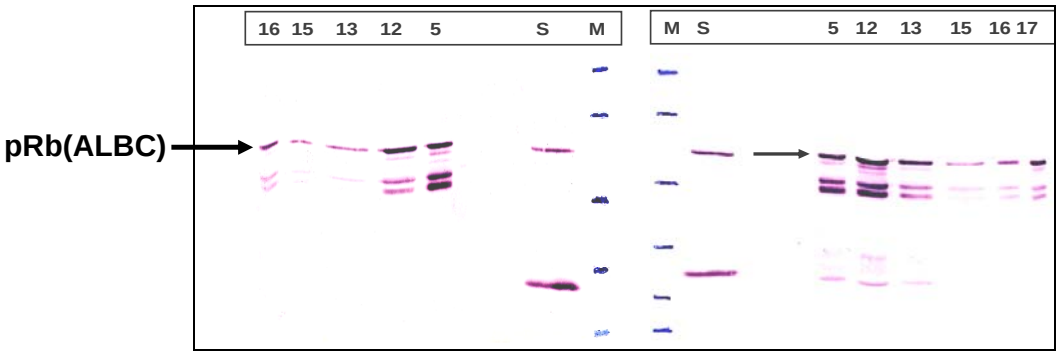

Figure. 2b Western blot analysis of the Mono Q purified protein samples with human pRb antibodies. *lane M and S are molecular mass marker and control pRb respectively; lanes 5, 12, 13, 15 and 16 are fraction numbers.* ***Figure. 2c Immuno-precipitation studies using His-tag antibodies.*** *Other details are as in Figure. 2b*

Gel filtration chromatography

Mono Q purified samples were passed through the superdex 75 gel filtration column. Figure. 3, shows the western blot of pRb purified from size exclusion chromatography. The pRb was nearly pure, however minor degradation is visible.

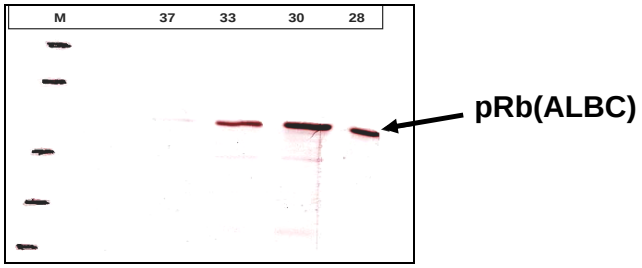

Figure. 3 Western blot of pRb purified from gel filtration chromatography. *lane M, represents molecular weight marker; Lanes 37, 33, 30 and 28 are fractions collected during purification.*

Structural integrity of the pRb large pocket was checked by a 1D proton NMR spectrum (Figure. 4). The spectrum shows partial signal dispersion at the aliphatic region (between +1.0 and -1.0 ppm) and at a region from 8.5 to 11 ppm, which suggested that the *E. coli* purified pRb (large pocket) was partially unfolded.

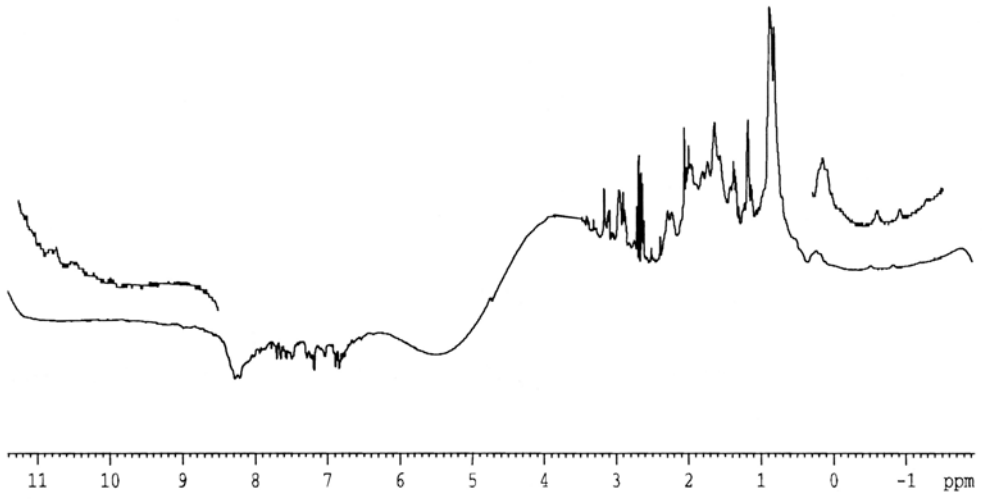

Figure. 4 The 1D proton spectrum of the pRb large pocket. *The highlighted regions are indicative for folded protein structures.*

1.3.1.3 Expression and purification of pRb (large pocket) from baculovirus

98% viable sf9 cells with a cell density of 2×10^7 cells/ml were seeded into a spinner flask. One liter of cells were infected with 10 ml of a hi-titer recombinant virus and allowed cells to grow at 27°C. After 72 hrs incubation, viral infected cells were harvested by centrifuging at 6,000 rpm for 30 min at 4°C. The pellet was resuspended in the Ni-NTA lysis buffer supplemented with the protease inhibitor cocktail and 10 mM β-ME. After sonication, cell debris were removed by centrifugation at 45,000 $\times$g for 90 min, at 4°C. Ni-NTA affinity purification performed with supernatant (lysate) resulted in copurification of pRb along with several impurities. Eluates of the Ni-NTA affinity column were pooled up and subjected to the cation exchange (mono Q) column chromatography followed by size exclusion chromatography. This whole process of purification resulted in purifying pRb (large pocket) up to 85% homogeneity.

1.3.1.4 Expression and purification of the small pocket of pRb from 4 liter *E. coli* cultures

The Rb gene that encodes the small pocket region of pRb spanning amino acids from 379 to 772 was subcloned into different prokaryotic expression vectors (see Materials). Through test expressions, pTrc construct was identified as the best construct to be used for pRb expression and purification. BL21 (DE3) Star cells carrying the pRb small pocket expression vector were cultured at 23°C. Recombinant protein expression

was induced with 1 mM IPTG. After cell lysis, His-pRb was purified using Ni-NTA affinity column chromatography followed by ion exchange chromatography and gel filtration. Figure. 5, shows a 10% SDS-PAGE of the anion exchange column indicating coelution of the *E. coli* host proteins along with pRb.

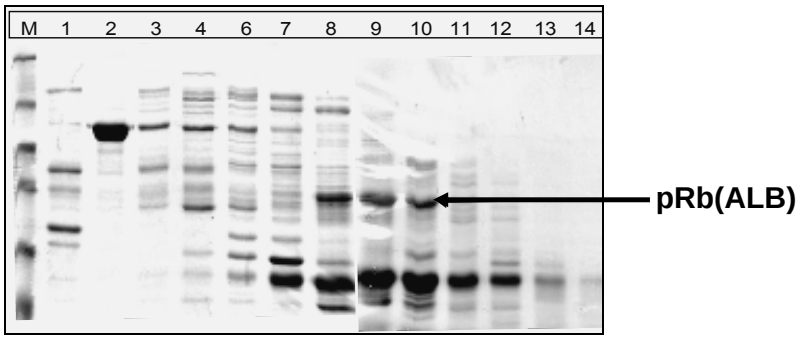

Figure. 5 12% SDS-PAGE of fractions eluted from an anion exchange column. *Lane M, molecular weight marker; lanes 1 to 14 are fraction numbers. Bands corresponding to pRb are indicated with arrow mark.*

An anion exchange purified protein was further fractionated by passing through a S-200 Gel filtration column (Figure. 6, lanes 1 to 4). SDS-PAGE analysis of pRb showed nearly pure pRb after gel filtration.

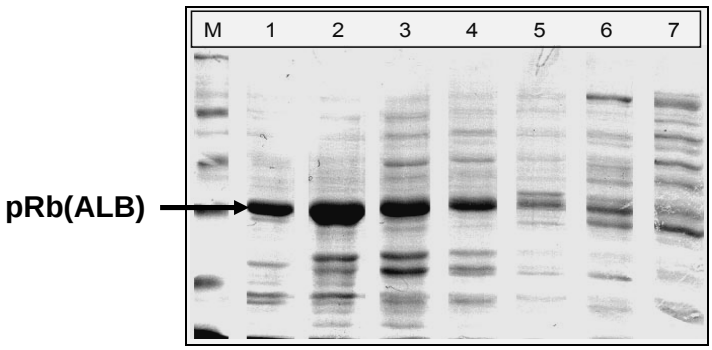

Figure. 6 12% SDS-PAGE of pRb (small pocket). *lane M, protein mass marker; lanes 1 to 7, fraction numbers.*

The *E. coli* purified pRb (small pocket) was characterized by immunoprecipitation studies (Figure. 7).

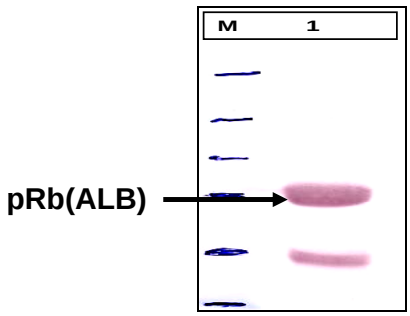

Figure. 7 Immunoblott analysis of the E. coli purified pRb (small pocket). *After storing at 4°C for five weeks, the protein was transferred to a nitrocellulose membrane and then antigens were detected with human pRb monoclonal antibodies. Lane M, represents molecular weight standards; lane 1 is human pRb purified from E. coli.*

Figure. 7, Lane 1 shows an interaction of the *E. coli* purified protein with human pRb monoclonal antibodies. A low molecular weight band is visible in addition to the expected pRb band. These results suggest that the protein that we purified in this study was pRb, which slowly degrades during storage at 4°C.

1.3.1.5 Expression and purification of the A/B pocket of pRb

The flexible loop between A and B domains of pRb (aa 578 to 644) was reported to effect its crystallization. Several earlier studies have showed that this loop has hardly any role in Rb involved protein protein interactions. We have deleted this loop for these reasons and named the construct as the A/B pocket of pRb. The deletion of the loop was achieved by oligonucleotide assisted polymerase chain reactions (see the Methods for details of oligos and thermal cycling parameters used for deletion mutagenesis and a strategy for deletion mutagenesis). PCR based deletion mutagenesis resulted in an open reading frame of the Rb gene containing desired deletion mutation. This ORF of Rb was cloned into plasmids containing the N-terminal GST tag and a His-tag (see Materials). GST tag increases solubility of the recombinant protein and both affinity tags aid in the separation of a desired protein from large number of contaminating molecules present in the crude extracts. DNA sequencing results of different plasmid constructs showed that the Rb ORF was cloned inframe to the *E. coli* translation initiation and termination signals.

In order to determine maximum expression efficiency, pilot expressions of the A/B pocket in different *E. coli* strains were performed at various conditions. The A/B pocket of pRb was expressed at high levels under His-tag, whereas the GST fused pRb (A/B) expressed at low levels. High expression of pRb (A/B) was seen in all *E. coli* strains at 37°C. However, pRb expressed at 37°C was found insoluble. Culturing cells at low temperature showed no effect on pRb solubility.

Increased solubility of pRb was seen when *E. coli* cells harbouring pRb expression vector (pRSET) were cultured in the presence of 10 mM potassium phosphate buffer pH 7.2 and 1 mM $MgSO_4$. The buffer keeps the pH of the cell growth medium (LB-medium) constant and provides physiological conditions, whereas Mg^{2+} ions assist in protein folding. Dying of cells after induction of pRb was observed, which allowed us to assume that pRb may be toxic to *E. coli* cells. By using BL21 Star (DE3) plysS cells as an expression system and growing cultures in the presence of 1% glucose, we could get good yields of pRb in a soluble form. The BL21 Star (DE3) plysS strain contains an additional plasmid, which encodes lysozyme. Lysozyme keeps the basal level expression of genes, whose expression is regulated by T7 RNA polymerase, low. Glucose also helps in inhibiting the basal level expression, which is essential for the expression of toxic proteins. After carrying out a series of pilot expressions, we found that the BL21 Star (DE3) plysS *E. coli* strain is the best strain for the pRb expression, and an LB medium supplemented with 10 mM potassium phosphate buffer pH 7.2, 1 mM $MgSO^4$ and 1% glucose as a growth medium to be used. Growing cells at 37°C up to an OD_{600} of 0.3 to 0.4 and inducing for pRb expression with 2 mM IPTG at 21°C when cells reached to log phase (0.76-0.8), and then allowing the recombinant protein expression at 14°C for 12 hrs resulted in high yields of pRb in a soluble form.

1.3.1.5.1 Purification of the A/B pocket of pRb

100 ml of overnight cultures of BL21 Star (DE3) plysS transformants were grown at 37°C. 17 ml of the overnight culture was subinoculated into a liter fresh LB medium (1:60 ratio). Rb expression cultures of *E. coli* were prepared by growing cells at conditions that were standardized previously. Expression cultures were harvested by spinning at 4200 xg for 30 min and then cells were lysed by lysozyme treatment followed by sonication. After removing cell debris by centrifuging at 40,000 xg for one hr, pH of the cell lysate was readjusted to 8.0 that help in an efficient binding of the His-

tagged protein to the nickel chelated matrix. Ni-NTA affinity purification was performed by allowing the His-tagged protein to bind to the Ni-NTA matrix, equilibrated with the lysis buffer, followed by washing non-specifically bound proteins, and then eluting the nickel bound His -tagged protein with a 250 mM imidazole gradient. The Ni-NTA purification profile and SDS-PAGE analysis is shown in Figure. 8a and 8b. Affinity purification results indicate that the His-tagged pRb is completely bound to the Ni-NTA resin (Figure. 8b, lane FT) and some of it was aggregated with *E. coli* proteins (Figure. 8b, lane WF). Figure. 8b, lanes 1-8 demonstrates the elution of few contaminant proteins along with pRb.

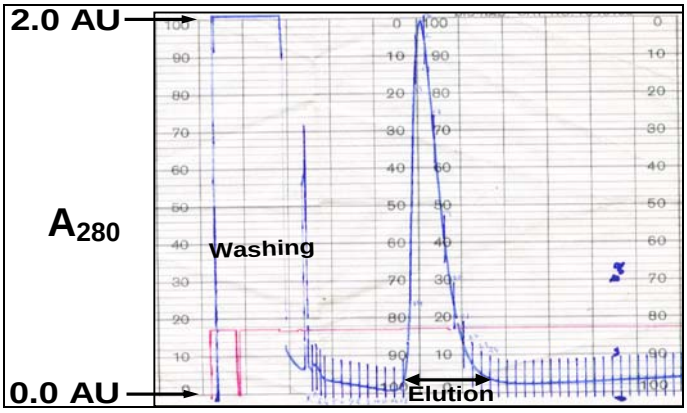

Figure. 8a A chart recorder chromatogram showing the Ni-NTA affinity column purification profile of pRb (A/B). *Peaks corresponding to the non-specifically bound protein and His-tagged pRb are labelled as washing and elution, respectively.*

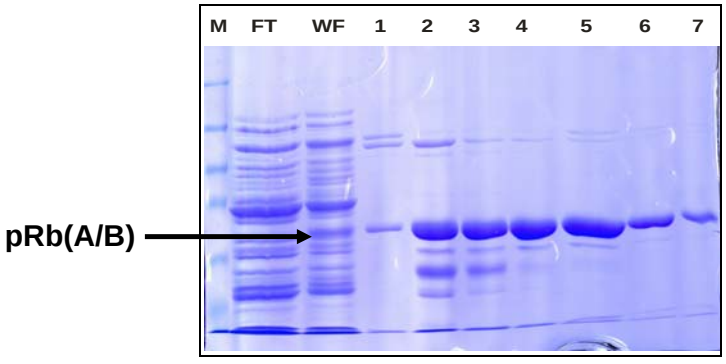

Figure. 8b 12% SDS-PAGE gel showing Ni-NTA affinity purification scheme. *Lane M, contains pre stained protein mass markers (NEB); Lane FT is flowthough; Lane WF is a fraction collected during washing with 50 mM imidazole; Lanes 1 to 7, register fractions eluted from the Ni-NTA column.*

Ni-NTA eluted fractions containing pRb were pooled up and subjected to cation exchange (Mono S) chromatography. Proteins were allowed to bind to the cation exchange resin equilibrated with the 25 mM MES buffer pH 6.0. Non-specifically bound proteins were washed with 25 mM MES buffer pH 6.0 and then the resin bound protein was eluted with a 1 M NaCl gradient in 25 mM MES buffer pH 6.0. Figure. 2, lanes 2-8 demonstrate that the protein purified on the Mono S column was homogenous and the band migrated at ~43 kDa exactly corresponds to the theoretical mass of the His-tagged A/B pocket region of pRb.

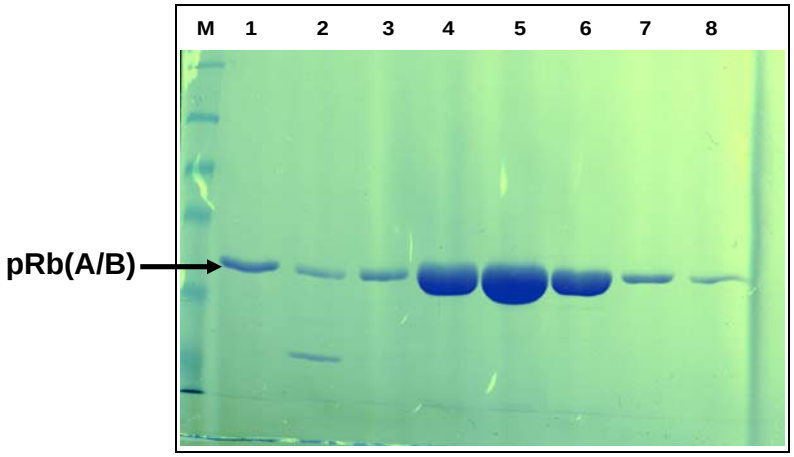

Figure. 9 12% SDS-PAGE of the mono S purified pRb (A/B). *8 µl of sample from each fraction was loaded on each well of the slab. Lane M is molecular weight standard; Lane 1 is fraction number 41 and Lanes 2-8 are fraction numbers 23, 30, 32, 36, 39, 43, and 48 subsequently.*

The mono S purified pRb was dialyzed against the dialysis buffer (see Materials) and then the His-tag was digested with Ek-Max entirokinase (invitrogen) in the presence of 3 mM $CaCl_2$ at 12°C for 10 - 12 hrs. Non-tagged pRb was separated by passing the reaction mixture through a S-75 gel filtration column. Gel filtration elution profile aligned with curves of molecular mass standards (Figure. 10) indicates that the mass of pRb after entirokinase digestion was ~39 kDa, which approximately corresponds to the calculated mass of the native A/B pocket of pRb.

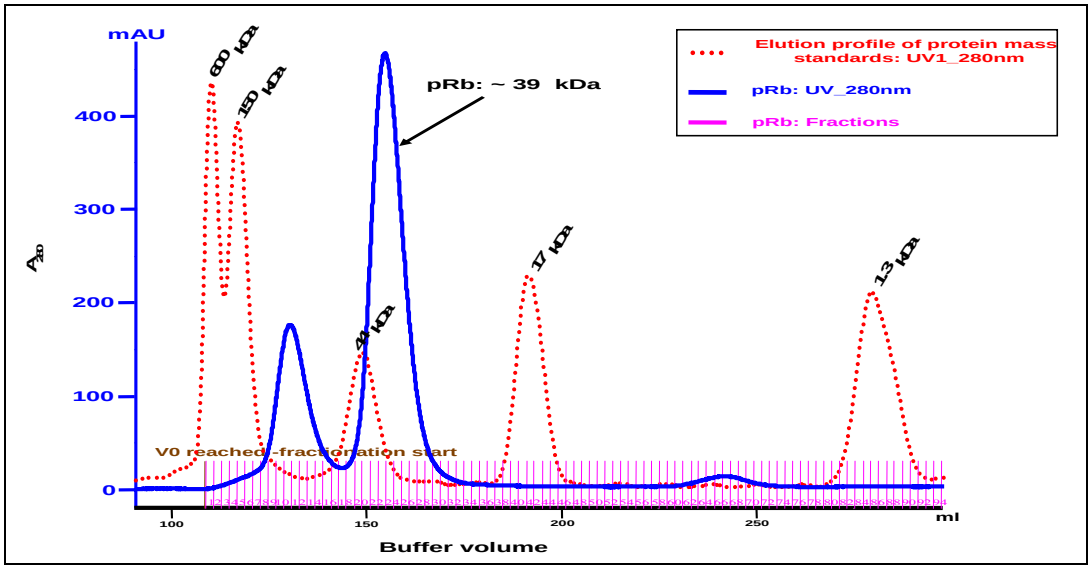

Figure.10 Purification of the native pRb (A/B) by gel filtration chromatography. *His-tagged pRb was digested with entirokinase to produce native pRb. Reaction mixture was separated on the S-75 gel filtration column. The UV absorption curves were aligned with the curves of protein mass standards. The solid blue colored line shows the UV absorption curve of pRb; the dotted line indicates the UV absorption curve of molecular mass standards; The Mass of each protein used as a standard is indicated. The Arrow mark represents the calculated mass of native pRb.*

1.3.1.5.2 Characterization of native pRb

The *E. coli* purified A/B pocket of retinoblastoma protein was characterized by Western blotting and the N-terminal amino acid analysis. Western blot analysis using human pRb monoclonal antibodies is shown in Figure. 11

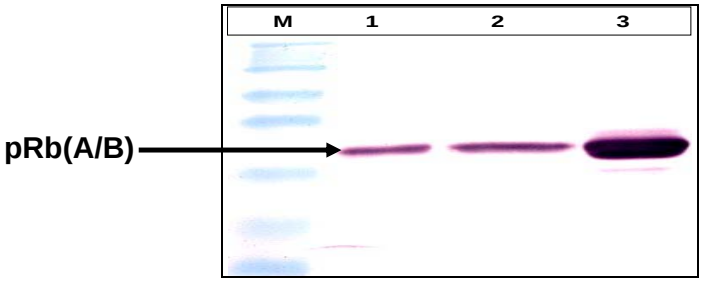

Figure. 11 Western blot of pRb (A/B). *M is molecular weight marker; lanes 1-3 are different concentrations of pRb after purification from E. coli.*

Interaction of human pRb monoclonal antibodies with the *E. coli* expressed and purified protein (Figure. 11, lanes 1-3) suggests that the protein that we purified in this study was pRb. The amino acid sequence of the protinase K digested peptides of the protein that we purified exactly matches with the amino acid sequence of human pRb (Figure. 12), which provides clear evidence that the protein under study was the human pRb.

A) MRGSHHHHHHGMASMTGGQQMGRDLYDDDDKDPSSRSAAGTMEFMNTIQQLMMILNS

SAAGT

A) ASDQPSENLISYFNNCTVNPKESILKRVK***DIGYIFK***EKFAKAVGQGCVEIGSQRYKLGVRLY

DIGYIFK

A) YRVMESMLKSEEERLSIQNFSKLLNDNIFHMSLLACALEVVMATYSRSTSQNLDSGTDLSF

A) PWILNVLNLKAFDFYKVIESFIKAEGNLTREMIKHLERCEHRIMESLAWLSDSPLFDLIKQSL

A) SLFYKKVYRLAYLRLNTLCERLLSEHPELEHIIWTLFQHTLQNEYELMRDRHLDQIMMCSMY

A) GICKVKNIDLKFKIIVTAYKDLPHAVQETFKRVLIKEEEYDSIIVFYNSVFMQRLK***TNILQYA***

TNILQYA

Figure. 12 The N-terminal amino acid sequence analysis of the E. coli purified pRb (A/B). *The amino acid sequence of pRb taken from Pub-Med is shown in (A). The N-terminal amino acid sequence of the entirokinase-digested pRb (purified from E. coli) and its homologous sequence of human pRb are marked in red colour. The amino acid sequence of the proteinase K digested pRb peptides and their homologous sequence in human pRb are underlined and marked in blue colour.*

The N-terminal amino acid sequence of the entirokinase digested pRb showed extermination of the histidine tag and production of a native protein (Figure. 12). To further ascertain whether the *E. coli* purified pRb was similar to that from human pRb, we performed a secondary structure analysis by CD spectroscopy and tertiary structural analysis by 1D ^{1}H proton NMR spectroscopy.

The CD spectrum of the *E. coli* purified pRb showed two minima at 208 and 222 nm and one maximum at 196 nm, which resemble signal seen with α-helical proteins (Figure. 13).

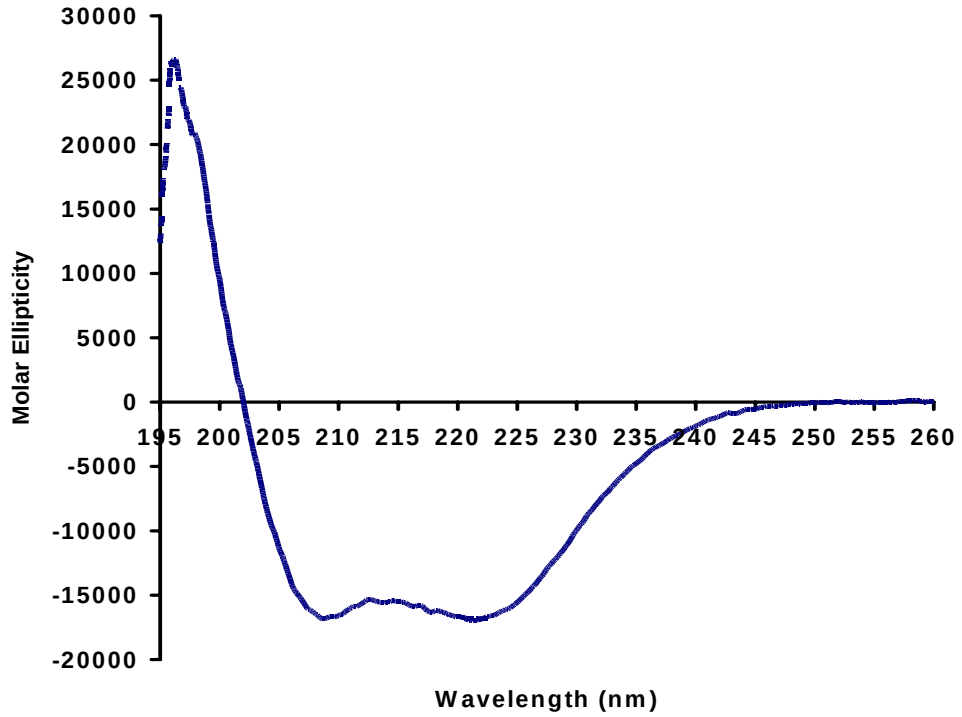

Figure. 13 Far UV CD-spectrum of pRb (A/B). *The CD spectrum of the native pRb (A/B) was measured as described under "Methods." The spectrum is shown after baseline correction.*

The crystal structure of the A/B pocket of pRb reported by Lee et al (Lee et al. 1998) revealed as it was a completely helical protein. By comparing our CD results with the existed crystal structure information, we concluded that the purified protein was a properly folded A/B pocket of human pRb.

The 1D proton NMR spectrum shows well dispersed chemical shifts at the amide region (+6.3 to 11 ppm), as well as at the aliphatic region (between +1.0 and -1.0 ppm), which indicates that the *E. coli* purified pRb (A/B) was completely structured (Figure. 14).

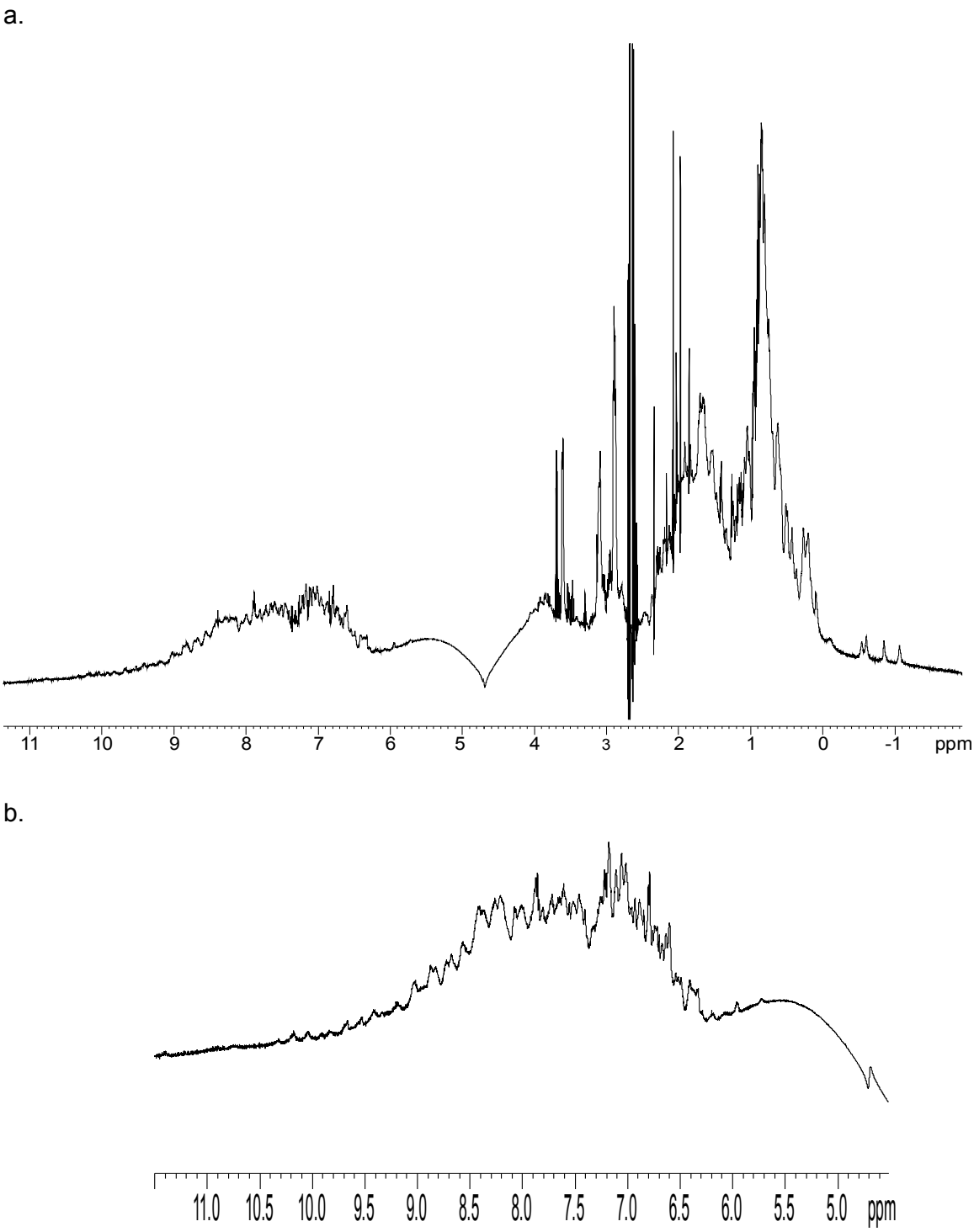

Figure. 14 1D NMR analysis of the E. coli purified pRb (A/B). *a) One dimensional proton NMR spectrum of pRb (A/B) at pH 7.2. b) The amide region of pRb (A/B). The proton spectrum of 0.8 mM protein in 10% D_2O was acquired on a Bruker AV-900 MHz spectrometer.*

1.3.1.5.3 Isotope labeling and NMR characterization of the A/B pocket of pRb

One liter of a minimal medium (see Materials for the recipe) supplemented with $^{15}NH_4Cl$ was inoculated with 20 ml of the overnight culture of BL21 Star (DE3) plysS transformants. The ^{15}N labelled pRb was expressed and purified using the same methods as for the unlabeled pRb, except that the ion exchange column purification step was replaced with the gel filtration purification. To assess whether the purified protein is labelled or not and its structural integrity, we acquired a ^{1}H-^{15}N HSQC spectrum showed in Figure. 15

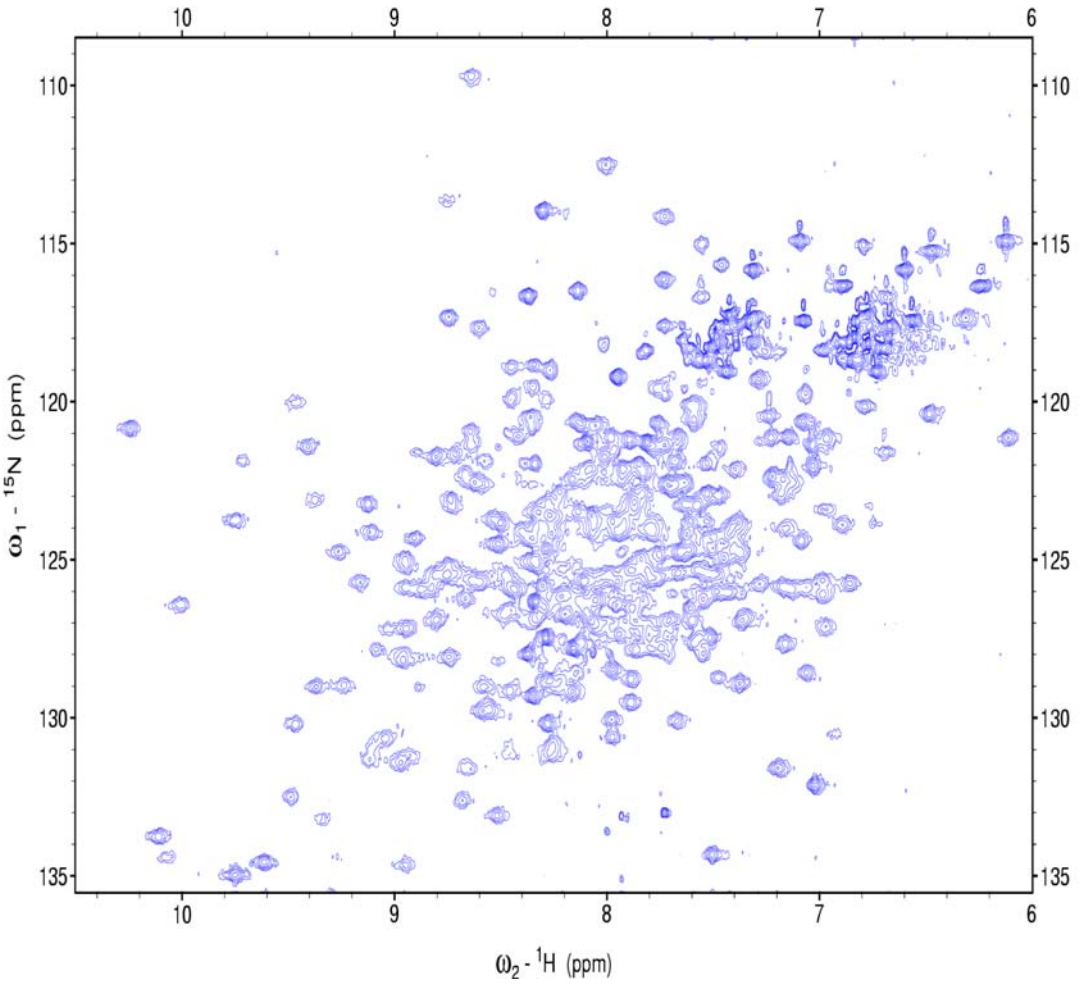

Figure. 15 ^{1}H-^{15}N HSQC spectrum of the E. coli purified pRb (A/B) at 23°C, pH 7.2. *The spectrum of ~0.8 mM pRb (A/B) in 10% D_2O was acquired on a Bruker AV-900 MHz spectrometer.*

The spectrum displays good signal dispersion in both dimensions, which is a characteristic feature of a folded protein. The spectrum also demonstrates some overlapped, broad peaks near the centre of the spectrum, which may be due to the large size of the protein.

In summary, we have developed a procedure to express large quantities of pRb (A/B) in *E. coli* in a soluble form and a three-step method to purify it in sufficient quantities for X-ray crystallography and NMR studies.

1.3.1.6 pRb and MyoD binding studies

Previous studies demonstrated that MyoD interact with the pocket domain of pRb (Gu et al., 1993). We examined these protein-protein interactions through pull-down assays and NMR binding studies (see methods for experimental details). The pull-down assay shows no pRb band (fig. 16, lanes 4, 5, 6 and 11) in the eluted fractions, which demonstrate that MyoD did not form complex with pRb.

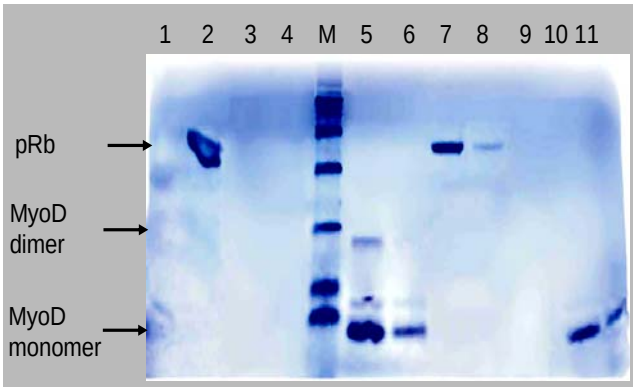

Figure. 16 In vitro binding assays. *E. coli purified pRb (ALB) was incubated with E. coli purified His-MyoD that was noncovelently coupled to Ni-NTA resin. After thorough washing the complex was eluted with 250 mM imidazole: lane 1, MyoD flow-through; 2 and 3 are pRb flow-through; 4, 5 and 6 are complex eluted with 250 mM imidazole; 7, 8 and 9 are pRb flow-through (amount of the bait was decreased to four times); 10 and 11 are complex eluted with 250 mM imidazole.*

NMR titrations were conducted on "selectively ^{15}N labelled" small pocket region of pRb (^{15}N-Lys) to investigate MyoD and pRb interactions. Movement of ^{1}H-^{15}N

resonances of pRb upon addition of E7 peptide (Fig 17a) indicates interaction of pRb with E7 peptide.

Fig. 17a

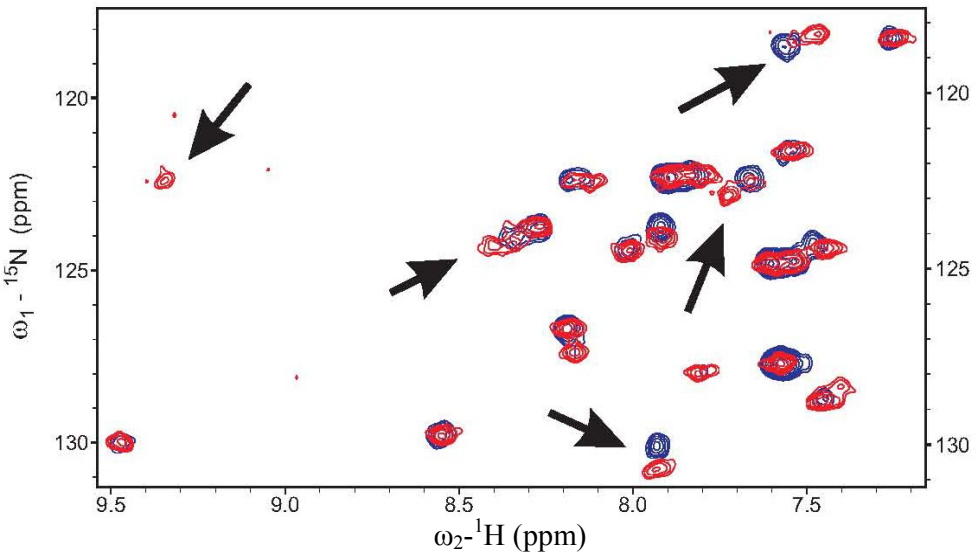

Fig. 17b

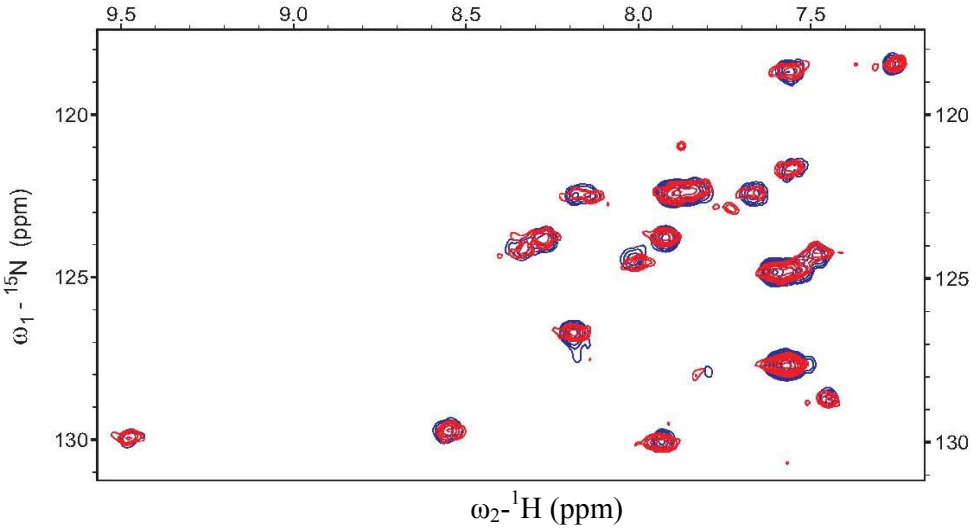

Figure. 17 NMR characterization of MyoD and pRb interactions. a) *^{1}H-^{15}N HSQC spectrum of ^{15}N-lysine labelled pRb after mixing with E7 peptide in equimolar ratio.* ***b)*** *^{1}H-^{15}N HSQC spectrum of ^{15}N-lysine labelled pRb after mixing with MyoD in equimolar ratio. Red color peaks represent ^{1}H-^{15}N resonances of pRb alone where as ^{1}H-^{15}N*

resonances of pRb in the presence of E7 peptide or MyoD are depicted in blue color. Arrows indicate resonance peaks that are moved upon protein-protein interactions.

Where as Fig 17b shows no changes in the ^{1}H-^{15}N resonances of pRb upon addition of MyoD which provide conclusive evidence that MyoD does not interact directly with pRb.

1.3.2 Discussion

Through biochemical and immunological studies, pRb has been reported to interact with viral oncoproteins and a plethora of cellular proteins such as kinases, transcription factors, and chromatin remodelling complexes. Availability of sufficient quantities of pure pRb is needed to probe all these interactions by alternative methods and to explain its mechanism of action in various functions. To date there are no reports on the purification of isotopic labelled pRb for NMR studies. Even though there are couple of reports on the production of truncated unlabelled pRb from *E. coli* (Edwards et al., 1992; Hensey et al., 1994; Huang et al., 1991), none of these expression and purification schemes were capable of providing sufficient quantities of pRb for structural investigations at laboratory scale. In this dissertation work, we report a purification scheme for the production of sufficient quantities of a homogeneous, stable and functional truncated form of labelled and unlabelled pRb from *E. coli* at laboratory scale.

As a part of current study, we have carried out *in vitro* binding studies between pRb and MyoD. Gu and co-workers have shown that MyoD interacts with pRb through its basic helix-loop-helix (bHLH) region (Gu et al., 1993) while later studies performed by three different groups failed to show interactions between MyoD and pRb *in vivo (Halevy et al., 1995; Li et al., 2000)*. However, we have performed *in vitro* binding studies to validate these contradictory reports and then to solve the pRb/MyoD complex structure. Pull-down experiments performed with pure pRb and MyoD demonstrated no interaction between pRb and MyoD. Gu at al. reported as MyoD interacts with the T-antigen binding region of pRb. On the other hand, the lysine patch located in the B-groove of pRb was reported to make direct contacts with viral oncoproteins such as SV40 large T-antigen and HPV E7 (Kim et al., 2001; Lee et al., 1998). Thus, we have

used a “selectively ^{15}N labelled” small pocket region of pRb (^{15}N-Lys) to investigate pRb/MyoD interactions. We have observed binding of E7 peptide to pRb whereas no interaction was detected between pRb and MyoD. Based on all these results we conclude that MyoD does not make physical contacts with pRb.

2 Identification of cleavage sites of calpain in the G_1 cyclin dependent kinase inhibitor $p19^{INK4d}$

2.1 Introduction

Calpains (EC 3.4.22.17) are a family of non-lysosomal, cysteine proteinases that show a Ca^{2+} dependent papain-like cysteine protease activity (Goll et al., 2003). The two ubiquitously expressed calpain forms, with proteolytic activities requiring μM and mM calcium, were identified and named as μ and m (also referred to as I and II) calpains, respectively (Dayton et al., 1981; Goll et al., 2003; Mellgren, 1980). Calpains are heterodimeric proteins, composed of a large 80-kDa catalytic subunit organized in four domains (I–IV) and a common small and 30-kDa regulatory subunit organized in two domains (V-VI). Domain II is a cysteine protease domain and contains the catalytic cysteine, histidine and asparagine residues. Domain IV is a Ca^{2+} binding domain in which five EF-hand motifs are present. The small regulatory subunit is composed of an N-terminal glycine-clustering hydrophobic region (domain V) and a C-terminal Ca^{2+} binding domain (domain VI). The hydrophobicity of the N-terminal domain (domain V) has been taken as an indication for its role in membrane anchoring (Inomata et al., 1989; Inomata et al., 1990; Kuboki et al., 1987; Kuboki et al., 1990; Lee et al., 1990; Molinari et al., 1994). Calpains have potential biological functions in apoptosis, pathology of degenerative diseases, in mediating intracellular calcium signals (Arora et al., 1996; Du et al., 1995; Spencer et al., 1995). A number of studies indicated that the calpains have a role in the cell cycle, specifically in the G_1 to S transition [reviewed in (Goll et al., 2003)]. For example, rapid loss of cyclin D levels in serum starved NIH 3T3 cells is restored by synthetic calpain inhibitors or by overexpression of an endogenous inhibitor of calpain, calpastatin (Choi et al., 1997). Calpain mediated degradation of $p21^{KIP1}$ which is a member of CIP1/KIP1 family of CDKIs had been reported in preadipocyte cell cycle progression and differentiation (Patel and Lane, 2000). However, biological role of calpain in the cell cycle regulation is still poorly understood.

Although the rules that govern calpain specificity have not yet been determined, experimental reports published so far indicate that proteolysis by calpains is limited and does not lead to small peptides suggesting that calpains may modulate functions of substrate proteins by cutting their interdomain regions (Croall and Demartino, 1991). In

this study, we attempt to characterize calpain preferred cleavage positions in $p19^{INK4d}$. $p19^{INK4d}$ is a 165 amino acid protein that comprise of ten α-helices assembled sequentially in five ankyrin repeats (Baumgartner et al., 1998) and it shares structural and biochemical properties of the other three INK4 family proteins, $p16^{INK4a}$, $p15^{INK4b}$ and $p18^{INK4c}$. The four INK4 family proteins negatively regulate the mammalian cell cycle by specifically binding and inhibiting cdk4/cdk6, which are strongly implicated in phosphorylation of the retinoblastoma tumor suppressor protein and there by in G_1-S controle (Bartek et al., 1997; Harper and Elledge, 1996; Morgan, 1995; Pines, 1996; Sherr and Roberts, 1999). Cdk inhibitors also have been implicated in terminal differentiation and senescence (Bartek et al., 1997; Ruas and Peters, 1998; Serrano et al., 1997; Sherr and Roberts, 1999). P16 inactivation by mutations is one of the most freequent defects contributing to tumorigenesis (Bartek et al., 1997; Ruas and Peters, 1998; Serrano, 1997; Sherr and Roberts, 1999). Inactivation of p19 through mutations contributes to bladder cancer (Tsutsumi et al., 1998) and, also defects in spermatogenesis in mice.

2.1.1 Aim of the project

The main aim of the project was to investigate whether $p19^{INK4D}$ would undergo proteolysis by calpain or not and if so what kind of specificity does calpain exhibit in p19 recognition and its cleavage. These studies help in understanding the probable mechanism of action of calpain in cell cycle regulation and provide information on rules governing its substrate specificity.

2.2 Materials and Methods

2.2.1 Materials

All materials used for this study were documented under “materials” section of chapter 1.

2.2.2 Methods

2.2.2.1 Proteolytic cleavage of p19 by μ-calpain

The *E. coli* expression vector containing p19 gene was obtained as previously described (Kalus et al., 1997). Proteolysis studies were carried out at 25˚C in 20 μl of

reaction mixture consisting of μ-calpain (purified from human erythrocytes (Gabrigelcic-Geiger et al., 2001) and p19 at the molar ratio of 1:50, and a calpain assay buffer (25 mM Tris-Hcl pH 7.3, 150 mM NaCl, 1 mM $CaCl_2$). After one hour incubation, the reaction was terminated by addition of the SDS-PAGE sample buffer followed by heating to 98°C for 5 min. Samples were resolved on 15% SDS-PAGE and stained with coomassie blue.

2.2.2.2 Calpain mediated proteolytic assays of p19 in the presence or absence of calcium and calpastatin

Inhibitory role of calpastatin on calpain was determined by incubating purified calpain, p19, and calpastatin domain I in the calpain assay buffer at a molar ratio of 1:50:1, respectively. Stability of p19 and calcium requirement for the calpain mediated proteolysis were investigated by performing two separate proteolytic cleavage assays of p19 incubated in the reaction buffer in the absence of calpain and presence of calcium; p19 incubated in the calpain reaction buffer in the absence of calcium and presence of calpain. All reactions were carried out for one hour and then stopped by addition of the SDS-PAGE sample buffer followed by heating to 98°C for 5 min.

Calpain treated samples were resolved on SDS-PAGE and then transferred onto the nitrocellulose membrane with the aid of semi-dry electro-blotting apparatus. Protein transfer from the gel onto the nitrocellulose membrane was carried out at 125 mV of constant current for one hour. Non-specific binding sites for immunoglobulins on the membrane were blocked with milk powder. The membrane was incubated initially with primary antibody and later with alkaline phosphatase conjugated secondary antibody. Membrane was thoroughly washed with Tris buffer and then developed by incubating with BCIP/NBT alkaline phosphatase substrate for 15 to 30 min.

2.2.2.3 N-Terminal amino acid analysis of fragments generated by calpain

Proteolytic reaction mixtures were resolved on SDS-PAGE and then transferred onto the PVDF membrane. Western transfer was carried out using semi dry electro-blotting apparatus at 125 mV of constant current for one and half hour. The protein blotted PVDF membrane was stained with coomassie blue. Coomassie stained bands were cut out from the membrane and used for N-terminal analysis by Edman degradation. Sequences obtained were used to map calpain cleavage sites and fragments generated from p19 by calpain mediated proteolysis.

2.3 Results and Discussion

2.3.1 Results

Figure 1a, (lane 1 and 4) and Figure 1b, (lane 1) shows that the p19 purified by our method was pure and not cleaved in the calpain assay buffer in the absence of calpain. Incubation of p19 with μ-calpain in the presence of 1 mM $CaCl_2$ resulted in p19 fragmentation (Figure 1a, lane 2, 3, 5 and 6). p19 was not cleaved in the presence of an endogenous calpain inhibitor, calpastatin, and calcium (Figure 1b, lane 5), or absence of calcium and calpastatin (Figure 1b, lane 4). Almost equal amount of p19 was cleaved by calpain in the presence of 5 mM (Figure 1b, lane 3) as compared to 1 mM $CaCl_2$ (Figure 1b, lane 2).

Figure 1A

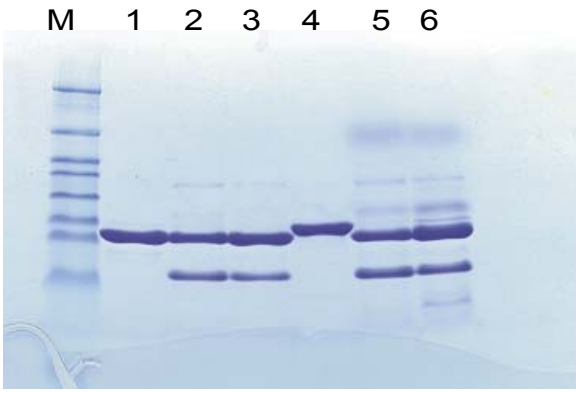

Figure 1B

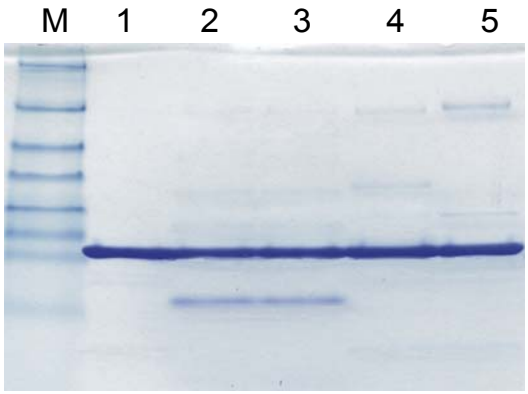

Figure 1. μ-calpain mediated proteolysis of p19. 1a) *lane M, prestained protein mass marker; lane1 and lane 4 are p19 without and with his-tag incubated in the calpain reaction buffer; lane 2, lane 5, are p19 without and with his-tag digested with calpain in the presence of Ca^{2+}, at a molar ratio of 50:1; lane 3 and 6 are p19 without and with his-tag digested with calpain in the presence of Ca^{2+}, at a molar ratio of 100:1.* ***1b)*** *calpastatin blocks calpain mediated p19 degradation. Lane M, pre stained protein mass marker; lane 1, p19 incubated in the calpain reaction buffer; lane 2 and 3 registers p19 digested with calpain in the absence of calpastatin and presence of 1 mM and 5 mM Ca^{2+} subsequently; lane 4 and 5 shows p19 digested with calpain in the absence of calpastatin and Ca^{2+} and in the presence of calpastatin and Ca^{2+} respectively.*

Figure 2, shows Western blot analysis of p19 and its cleavage products.

Figure 2

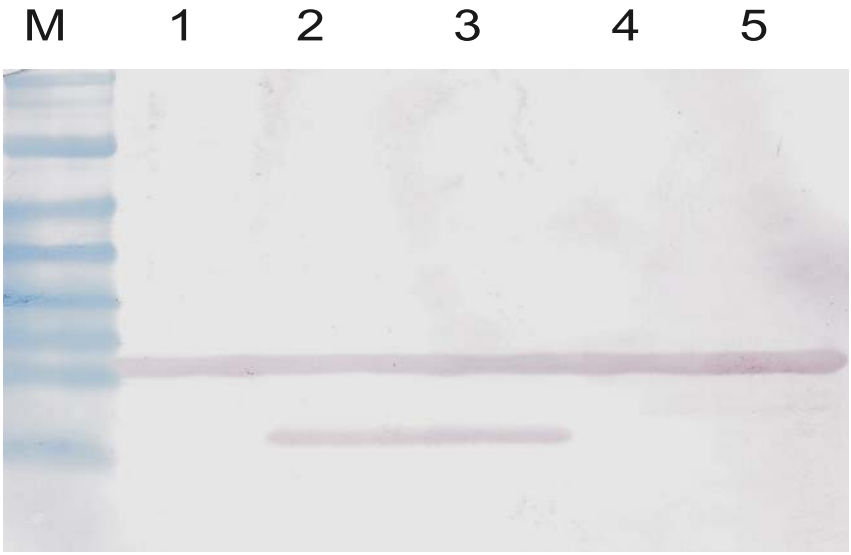

Figure 2. Western blott of p19 fragments generated by calpain. *p19 digested with calpain in the presence or absence of calcium and calpastatin, resolved on SDS-PAGE and transferred onto the nitrocellulose membrane. Non-cleaved and cleaved fragments of p19 were detected by immunoassaying with p19 polyclonal antibodies. Figure legends are as in Figure 1b.*

The p19 cleavage products blotted on PVDF membrane were subjected to N-terminal amino acid analysis by Edman degradation and the sequence of various fragments obtained were as follows: LLHREL, KQGASP, EVRRLL, ALQVMM, IHLAVQ, FLAAES. Possible calpain cleavage sites in p19 were identified and are schematically shown in Figure 3a. Fragments containing LLHREL and KQGASP as an N-terminal amino acid sequence were obtained in detectable amounts from reverse phase HPLC and hence we have concluded these two cleavage sites located between histidine 29 and arginine 30, glysine 64 and alanine 65 as major cleavage sites of calpain and remaining four fragments were obtained in low quantities and thus named as minor cleavage sites.

Figure 3A

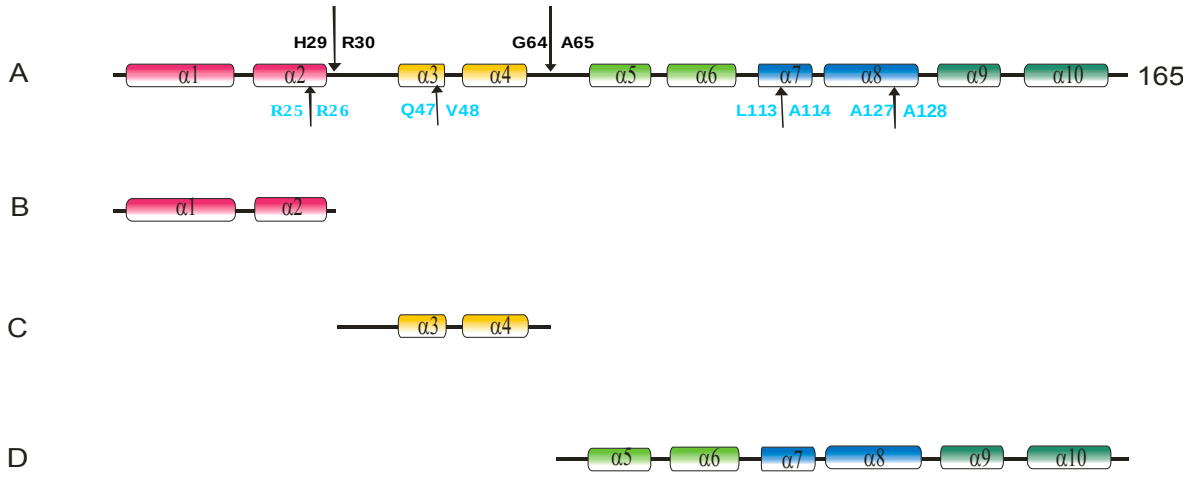

Figure 3a. Schematic representation of domain organization and calpain cleavage sites of p19. *Peptides generated from p19 in the calpain cleavage reaction were analyzed by N-terminal amino acid sequencing. Downward and upward arrows indicates major and minor calpain cleavage site subsequently. Fragments generated by calpain are schematically shown below the full-length sequence of p19.*

Figure 3b. shows the positions of the major calpain cleavage sites in the three-dimensional structure of p19.

Figure 3B

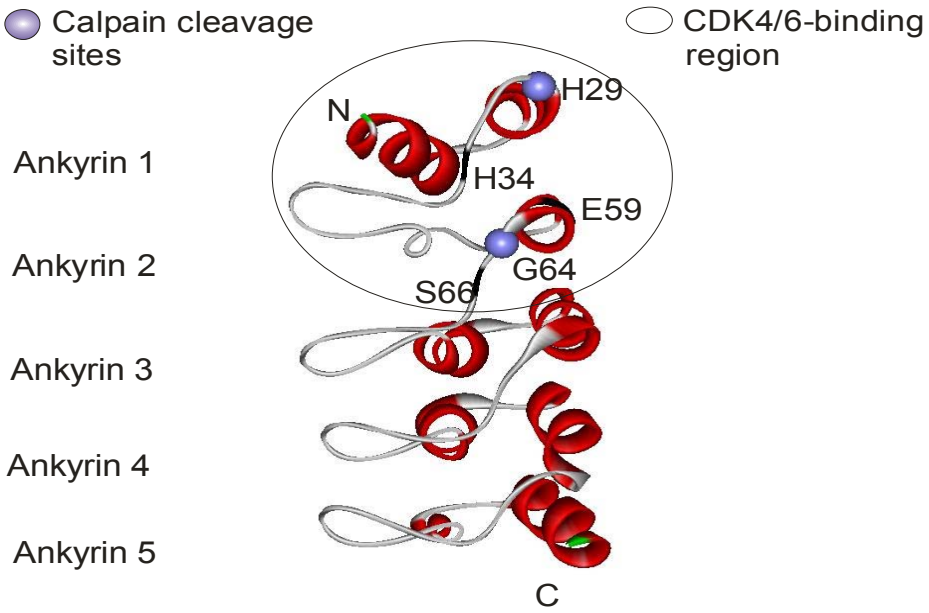

Figure 3b. Ribbon diagram, schematically depicts p19 tertiary structure and its binding region to cdk4/cdk6. p19 consist of 10 α-helices assembled as five ankyrin repeats sequentially, forming an elongated structure. Ankyrin repeat 1 and 2 bind to G_1-cdk4/cdk6, represented with a circle. The calpain cleavage sites of p19 are denoted with blue colored spheres. Flexible amino acid residues detected by NMR relaxation studies (H34, E59 and S66) are labelled and the regions corresponding to the respective amino acid residues are marked in black.

2.3.2 Discussion

Transition from the G_1 to S phase of the mammalian cell cycle is regulated by the Rb/E2F pathway (Weinberg, 1995). Cyclin D-cyclin dependent kinase-4/6 complexes phosphorylate the retinoblastoma protein (pRb), which frees E2F from the Rb/E2F complex. The freed E2F activates the transcription of genes involved in cell proliferation (Leone et al., 1998; Weinberg, 1995), p53 dependent (Bates et al., 1998; DeGregori et al., 1997) and independent apoptosis (Irwin et al., 2000). INK4 inhibitors specifically inhibit the G_1 cyclin dependent kinase mediated phosphorylation of pRb and thus the normal function of Rb/E2F pathway is deregulated. INK4 inhibitors exert their action by binding directly to cdk4/6 through their two N-terminal ankyrin repeats (Brotherton et al., 1998; Russo et al., 1998). It is interesting to see that the major calpain cleavage sites in p19 are located exactly in these two ankyrin repeats. Calpains therefore should influence the INK4 inhibitor bindings to cdk4/6 and thus may take part in the regulation of this binding *in vivo*.

There is a limited number of reports on substrate specificity of calpains and these have been reviewed by Croall and Demartino (Croall and Demartino, 1991) and more recently by Goll et al (Goll et al., 2003). Early studies suggested that the calpains preferentially cleave peptide bonds with a Leu or a Val residue in the P2 position. A more complete data, however, indicated that substrate specificity of the calpains is controlled by the conformation of polypeptide chain and not by amino acid sequence (Croall et al., 1996; Harris et al., 1988; Stabach et al., 1997). In general the literature data indicate that the calpains cleave target proteins at a limited number of sites and produce large polypeptide fragments rather than small peptides or amino acids (Croall and Demartino, 1991; Goll et al., 2003; Sasaki et al., 1984). A typical example is

provided by the m-calpain proteolysis of vimentin. Vimentin belongs to the intermediate filament (IF) family of proteins (Fuchs and Weber, 1994). All IF proteins share a common structural organization of the dimer that includes the central coiled-coil 'rod' domain flanked by the 'head' and 'tail' domains at both ends (Fuchs and Weber, 1994; Strelkov et al., 2002).

The α-helical core part is not continuous, however, but interrupted in several places, resulting in four consecutive α-helical segments that are connected by linkers. The major calpain proteolytic fragments in vimentin arise from cleavage in the unordered amino-terminal headpiece, the tail domain, and are followed by cleavage in the linker that separates two major coiled-coil domains (Fischer et al., 1986). Another example, related to our α-helical p19, is provided by α-tropomyosin, whose polypeptide is 100% α-helical. Nine of the 11 calpain cleavages in the α-tropomyosin polypeptide are in the COOH-terminal half of the molecule (Croall and Demartino, 1991). The COOH-terminal half of the helix is significantly less stable than the NH2-terminal half, again suggesting that the substrate specificity of the calpains depends on the conformation of the polypeptide, with a more open structure favouring cleavage. The p19 caplain cleavage seems to show still other features. The major calpain cleavage sites are located at the end of the second helix (α-2) of the first ankyrin repeat (His 29) and again at the end of the second helix (α-4) of the second ankyrin repeat Gly 64 (Figure 4). His 29 and Arg 30 are in the α-helical conformation, the amide proton of His 29 makes a hydrogen bond with C=O of Arg 25. Gly 64 participates in a semi-helical loop, which follows helix α-4. Both major cleavage sites are therefore located immediately after well-structured, stable α-helices. Our previous NMR relaxation measurements on $p19^{INK4d}$ showed that most of the backbone of $p19^{INK4d}$ exists in a well-defined structure of limited conformational flexibility on the nanosecond to picosecond time-scales (Renner et al., 1998). The exceptions were short stretches around residues Val 69 and Glu 129, which are flexible on this fast time scale. Also considerable amounts of slower exchange broadening were found for several residues throughout the sequence; these were located mostly in the second ankyrin repeat, and in the beginning and end of loops, connecting ankyrin repeats. Gly 64 is close to Val 69, and a minor cleavage site residue Ala 127 is close to Glu 129. However, we could not find any clear correlation between all "flexible" residues and their locations in the close neighborhood to the calpain cleavage sites. Figure 4, shows which residues are solvent exposed in p19. The His 29/Arg 30 cleavage site is

one of the most solvent exposed, however, the Gly 64/Ala 65 site is not; and therefore no correlation can again be detected.

Figure 4

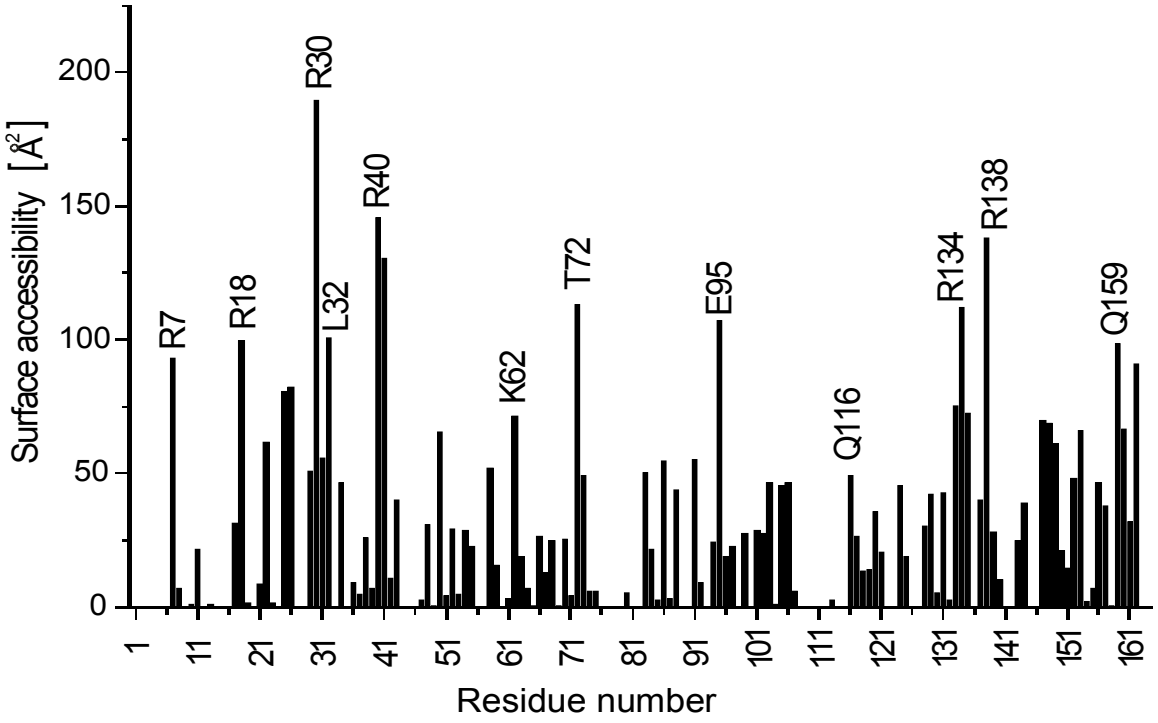

Figure 4. Surface accessibility plot of p19. The above plot indicates the surface accessibility of each residue of p19 in square angstrom units [Å^2]. The residues with higher surface accessibilities are labelled and are the most solvent exposed ones. The His29/Arg30 cleavage site is one among the solvent exposed, however, the Gly64/Ala65 site, although a calpain cleavage site, does not have a significant solvent exposed region.

In conclusion, our data seem to show new characteristics of calpain action in that calpains cleaved p19 immediately to the stable α-helical segments of the protein, but not necessarily at the residues of linker polypeptide segments that are most exposed to solvent or that have high flexibility.

3 Zusammenfassung

Das Retinoblastoma Tumor Supressor Protein pRb ist ein Phosphoprotein des Zellkerns, das als negativer Regulator der zellulären Proliferation und Apoptose fungiert und ein Promoter der Zelldifferenzierung ist. Alle seine physiologischen Funktionen wurden aufgrund seiner Fähigkeit beschrieben, mit einem Großteil der zellulären und viralen Onkoproteine zu interagieren. Detaillierte strukturelle und funktionelle Analysen von pRb wurde dadurch erschwert, dass das saubere Protein fehlte. Diese Arbeit berichtet über den Aufbau, die Expression und die Dreischrittreinigung der A/B-Taschenregion des pRb in einem bakteriellen Expressionssystem. Das Protokoll erlaubt die Produktion von 5-6 mg/l sauberem ungelabeltem pRb und 3-4 mg/l isotopen-gelabeltem pRb in einer *E. coli*-Kultur. Die molekulare Mase des gereinigten Proteins wurde aufgrund von SDS-PAGE und Gel filtration auf ca. 39 kDa geschätzt. N-terminale Aminosäurenanalyse und Westernblotuntersuchungen wurden benutzt, um das aus *E. coli* gereinigte humane pRb zu charakterisieren. Die Sekundär- und Tertiärstruktur wurden durch CD-Messungen und NMR-Spektroskopie überprüft. Die Präparation von pRB, über die hier berichtet wird, liefert ausreichende Mengen von diesem Protein für eine detaillierte funktionelle und strukturelle Charakterisierung des Reinoblasmaproteins. Das isotopen-gelabelte Protein kann benutzt werden, um die vorgeschlagenen pRb Protein-Protein-Wechselwirkungen zu überprüfen, wie auch für Strukturbestimmung und “drug-design”. Das ungelabelte Protein kann benutzt werden, um Komplexe von pRb und seiner Partnerproteine zu machen. Das Lösen der Kristallstrukturen dieser Komplexe mag den Handlungsmechanismus des pRb in verschiedenen zellulären Prozessen erklären.

Eine Anwendung dieser Arbeit ist die Untersuchung der Interaktion zwischen pRb und MyoD. MyoD gehört zu einer Gruppe von muskelspezifischen, helix-loop-helix Motif zeigende Transkriptionsfaktoren, welche essentiell für die Differenzierung von Muskelzellen in Vertebraten sind. Vorangegangene Studien zeigten daß MyoD mit der sog “small pocket domain” von pRb interagiert. Durch spezifische Binde-Essays und NMR Titrationen konnten wir mit unserer Arbeit zeigen, daß die “small pocket domain” des Retinoblastoma-proteins nicht mit MyoD in vitro interagiert, wie Vorangegangene Studien zeigten.

Calpaine sind Cysteinproteasen, die in der calciumvermittelten Signaltransduktion, der Apoptose und degenerativen Krankheiten eine Rolle spielen. Calpaine sind wichtig für die Regulation des Zellzyklus, aber Regeln, die die Calpainspaltungsspezifität erklären, sind wenig verstanden. Diese Arbeit berichtet über in vitro Untersuchungen des Schemas der Calpain-Proteolyse des $p19^{INK4d}$ Proteins, einem cyclinabhängigen cdk4/6 Inhibitors, der den Zellzyklus von Säugern negativ reguliert. Die Daten, die hier vorgestellt werden, zeigen neue Eigenschaften der Calpain-Aktion: Calpaine schneiden $p19^{INK4d}$ unmittelbar nach stabilen α-helikalen Segmenten im Protein, aber nicht notwendigerweise bei Resten der Linkerpolypeptidsegmente, die am meisten dem Lösungsmittel zugänglich sind oder die hoch flexibel sind. Dies steht im Gegensatz zu Eigenschaften der Calpaine, die im Zusammenhang mit der Spezifität der Calpaine für ihre Substrate beobachtet wurden. Es wurde ebenfalls beobachtet, dass cdk6 nicht von Calpain geschnitten wird, was impliziert, dass Calpain in den Zellzyklus eingebunden sein kann, um den regulatorischen Proteinumsatz durch Cycline und cdk-Inhibitoren zu regeln.

4 Summary

The retinoblastoma tumor suppressor protein, pRb, is a nuclear phosphoprotein that acts as a negative regulator of cellular proliferation and apoptosis, and a promoter of cell differentiation. All of its physiological functions were ascribed based on its ability to interact with a plethora of cellular and viral oncoproteins. However, detailed structural and functional analysis of pRb has been hampered by a lack of pure protein. In the presented thesis, we report the construction, expression and three-step purification of the A/B pocket region of pRb in a bacterial expression system. Our protocol allows the production of 5-6 mg of pure unlabelled pRb and 3-4 mg of isotopic labelled pRb per liter of *E. coli* culture. The molecular mass of the purified protein was estimated to be ~39 kDa by SDS-PAGE and gel filtration. N-terminal amino acid analysis and Western blot studies were used to characterize the *E. coli* purified human pRb. The secondary and tertiary structural integrity of the protein was investigated by CD and NMR spectroscopy. The preparation of pRb reported here provides sufficient amounts of this protein for a detailed functional and structural characterization of the retinoblastoma protein. The isotopic labelled protein can be used to validate proposed pRb protein-protein interactions as well as for structure determination and drug design. The unlabelled protein can be used to make complexes of pRb and its partner proteins, and solving crystal structures of these complexes may explain the mechanism of action of pRb in various cellular processes.

As an application of this work, we have probed interactions between pRb and MyoD. MyoD belongs to a group of muscle specific basic helix-loop-helix (bHLH) transcription factors that are essential for muscle cell differentiation in vertebrates. Preceding studies showed interaction of MyoD with the small pocket domain of pRb. Through pull-down assays and NMR titrations, here we demonstrate that the small pocket domain of retinoblastoma protein does not interact with MyoD *in vitro* as previous studies reported.

Calpains are cysteine proteases implicated in Ca^{2+} mediated signal transduction, apoptosis and degenerative diseases. Calpains play a role in the cell cycle regula-

tion, but the physiological function of calpains in the cell cycle and rules that govern calpain cleavage specificity are poorly understood. We report here in this thesis in vitro studies on the pattern of calpain proteolysis of the $p19^{INK4d}$ protein, a cyclin-dependent CDK4/6 inhibitor that negatively regulates the mammalian cell cycle. The data presented here show new characteristics of calpain action: calpains cleave $p19^{INK4d}$ immediately after stable α-helical segments of the protein, but not necessarily at residues of linker polypeptide segments that are most exposed to solvent or that have high flexibility, in contrast to features observed so far in the specificity of calpains for their substrates. We also observed that CDK6 is not cleaved by calpain, suggesting that calpain may be involved in the cell cycle by regulating the cell cycle regulatory protein turnover through cyclins and CDK inhibitors.

5 References

Abdelhafiz, H.A., Heasley, L.E., Kyriakis, J.M., Avruch, J., Kroll, D.J., Johnson, G.L. and Hoeffler, J.P. (1992) Activating Transcription Factor-Ii DNA-Binding Activity Is Stimulated by Phosphorylation Catalyzed by P42 and P54 Microtubule-Associated Protein-Kinases. *Molecular Endocrinology*, **6**, 2079-2089.

Ajchenbaum, F., Ando, K., Decaprio, J.A. and Griffin, J.D. (1993) Independent Regulation of Human D-Type Cyclin Gene-Expression During G1-Phase in Primary Human Lymphocytes-T. *Journal of Biological Chemistry*, **268**, 4113-4119.

Akama, Y., Yasui, W., Yokozaki, H., Kuniyasu, H., Kitahara, K., Ishikawa, T. and Tahara, E. (1995) Frequent Amplification of the Cyclin-E Gene in Human Gastric Carcinomas. *Japanese Journal of Cancer Research*, **86**, 617-621.

Akira, S., Isshiki, H., Sugita, T., Tanabe, O., Kinoshita, S., Nishio, Y., Nakajima, T., Hirano, T. and Kishimoto, T. (1990) A Nuclear Factor for Il-6 Expression (Nf-Il6) Is a Member of a C/Ebp Family. *Embo Journal*, **9**, 1897-1906.

Alcalay, M., Tomassoni, L., Colombo, E., Stoldt, S., Grignani, F., Fagioli, M., Szekely, L., Helin, K. and Pelicci, P.G. (1998) The promyelocytic leukemia gene product (PML) forms stable complexes with the retinoblastoma protein. *Molecular and Cellular Biology*, **18**, 1084-1093.

Alcalay, M., Zangrilli, D., Fagioli, M., Pandolfi, P.P., Mencarelli, A., Lococo, F., Biondi, A., Grignani, F. and Pelicci, P.G. (1992) Expression Pattern of the Rar-Alpha-Pml Fusion Gene in Acute Promyelocytic Leukemia. *Proceedings of the National Academy of Sciences of the United States of America*, **89**, 4840-4844.

Angel, P. and Karin, M. (1991) The Role of Jun, Fos and the Ap-1 Complex in Cell-Proliferation and Transformation. *Biochimica Et Biophysica Acta*, **1072**, 129-157.

Anneren, C. and Welsh, M. (2000) Role of the Bsk/Iyk non-receptor tyrosine kinase for the control of growth and hormone production in RINm5F cells. *Growth Factors*, **17**, 233-247.

Arora, A.S., deGroen, P.C., Croall, D.E., Emori, Y. and Gores, G.J. (1996) Hepatocellular carcinoma cells resist necrosis during anoxia by preventing phospholipase-mediated calpain activation. *Journal of Cellular Physiology*, **167**, 434-442.

Baldi, A., Boccia, V., Claudio, P.P., DeLuca, A. and Giordano, A. (1996) Genomic structure of the human retinoblastoma-related Rb2/p130 gene. *Proceedings of the National Academy of Sciences of the United States of America*, **93**, 4629-4632.

Bartek, J., Bartkova, J. and Lukas, J. (1997) The retinoblastoma protein pathway in cell cycle control and cancer. *Experimental Cell Research*, **237**, 1-6.

Bates, S., Phillips, A.C., Clark, P.A., Stott, F., Peters, G., Ludwig, R.L. and Vousden, K.H. (1998) p14(ARF) links the tumour suppressors RB and p53. *Nature*, **395**, 124-125.

Baumgartner, R., Fernandez-Catalan, C., Winoto, A., Huber, R., Engh, R.A. and Holak, T.A. (1998) Structure of human cyclin-dependent kinase inhibitor p19(INK4d): comparison to known ankyrin-repeat-containing structures and implications for the dysfunction of tumor suppressor p16(INK4a). *Structure with Folding & Design*, **6**, 1279-1290.

Borden, K.L.B., Boddy, M.N., Lally, J., Oreilly, N.J., Martin, S., Howe, K., Solomon, E. and Freemont, P.S. (1995) The Solution Structure of the Ring Finger Domain from the Acute Promyelocytic Leukemia Proto-Oncoprotein Pml. *Embo Journal*, **14**, 1532-1541.

Borden, K.L.B., Lally, J.M., Martin, S.R., Oreilly, N.J., Solomon, E. and Freemont, P.S. (1996) In vivo and in vitro characterization of the B1 and B2 zinc-binding domains from the acute promyelocytic leukemia protooncoprotein PML. *Proceedings of the National Academy of Sciences of the United States of America*, **93**, 1601-1606.

Botz, J., ZerfassThome, K., Spitkovsky, D., Delius, H., Vogt, B., Eilers, M., Hatzigeorgiou, A. and JansenDurr, P. (1996) Cell cycle regulation of the murine cyclin E gene depends on an E2F binding site in the promoter. *Molecular and Cellular Biology*, **16**, 3401-3409.

Brehm, A., Miska, E.A., McCance, D.J., Reid, J.L., Bannister, A.J. and Kouzarides, T. (1998) Retinoblastoma protein recruits histone deacetylase to repress transcription. *Nature*, **391**, 597-601.

Bremner, R., Cohen, B.L., Sopta, M., Hamel, P.A., Ingles, C.J., Gallie, B.L. and Phillips, R.A. (1995) Direct Transcriptional Repression by Prb and Its Reversal by Specific Cyclins. *Molecular and Cellular Biology*, **15**, 3256-3265.

Briata, P., Danna, F., Franzi, A.T. and Gherzi, R. (1993) Ap-1 Activity During Normal Human Keratinocyte Differentiation - Evidence for a Cytosolic Modulator of Ap-1 DNA-Binding. *Experimental Cell Research*, **204**, 136-146.

Brotherton, D.H., Dhanaraj, V., Wick, S., Brizuela, L., Domaille, P.J., Volyanik, E., Xu, X., Parisini, E., Smith, B.O., Archer, S.J., Serrano, M., Brenner, S.L., Blundell, T.L. and Laue, E.D. (1998) Crystal structure of the complex of the cyclin D dependent kinase Cdk6 bound to the cell-cycle inhibitor p19(INK4d). *Nature*, **395**, 244-250.

Buchkovich, K., Duffy, L.A. and Harlow, E. (1989) The Retinoblastoma Protein Is Phosphorylated During Specific Phases of the Cell-Cycle. *Cell*, **58**, 1097-1105.

Cance, W.G., Craven, R.J., Bergman, M., Xu, L.H., Alitalo, K. and Liu, E.T. (1994) Rak, a Novel Nuclear Tyrosine Kinase Expressed in Epithelial-Cells. *Cell Growth & Differentiation*, **5**, 1347-1355.

Carnero, A. (2002) Targeting the cell cycle for cancer therapy. *British Journal of Cancer*, **87**, 129-133.

Castano, E., Kleyner, Y. and Dynlacht, B.D. (1998) Dual cyclin-binding domains are required for p107 to function as a kinase inhibitor. *Molecular and Cellular Biology*, **18**, 5380-5391.

Chandrasekharan, S., Qiu, T.H., Alkharouf, N., Brantley, K., Mitchell, J.B. and Liu, E.T. (2002) Characterization of mice deficient in the Src family nonreceptor tyrosine kinase Frk/rak. *Molecular and Cellular Biology*, **22**, 5235-5247.

Chang, K.H., Chen, Y.M., Chen, T.T., Chou, W.H., Chen, P.L., Ma, Y.Y., YangFeng, T.L., Leng, X.H., Tsai, M.J., Omalley, B.W. and Lee, W.H. (1997) A thyroid hormone receptor coactivator negatively regulated by the retinoblastoma protein. *Proceedings of the National Academy of Sciences of the United States of America*, **94**, 9040-9045.

Charles, A., Tang, X.R., Crouch, E., Brody, J.S. and Xiao, Z.X.J. (2001) Retinoblastoma protein complexes with C/EBP proteins and activates C/EBP-mediated transcription. *Journal of Cellular Biochemistry*, **83**, 414-425.

Chauhan, D., Hideshima, T., Treon, S., Teoh, G., Raje, N., Yoshihimito, S., Tai, Y.T., Li, W.W., Fan, J.G., DeCaprio, J. and Anderson, K.C. (1999) Functional interaction between retinoblastoma protein and stress-activated protein kinase in multiple myeloma cells. *Cancer Research*, **59**, 1192-1195.

Chellappan, S., Kraus, V.B., Kroger, B., Munger, K., Howley, P.M., Phelps, W.C. and Nevins, J.R. (1992) Adenovirus-E1a, Simian Virus-40 Tumor-Antigen, and Human Papillomavirus-E7 Protein Share the Capacity to Disrupt the Interaction between Transcription Factor-E2f and the Retinoblastoma Gene-Product. *Proceedings of the National Academy of Sciences of the United States of America*, **89**, 4549-4553.

Chellappan, S.P., Hiebert, S., Mudryj, M., Horowitz, J.M. and Nevins, J.R. (1991) The E2f Transcription Factor Is a Cellular Target for the Rb Protein. *Cell*, **65**, 1053-1061.

Chen, P.L., Riley, D.J., Chen, Y.M. and Lee, W.H. (1996a) Retinoblastoma protein positively regulates terminal adipocyte differentiation through direct interaction with C/EBPs. *Genes & Development*, **10**, 2794-2804.

Chen, P.L., Riley, D.J., ChenKiang, S. and Lee, W.H. (1996b) Retinoblastoma protein directly interacts with and activates the transcription factor NF-IL6. *Proceedings of the National Academy of Sciences of the United States of America*, **93**, 465-469.

Chen, P.L., Scully, P., Shew, J.Y., Wang, J.Y.J. and Lee, W.H. (1989) Phosphorylation of the Retinoblastoma Gene-Product Is Modulated During the Cell-Cycle and Cellular-Differentiation. *Cell*, **58**, 1193-1198.

Chen, S. and Paucha, E. (1990) Identification of a Region of Simian Virus-40 Large T-Antigen Required for Cell-Transformation. *Journal of Virology*, **64**, 3350-3357.

Choi, Y.H., Lee, S.J., Nguyen, P., Jang, J.S., Lee, J., Wu, M.L., Takano, E., Maki, M., Henkart, P.A. and Trepel, J.B. (1997) Regulation of cyclin D1 by calpain protease. *Journal of Biological Chemistry*, **272**, 28479-28484.

Choubey, D. and Lengyel, P. (1995) Binding of an Interferon-Inducible Protein (P202) to the Retinoblastoma Protein. *Journal of Biological Chemistry*, **270**, 6134-6140.

Choubey, D., Li, S.J., Datta, B., Gutterman, J.U. and Lengyel, P. (1996) Inhibition of E2F-mediated transcription by p202. *Embo Journal*, **15**, 5668-5678.

Chow, K.N.B. and Dean, D.C. (1996) Domains A and B in the Rb pocket interact to form a transcriptional repressor motif. *Molecular and Cellular Biology*, **16**, 4862-4868.

Clurman, B.E., Sheaff, R.J., Thress, K., Groudine, M. and Roberts, J.M. (1996) Turnover of cyclin E by the ubiquitin-proteasome pathway is regulated by cdk2 binding and cyclin phosphorylation. *Genes & Development*, **10**, 1979-1990.

Craven, R.J., Cance, W.G. and Liu, E.T. (1995) The Nuclear Tyrosine Kinase Rak Associates with the Retinoblastoma Protein Prb. *Cancer Research*, **55**, 3969-3972.

Croall, D.E., Chacko, S. and Wang, Z. (1996) Cleavage of caldesmon and calponin by calpain: Substrate recognition is not dependent on calmodulin binding domains. *Biochimica Et Biophysica Acta-Protein Structure and Molecular Enzymology*, **1298**, 276-284.

Croall, D.E. and Demartino, G.N. (1991) Calcium-Activated Neutral Protease (Calpain) System - Structure, Function, and Regulation. *Physiological Reviews*, **71**, 813-847.

Darlington, G.J., Ross, S.E. and MacDougald, O.A. (1998) The role of C/EBP genes in adipocyte differentiation. *Journal of Biological Chemistry*, **273**, 30057-30060.

Daston, G., Lamar, E., Olivier, M. and Goulding, M. (1996) Pax-3 is necessary for migration but not differentiation of limb muscle precursors in the mouse. *Development*, **122**, 1017-1027.

Datta, B., Min, W., Burma, S. and Lengyel, P. (1998) Increase in p202 expression during skeletal muscle differentiation: Inhibition of MyoD protein expression and activity by p202. *Molecular and Cellular Biology*, **18**, 1074-1083.

Dayton, W.R., Schollmeyer, J.V., Lepley, R.A. and Cortes, L.R. (1981) A Calcium-Activated Protease Possibly Involved in Myofibrillar Protein-Turnover - Isolation of a Low-Calcium-Requiring Form of the Protease. *Biochimica Et Biophysica Acta*, **659**, 48-61.

Decaprio, J.A., Furukawa, Y., Ajchenbaum, F., Griffin, J.D. and Livingston, D.M. (1992) The Retinoblastoma-Susceptibility Gene-Product Becomes Phosphorylated in Multiple Stages During Cell-Cycle Entry and Progression. *Proceedings of the National Academy of Sciences of the United States of America*, **89**, 1795-1798.

Decaprio, J.A., Ludlow, J.W., Lynch, D., Furukawa, Y., Griffin, J., Piwnicaworms, H., Huang, C.M. and Livingston, D.M. (1989) The Product of the Retinoblastoma Susceptibility Gene Has Properties of a Cell-Cycle Regulatory Element. *Cell*, **58**, 1085-1095.

Degregori, J., Kowalik, T. and Nevins, J.R. (1995) Cellular Targets for Activation by the E2f1 Transcription Factor Include DNA Synthesis- and G(1)/S-Regulatory Genes. *Molecular and Cellular Biology*, **15**, 4215-4224.

DeGregori, J., Leone, G., Miron, A., Jakoi, L. and Nevins, J.R. (1997) Distinct roles for E2F proteins in cell growth control and apoptosis. *Proceedings of the National Academy of Sciences of the United States of America*, **94**, 7245-7250.

Diehl, A.M. (1998) Roles of CCAAT/Enhancer-binding proteins in regulation of liver regenerative growth. *Journal of Biological Chemistry*, **273**, 30843-30846.

Dowdy, S.F., Hinds, P.W., Louie, K., Reed, S.I., Arnold, A. and Weinberg, R.A. (1993) Physical Interaction of the Retinoblastoma Protein with Human D-Cyclins. *Cell*, **73**, 499-511.

Dryja, T.P., Rapaport, J., McGee, T.L., Nork, T.M. and Schwartz, T.L. (1993) Molecular Etiology of Low-Penetrance Retinoblastoma in 2 Pedigrees. *American Journal of Human Genetics*, **52**, 1122-1128.

Du, X.P., Saido, T.C., Tsubuki, S., Indig, F.E., Williams, M.J. and Ginsberg, M.H. (1995) Calpain Cleavage of the Cytoplasmic Domain of the Integrin Beta(3) Subunit. *Journal of Biological Chemistry*, **270**, 26146-26151.

Dunaief, J.L., Strober, B.E., Guha, S., Khavari, P.A., Alin, K., Luban, J., Begemann, M., Crabtree, G.R. and Goff, S.P. (1994) The Retinoblastoma Protein and Brg1 Form a Complex and Cooperate to Induce Cell-Cycle Arrest. *Cell*, **79**, 119-130.

Durfee, T., Becherer, K., Chen, P.L., Yeh, S.H., Yang, Y.Z., Kilburn, A.E., Lee, W.H. and Elledge, S.J. (1993) The Retinoblastoma Protein Associates with the Protein Phosphatase Type-1 Catalytic Subunit. *Genes & Development*, **7**, 555-569.

Durfee, T., Mancini, M.A., Jones, D., Elledge, S.J. and Lee, W.H. (1994) The Amino-Terminal Region of the Retinoblastoma Gene-Product Binds a Novel Nuclear Matrix Protein That Colocalizes to Centers for Rna Processing. *Journal of Cell Biology*, **127**, 609-622.

Duronio, R.J. and Ofarrell, P.H. (1995) Developmental Control of the G(1) to S-Transition in Drosophila - Cyclin-E Is a Limiting Downstream Target of E2f. *Genes & Development*, **9**, 1456-1468.

Dynlacht, B.D., Flores, O., Lees, J.A. and Harlow, E. (1994) Differential Regulation of E2f Transactivation by Cyclin Cdk2 Complexes. *Genes & Development*, **8**, 1772-1786.

Dyson, N. (1998) The regulation of E2F by pRB-family proteins. *Genes & Development*, **12**, 2245-2262.

Dyson, N., Guida, P., McCall, C. and Harlow, E. (1992) Adenovirus-E1a Makes 2 Distinct Contacts with the Retinoblastoma Protein. *Journal of Virology*, **66**, 4606-4611.

Dyson, N., Howley, P.M., Munger, K. and Harlow, E. (1989) The Human Papilloma Virus-16 E7-Oncoprotein Is Able to Bind to the Retinoblastoma Gene-Product. *Science*, **243**, 934-937.

Edwards, G.M., Huber, H.E., Defeojones, D., Vuocolo, G., Goodhart, P.J., Maigetter, R.Z., Sanyal, G., Oliff, A. and Heimbrook, D.C. (1992) Purification and Characterization of a Functionally Homogeneous 60-Kda Species of the Retinoblastoma Gene-Product. *Journal of Biological Chemistry*, **267**, 7971-7974.

Egan, C., Bayley, S.T. and Branton, P.E. (1989) Binding of the Rb1 Protein to E1a Products Is Required for Adenovirus Transformation. *Oncogene*, **4**, 383-388.

Egan, C., Jelsma, T.N., Howe, J.A., Bayley, S.T., Ferguson, B. and Branton, P.E. (1988) Mapping of Cellular Protein-Binding Sites on the Products of Early-Region-1a of Human Adenovirus Type-5. *Molecular and Cellular Biology*, **8**, 3955-3959.

Epstein, J.A., Shapiro, D.N., Cheng, J., Lam, P.Y.P. and Maas, R.L. (1996) Pax3 modulates expression of the c-Met receptor during limb muscle development. *Proceedings of the National Academy of Sciences of the United States of America*, **93**, 4213-4218.

Evans, T., Rosenthal, E.T., Youngblom, J., Distel, D. and Hunt, T. (1983) Cyclin - a Protein Specified by Maternal Messenger-Rna in Sea-Urchin Eggs That Is Destroyed at Each Cleavage Division. *Cell*, **33**, 389-396.

Ewen, M.E., Faha, B., Harlow, E. and Livingston, D.M. (1992) Interaction of P107 with Cyclin-a Independent of Complex-Formation with Viral Oncoproteins. *Science*, **255**, 85-87.

Ewen, M.E., Ludlow, J.W., Marsilio, E., Decaprio, J.A., Millikan, R.C., Cheng, S.H., Paucha, E. and Livingston, D.M. (1989) An N-Terminal Transformation-Governing Sequence of Sv40 Large T-Antigen Contributes to the Binding of Both P110rb and a 2nd Cellular Protein, P120. *Cell*, **58**, 257-267.

Ewen, M.E., Sluss, H.K., Sherr, C.J., Matsushime, H., Kato, J.Y. and Livingston, D.M. (1993) Functional Interactions of the Retinoblastoma Protein with Mammalian D-Type Cyclins. *Cell*, **73**, 487-497.

Ewen, M.E., Xing, Y.G., Lawrence, J.B. and Livingston, D.M. (1991) Molecular-Cloning, Chromosomal Mapping, and Expression of the Cdna for P107, a Retinoblastoma Gene Product-Related Protein. *Cell*, **66**, 1155-1164.

Faha, B., Ewen, M.E., Tsai, L.H., Livingston, D.M. and Harlow, E. (1992) Interaction between Human Cyclin-a and Adenovirus E1a-Associated P107 Protein. *Science*, **255**, 87-90.

Fischer, S., Vandekerckhove, J., Ampe, C., Traub, P. and Weber, K. (1986) Protein-Chemical Identification of the Major Cleavage Sites of the Ca2 Proteinase on Murine Vimentin, the Mesenchymal Intermediate Filament Protein. *Biological Chemistry Hoppe-Seyler*, **367**, 1147-1152.

Flemington, E.K., Speck, S.H. and Kaelin, W.G. (1993) E2f-1-Mediated Transactivation Is Inhibited by Complex-Formation with the Retinoblastoma Susceptibility Gene-Product. *Proceedings of the National Academy of Sciences of the United States of America*, **90**, 6914-6918.

Fuchs, E. and Weber, K. (1994) Intermediate Filaments - Structure, Dynamics, Function, and Disease. *Annual Review of Biochemistry*, **63**, 345-382.

Gartel, A.L., Goufman, E., Tevosian, S.G., Shih, H., Yee, A.S. and Tyner, A.L. (1998) Activation and repression of p21(WAF1/CIP1) transcription by RB binding proteins. *Oncogene*, **17**, 3463-3469.

Gaubatz, S., Lees, J.A., Lindeman, G.J. and Livingston, D.M. (2001) E2F4 is exported from the nucleus in a CRM1-dependent manner. *Molecular and Cellular Biology*, **21**, 1384-1392.

Geng, Y., Eaton, E.N., Picon, M., Roberts, J.M., Lundberg, A.S., Gifford, A., Sardet, C. and Weinberg, R.A. (1996) Regulation of cyclin E transcription by E2Fs and retinoblastoma protein. *Oncogene*, **12**, 1173-1180.

Goll, D.E., Thompson, V.F., Li, H.Q., Wei, W. and Cong, J.Y. (2003) The calpain system. *Physiological Reviews*, **83**, 731-801.

Grana, X. and Reddy, E.P. (1995) Cell-Cycle Control in Mammalian-Cells - Role of Cyclins, Cyclin-Dependent Kinases (Gdks), Growth Suppressor Genes and Cyclin-Dependent Kinase Inhibitors (Ckis). *Oncogene*, **11**, 211-219.

Grignani, F., Fagioli, M., Alcalay, M., Longo, L., Pandolfi, P.P., Donti, E., Biondi, A., Lococo, F. and Pelicci, P.G. (1994) Acute Promyelocytic Leukemia - from Genetics to Treatment. *Blood*, **83**, 10-25.

Gu, W., Schneider, J.W., Condorelli, G., Kaushal, S., Mahdavi, V. and Nadalginard, B. (1993) Interaction of Myogenic Factors and the Retinoblastoma Protein Mediates Muscle-Cell Commitment and Differentiation. *Cell*, **72**, 309-324.

Hahn, W.C. and Weinberg, R.A. (2002) Modelling the molecular circuitry of cancer. *Nature Reviews Cancer*, **2**, 331-341.

Halevy, O., Novitch, B.G., Spicer, D.B., Skapek, S.X., Rhee, J., Hannon, G.J., Beach, D. and Lassar, A.B. (1995) Correlation of Terminal Cell-Cycle Arrest of Skeletal-Muscle with Induction of P21 by Myod. *Science*, **267**, 1018-1021.

Hall, M. and Peters, G. (1996) Genetic alterations of cyclins, cyclin-dependent kinases, and Cdk inhibitors in human cancer. In *Advances in Cancer Research, Vol 68*, Vol. 68, pp. 67-108.

Hamel, P.A., Phillips, R.A., Muncaster, M. and Gallie, B.L. (1993) Speculations on the Roles of Rb1 in Tissue-Specific Differentiation, Tumor Initiation, and Tumor Progression. *Faseb Journal*, **7**, 846-854.

Hannan, K.M., Hannan, R.D., Smith, S.D., Jefferson, L.S., Lun, M.Y. and Rothblum, L.I. (2000) Rb and p130 regulate RNA polymerase I transcription: Rb disrupts the interaction between UBF and SL-1. *Oncogene*, **19**, 4988-4999.

Hannon, G.J., Demetrick, D. and Beach, D. (1993) Isolation of the Rb-Related P130 through Its Interaction with Cdk2 and Cyclins. *Genes & Development*, **7**, 2378-2391.

Harper, J.W. and Elledge, S.J. (1996) Cdk inhibitors in development and cancer. *Current Opinion in Genetics & Development*, **6**, 56-64.

Harris, A.S., Croall, D.E. and Morrow, J.S. (1988) The Calmodulin-Binding Site in Alpha-Fodrin Is near the Calcium-Dependent Protease-I Cleavage Site. *Journal of Biological Chemistry*, **263**, 15754-15761.

Hausen, H.Z. (1991) Viruses in Human Cancers. *Science*, **254**, 1167-1173.

He, J., Allen, J.R., Collins, V.P., Allalunisturner, M.J., Godbout, R., Day, R.S. and James, C.D. (1994) Cdk4 Amplification Is an Alternative Mechanism to P16 Gene Homozygous Deletion in Glioma Cell-Lines. *Cancer Research*, **54**, 5804-5807.

Heichman, K.A. and Roberts, J.M. (1994) Rules to Replicate By. *Cell*, **79**, 557-562.

Helin, K., Harlow, E. and Fattaey, A. (1993) Inhibition of E2f-1 Transactivation by Direct Binding of the Retinoblastoma Protein. *Molecular and Cellular Biology*, **13**, 6501-6508.

Helt, A.M. and Galloway, D.A. (2001) Destabilization of the retinoblastoma tumor suppressor by human papillomavirus type 16 E7 is not sufficient to overcome cell cycle arrest in human keratinocytes. *Journal of Virology*, **75**, 6737-6747.

Helt, A.M. and Galloway, D.A. (2003) Mechanisms by which DNA tumor virus oncoproteins target the Rb family of pocket proteins. *Carcinogenesis*, **24**, 159-169.

Hensey, C.E., Hong, F., Durfee, T., Qian, Y.W., Lee, E. and Lee, W.H. (1994) Identification of Discrete Structural Domains in the Retinoblastoma Protein - Amino-Terminal Domain Is Required for Its Oligomerization. *Journal of Biological Chemistry*, **269**, 1380-1387.

Hiebert, S.W. (1993) Regions of the Retinoblastoma Gene-Product Required for Its Interaction with the E2f Transcription Factor Are Necessary of E2 Promoter Repression and Prb-Mediated Growth Suppression. *Molecular and Cellular Biology*, **13**, 3384-3391.

Hogg, A., Bia, B., Onadim, Z. and Cowell, J.K. (1993) Molecular Mechanisms of Oncogenic Mutations in Tumors from Patients with Bilateral and Unilateral Retinoblastoma. *Proceedings of the National Academy of Sciences of the United States of America*, **90**, 7351-7355.

Hong, F.D., Huang, H.J.S., To, H., Young, L.J.S., Oro, A., Bookstein, R., Lee, E. and Lee, W.H. (1989) Structure of the Human Retinoblastoma Gene. *Proceedings of the National Academy of Sciences of the United States of America*, **86**, 5502-5506.

Horowitz, J.M., Park, S.H., Bogenmann, E., Cheng, J.C., Yandell, D.W., Kaye, F.J., Minna, J.D., Dryja, T.P. and Weinberg, R.A. (1990) Frequent Inactivation of the Retinoblastoma Antioncogene Is Restricted to a Subset of Human Tumor-Cells. *Proceedings of the National Academy of Sciences of the United States of America*, **87**, 2775-2779.

Hu, Q.J., Dyson, N. and Harlow, E. (1990) The Regions of the Retinoblastoma Protein Needed for Binding to Adenovirus-E1a or Adenovirus-Sv40 Large T-Antigen Are Common Sites for Mutations. *Embo Journal*, **9**, 1147-1155.

Huang, S., Lee, W.H. and Lee, E. (1991) A Cellular Protein That Competes with Sv40 T-Antigen for Binding to the Retinoblastoma Gene-Product. *Nature*, **350**, 160-162.

Huang, S., Shin, E., Sheppard, K.A., Chokroverty, L., Shan, B., Qian, Y.W., Lee, E. and Yee, A.S. (1992) The Retinoblastoma Protein Region Required for Interaction with the E2f Transcription Factor Includes the T/E1a Binding and Carboxy-Terminal Sequences. *DNA and Cell Biology*, **11**, 539-548.

Huang, S., Wang, N.P., Tseng, B.Y., Lee, W.H. and Lee, E. (1990) 2 Distinct and Frequently Mutated Regions of Retinoblastoma Protein Are Required for Binding to Sv40 T-Antigen. *Embo Journal*, **9**, 1815-1822.

Imai, Y., Matsushima, Y., Sugimura, T. and Terada, M. (1991) Purification and Characterization of Human Papillomavirus Type-16 E7 Protein with Preferential Binding-Capacity to the Underphosphorylated Form of Retinoblastoma Gene-Product. *Journal of Virology*, **65**, 4966-4972.

Inomata, M., Hayashi, M., Nakamura, M., Saito, Y. and Kawashima, S. (1989) Properties of Erythrocyte-Membrane Binding and Autolytic Activation of Calcium-Activated Neutral Protease. *Journal of Biological Chemistry*, **264**, 18838-18843.

Inomata, M., Saito, Y., Kon, K. and Kawashima, S. (1990) Binding-Sites for Calcium-Activated Neutral Protease on Erythrocyte-Membranes Are Not Membrane Phospholipids. *Biochemical and Biophysical Research Communications*, **171**, 625-632.

Irwin, M., Marin, M.C., Phillips, A.C., Seelan, R.S., Smith, D.I., Liu, W.G., Flores, E.R., Tsai, K.Y., Jacks, T., Vousden, K.H. and Kaelin, W.G. (2000) Role for the p53 homologue p73 in E2F-1-induced apoptosis. *Nature*, **407**, 645-648.

Jelsma, T.N., Howe, J.A., Mymryk, J.S., Evelegh, C.M., Cunniff, N.F.A. and Bayley, S.T. (1989) Sequences in E1a Proteins of Human Adenovirus-5 Required for Cell-Transformation, Repression of a Transcriptional Enhancer, and Induction of Proliferating Cell Nuclear Antigen. *Virology*, **171**, 120-130.

Johnson, D.G., Ohtani, K. and Nevins, J.R. (1994) Autoregulatory Control of E2f1 Expression in Response to Positive and Negative Regulators of Cell-Cycle Progression. *Genes & Development*, **8**, 1514-1525.

Kaelin, W.G., Ewen, M.E. and Livingston, D.M. (1990) Definition of the Minimal Simian Virus-40 Large T-Antigen-Binding and Adenovirus E1a-Binding Domain in the Retinoblastoma Gene-Product. *Molecular and Cellular Biology*, **10**, 3761-3769.

Kastner, P., Perez, A., Lutz, Y., Rochetteegly, C., Gaub, M.P., Durand, B., Lanotte, M., Berger, R. and Chambon, P. (1992) Structure, Localization and Transcriptional Properties of 2 Classes of Retinoic Acid Receptor-Alpha Fusion Proteins in Acute Promyelocytic Leukemia (Apl) - Structural Similarities with a New Family of Oncoproteins. *Embo Journal*, **11**, 629-642.

Kato, J., Matsushime, H., Hiebert, S.W., Ewen, M.E. and Sherr, C.J. (1993) Direct Binding of Cyclin-D to the Retinoblastoma Gene-Product (Prb) and Prb

Phosphorylation by the Cyclin D-Dependent Kinase Cdk4. *Genes & Development*, **7**, 331-342.

Kato, J.Y., Matsuoka, M., Polyak, K., Massague, J. and Sherr, C.J. (1994) Cyclic-Amp-Induced G1 Phase Arrest Mediated by an Inhibitor (P27(Kip1)) of Cyclin-Dependent Kinase-4 Activation. *Cell*, **79**, 487-496.

Keyomarsi, K., Conte, D., Toyofuku, W. and Fox, M.P. (1995) Deregulation of Cyclin-E in Breast-Cancer. *Oncogene*, **11**, 941-950.

Keyomarsi, K., Oleary, N., Molnar, G., Lees, E., Fingert, H.J. and Pardee, A.B. (1994) Cyclin-E, a Potential Prognostic Marker for Breast-Cancer. *Cancer Research*, **54**, 380-385.

Khavari, P.A., Peterson, C.L., Tamkun, J.W., Mendel, D.B. and Crabtree, G.R. (1993) Brg1 Contains a Conserved Domain of the Swi2/Snf2 Family Necessary for Normal Mitotic Growth and Transcription. *Nature*, **366**, 170-174.

Kim, H.Y., Ahn, B.Y. and Cho, Y. (2001) Structural basis for the inactivation of retinoblastoma tumor suppressor by SV40 large T antigen. *Embo Journal*, **20**, 295-304.

Kim, S.J., Wagner, S., Liu, F., Oreilly, M.A., Robbins, P.D. and Green, M.R. (1992) Retinoblastoma Gene-Product Activates Expression of the Human Tgf-Beta-2 Gene through Transcription Factor Atf-2. *Nature*, **358**, 331-334.

Kitahara, K., Yasui, W., Kuniyasu, H., Yokozaki, H., Akama, Y., Yunotani, S., Hisatsugu, T. and Tahara, E. (1995) Concurrent Amplification of Cyclin-E and Cdk2 Genes in Colorectal Carcinomas. *International Journal of Cancer*, **62**, 25-28.

Krek, W., Ewen, M.E., Shirodkar, S., Arany, Z., Kaelin, W.G. and Livingston, D.M. (1994) Negative Regulation of the Growth-Promoting Transcription Factor E2f-1 by a Stably Bound Cyclin a-Dependent Protein-Kinase. *Cell*, **78**, 161-172.

Kuboki, M., Ishii, H. and Kazama, M. (1987) Procalpain Is Activated on the Plasma-Membrane and the Calpain Acts on the Membrane. *Biochimica Et Biophysica Acta*, **929**, 164-172.

Kuboki, M., Ishii, H. and Kazama, M. (1990) Characterization of Calpain-I Binding-Proteins in Human Erythrocyte Plasma-Membrane. *Journal of Biochemistry*, **107**, 776-780.

Labbaye, C., Valtieri, M., Grignani, F., Luchetti, L., Masella, B., Alcalay, M., Testa, U. and Peschle, C. (1999) Expression and role of PML gene in normal adult hematopoiesis: functional interaction between PML and Rb proteins in erythropoiesis. *Oncogene*, **18**, 3529-3540.

Lavender, P., Vandel, L., Bannister, A.J. and Kouzarides, T. (1997) The HMG-box transcription factor HBP1 is targeted by the pocket proteins and E1A. *Oncogene*, **14**, 2721-2728.

Lee, J., Wang, Z.Y., Luoh, S.M., Wood, W.I. and Scadden, D.T. (1994) Cloning of Frk, a Novel Human Intracellular Src-Like Tyrosine Kinase-Encoding Gene. *Gene*, **138**, 247-251.

Lee, J.O., Russo, A.A. and Pavletich, N.P. (1998) Structure of the retinoblastoma tumour-suppressor pocket domain bound to a peptide from HPV E7. *Nature*, **391**, 859-865.

Lee, W.H., Shew, J.Y., Hong, F.D., Sery, T.W., Donoso, L.A., Young, L.J., Bookstein, R. and Lee, E. (1987) The Retinoblastoma Susceptibility Gene Encodes a Nuclear Phosphoprotein Associated with DNA-Binding Activity. *Nature*, **329**, 642-645.

Lee, W.J., Adachi, Y., Maki, M., Hatanaka, M. and Murachi, T. (1990) Factors Influencing the Binding of Calpain-I to Human Erythrocyte inside-out Vesicles. *Biochemistry International*, **22**, 163-171.

Lees, E., Faha, B., Dulic, V., Reed, S.I. and Harlow, E. (1992) Cyclin-E Cdk2 and Cyclin-a Cdk2 Kinases Associate with P107 and E2f in a Temporally Distinct Manner. *Genes & Development*, **6**, 1874-1885.

Lekstrom-Himes, J. and Xanthopoulos, K.G. (1998) Biological role of the CCAAT enhancer-binding protein family of transcription factors. *Journal of Biological Chemistry*, **273**, 28545-28548.

Leone, G., DeGregori, J., Yan, Z., Jakoi, L., Ishida, S., Williams, R.S. and Nevins, J.R. (1998) E2F3 activity is regulated during the cell cycle and is required for the induction of S phase. *Genes & Development*, **12**, 2120-2130.

Lesage, F., Hugnot, J.P., Amri, E.Z., Grimaldi, P., Barhanin, J. and Lazdunski, M. (1994) Expression Cloning in K+ Transport Defective Yeast and Distribution of Hbp1, a New Putative Hmg Transcriptional Regulator. *Nucleic Acids Research*, **22**, 3685-3688.

Li, E., Bestor, T.H. and Jaenisch, R. (1992) Targeted Mutation of the DNA Methyltransferase Gene Results in Embryonic Lethality. *Cell*, **69**, 915-926.

Li, F.Q., Coonrod, A. and Horwitz, M. (2000) Selection of a dominant negative retinoblastoma protein (RB) inhibiting satellite myoblast differentiation implies an indirect interaction between MyoD and RB. *Molecular and Cellular Biology*, **20**, 5129-5139.

Li, H. and Wicks, W.D. (2001) Retinoblastoma protein interacts with ATF2 and JNK/p38 in stimulating the transforming growth factor-beta 2 promoter. *Archives of Biochemistry and Biophysics*, **394**, 1-12.

Li, S.F., Shiozawa, T., Nakayama, K., Nikaido, T. and Fujii, S. (1996) Stepwise abnormality of sex steroid hormone receptors, tumor suppressor gene products (p53 and Rb), and cyclin E in uterine endometrioid carcinoma. *Cancer*, **77**, 321-329.

Li, Y., Graham, C., Lacy, S., Duncan, A.M.V. and Whyte, P. (1993) The Adenovirus-E1a-Associated 130-Kd Protein Is Encoded by a Member of the Retinoblastoma

Gene Family and Physically Interacts with Cyclin-a and Cyclin-E. *Genes & Development*, **7**, 2366-2377.

Livingstone, C., Patel, G. and Jones, N. (1995) Atf-2 Contains a Phosphorylation-Dependent Transcriptional Activation Domain. *Embo Journal*, **14**, 1785-1797.

Lovering, R., Hanson, I.M., Borden, K.L.B., Martin, S., Oreilly, N.J., Evan, G.I., Rahman, D., Pappin, D.J.C., Trowsdale, J. and Freemont, P.S. (1993) Identification and Preliminary Characterization of a Protein Motif Related to the Zinc Finger. *Proceedings of the National Academy of Sciences of the United States of America*, **90**, 2112-2116.

Luo, R.X., Postigo, A.A. and Dean, D.C. (1998) Rb interacts with histone deacetylase to repress transcription. *Cell*, **92**, 463-473.

Magnaghi-Jaulin, L., Groisman, R., Naguibneva, I., Robin, P., Lorain, S., Le Villain, J.P., Troalen, F., Trouche, D. and Harel-Bellan, A. (1998) Retinoblastoma protein represses transcription by recruiting a histone deacetylase. *Nature*, **391**, 601-605.

Martelli, F., Cenciarelli, C., Santarelli, G., Polikar, B., Felsani, A. and Caruso, M. (1994) Myod Induces Retinoblastoma Gene-Expression During Myogenic Differentiation. *Oncogene*, **9**, 3579-3590.

Matsushime, H., Roussel, M.F., Ashmun, R.A. and Sherr, C.J. (1991) Colony-Stimulating Factor-I Regulates Novel Cyclins During the G1 Phase of the Cell-Cycle. *Cell*, **65**, 701-713.

Mellgren, R.L. (1980) Canine Cardiac Calcium-Dependent Proteases - Resolution of 2 Forms with Different Requirements for Calcium. *Febs Letters*, **109**, 129-133.

Mihara, K., Cao, X.R., Yen, A., Chandler, S., Driscoll, B., Murphree, A.L., Tang, A. and Fung, Y.K.T. (1989) Cell-Cycle Dependent Regulation of Phosphorylation of the Human Retinoblastoma Gene-Product. *Science*, **246**, 1300-1303.

Minshull, J., Blow, J.J. and Hunt, T. (1989) Translation of Cyclin Messenger-Rna Is Necessary for Extracts of Activated Xenopus Eggs to Enter Mitosis. *Cell*, **56**, 947-956.

Mittnacht, S. (1998) Control of pRB phosphorylation. *Current Opinion in Genetics & Development*, **8**, 21-27.

Molinari, M., Anagli, J. and Carafoli, E. (1994) Ca2+-Activated Neutral Protease Is Active in the Erythrocyte-Membrane in Its Nonautolyzed 80-Kda Form. *Journal of Biological Chemistry*, **269**, 27992-27995.

Moran, B. and Zerler, B. (1988) Interactions between Cell Growth-Regulating Domains in the Products of the Adenovirus E1a Oncogene. *Molecular and Cellular Biology*, **8**, 1756-1764.

Moran, E. and Mathews, M.B. (1987) Multiple Functional Domains in the Adenovirus E1a Gene. *Cell*, **48**, 177-178.

Morgan, D.O. (1995) Principles of Cdk Regulation. *Nature*, **374**, 131-134.

Morkel, M., Wenkel, J., Bannister, A.J., Kouzarides, T. and Hagemeier, C. (1997) An E2F-like repressor of transcription. *Nature*, **390**, 567-568.

Nakanishi, M., Kaneko, Y., Matsushime, H. and Ikeda, K. (1999) Direct interaction of p21 cyclin-dependent kinase inhibitor with the retinoblastoma tumor suppressor protein. *Biochemical and Biophysical Research Communications*, **263**, 35-40.

Narayan, S., Widen, S.G., Beard, W.A. and Wilson, S.H. (1994) Rna-Polymerase-Ii Transcription .2. Rate of Promoter Clearance Is Enhanced by a Purified Activating Transcription Factor Camp Response Element-Binding Protein. *Journal of Biological Chemistry*, **269**, 12755-12763.

Nead, M.A., Baglia, L.A., Antinore, M.J., Ludlow, J.W. and McCance, D.J. (1998) Rb binds c-Jun and activates transcription. *Embo Journal*, **17**, 2342-2352.

Neuman, E., Flemington, E.K., Sellers, W.R. and Kaelin, W.G. (1994) Transcription of the E2f-1 Gene Is Rendered Cell-Cycle Dependent by E2f DNA-Binding Sites within Its Promoter. *Molecular and Cellular Biology*, **14**, 6607-6615.

Nevins, J.R. (1992) E2f - a Link between the Rb Tumor Suppressor Protein and Viral Oncoproteins. *Science*, **258**, 424-429.

Nevins, J.R. (1998) Toward an understanding of the functional complexity of the E2F and retinoblastoma families. *Cell Growth & Differentiation*, **9**, 585-593.

Nevins, J.R. (2001) The Rb/E2F pathway and cancer. *Human Molecular Genetics*, **10**, 699-703.

Nicolas, E., Morales, V., Magnaghi-Jaulin, L., Harel-Bellan, A., Richard-Foy, H. and Trouche, D. (2000) RbAp48 belongs to the histone deacetylase complex that associates with the retinoblastoma protein. *Journal of Biological Chemistry*, **275**, 9797-9804.

Nigg, E.A. (1995) Cyclin-Dependent Protein-Kinases - Key Regulators of the Eukaryotic Cell-Cycle. *Bioessays*, **17**, 471-480.

Norbury, C. and Nurse, P. (1992) Animal-Cell Cycles and Their Control. *Annual Review of Biochemistry*, **61**, 441-470.

Nourse, J., Firpo, E., Flanagan, W.M., Coats, S., Polyak, K., Lee, M.H., Massague, J., Crabtree, G.R. and Roberts, J.M. (1994) Interleukin-2-Mediated Elimination of the P27(Kip1) Cyclin-Dependent Kinase Inhibitor Prevented by Rapamycin. *Nature*, **372**, 570-573.

Novitch, B.G., Mulligan, G.J., Jacks, T. and Lassar, A.B. (1996) Skeletal muscle cells lacking the retinoblastoma protein display defects in muscle gene expression and accumulate in S and G(2) phases of the cell cycle. *Journal of Cell Biology*, **135**, 441-456.

Nurse, P. (2000) A long twentieth century of the cell cycle and beyond. *Cell*, **100**, 71-78.

Oberg-Welsh, C., Anneren, C. and Welsh, M. (1998) Mutation of C-terminal tyrosine residues Y497/Y504 of the Src-family member Bsk/Iyk decreases NIH3T3 cell proliferation. *Growth Factors*, **16**, 111-124.

Oft, M., Peli, J., Rudaz, C., Schwarz, H., Beug, H. and Reichmann, E. (1996) TGF-beta 1 and Ha-Ras collaborate in modulating the phenotypic plasticity and invasiveness of epithelial tumor cells. *Genes & Development*, **10**, 2462-2477.

Ogawa, H., Ishiguro, K., Gaubatz, S., Livingston, D.M. and Nakatani, Y. (2002) A complex with chromatin modifiers that occupies E2F-and Myc-responsive genes in G(0) cells. *Science*, **296**, 1132-1136.

Ohtani, K., DeGregori, J. and Nevins, J.R. (1995) Regulation of the cyclin E gene by transcription factor E2F1. *Proceedings of the National Academy of Sciences of the United States of America*, **92**, 12146-12150.

Okano, M., Bell, D.W., Haber, D.A. and Li, E. (1999) DNA methyltransferases Dnmt3a and Dnmt3b are essential for de novo methylation and mammalian development. *Cell*, **99**, 247-257.

Olson, E.N. and Klein, W.H. (1994) Bhlh Factors in Muscle Development - Dead Lines and Commitments, What to Leave in and What to Leave Out. *Genes & Development*, **8**, 1-8.

Ortega, S., Malumbres, M. and Barbacid, M. (2002) Cyclin D-dependent kinases, INK4 inhibitors and cancer. *Biochimica Et Biophysica Acta-Reviews on Cancer*, **1602**, 73-87.

Pardee, A.B. (1989) G1 Events and Regulation of Cell-Proliferation. *Science*, **246**, 603-608.

Parthun, M.R., Widom, J. and Gottschling, D.E. (1996) The major cytoplasmic histone acetyltransferase in yeast: Links to chromatin replication and histone metabolism. *Cell*, **87**, 85-94.

Patel, Y.M. and Lane, M.D. (2000) Mitotic clonal expansion during preadipocyte differentiation: Calpain-mediated turnover of p27. *Journal of Biological Chemistry*, **275**, 17653-17660.

Patrick, D.R., Oliff, A. and Heimbrook, D.C. (1994) Identification of a Novel Retinoblastoma Gene-Product Binding-Site on Human Papillomavirus Type-16 E7 Protein. *Journal of Biological Chemistry*, **269**, 6842-6850.

Perez, A., Kastner, P., Sethi, S., Lutz, Y., Reibel, C. and Chambon, P. (1993) Pmlrar Homodimers - Distinct DNA-Binding Properties and Heteromeric Interactions with Rxr. *Embo Journal*, **12**, 3171-3182.

Pfarr, C.M., Mechta, F., Spyrou, G., Lallemand, D., Carillo, S. and Yaniv, M. (1994) Mouse Jund Negatively Regulates Fibroblast Growth and Antagonizes Transformation by Ras. *Cell*, **76**, 747-760.

Phillips, A.C., Bates, S., Ryan, K.M., Helin, K. and Vousden, K.H. (1997) Induction of DNA synthesis and apoptosis are separable functions of E2F-1. *Genes & Development*, **11**, 1853-1863.

Phillips, A.C., Ernst, M.K., Bates, S., Rice, N.R. and Vousden, K.H. (1999) E2F-1 potentiates cell death by blocking antiapoptotic signaling pathways. *Molecular Cell*, **4**, 771-781.

Pines, J. (1996) Cell cycle: Reaching for a role for the Cks proteins. *Current Biology*, **6**, 1399-1402.

Poli, V. (1998) The role of C/EBP isoforms in the control of inflammatory and native immunity functions. *Journal of Biological Chemistry*, **273**, 29279-29282.

Polyak, K., Kato, J.Y., Solomon, M.J., Sherr, C.J., Massague, J., Roberts, J.M. and Koff, A. (1994a) P27(Kip1), a Cyclin-Cdk Inhibitor, Links Transforming Growth-Factor-Beta and Contact Inhibition to Cell-Cycle Arrest. *Genes & Development*, **8**, 9-22.

Polyak, K., Lee, M.H., Erdjumentbromage, H., Koff, A., Roberts, J.M., Tempst, P. and Massague, J. (1994b) Cloning of P27(Kip1), a Cyclin-Dependent Kinase Inhibitor and a Potential Mediator of Extracellular Antimitogenic Signals. *Cell*, **78**, 59-66.

Qian, Y.W. and Lee, E. (1995) Dual Retinoblastoma-Binding Proteins with Properties Related to a Negative Regulator of Ras in Yeast. *Journal of Biological Chemistry*, **270**, 25507-25513.

Qian, Y.W., Wang, Y.C.J., Hollingsworth, R.E., Jones, D., Ling, N. and Lee, E. (1993) A Retinoblastoma-Binding Protein Related to a Negative Regulator of Ras in Yeast. *Nature*, **364**, 648-652.

Qian, Y.Y., Luckey, C., Horton, L., Esser, M. and Templeton, D.J. (1992) Biological Function of the Retinoblastoma Protein Requires Distinct Domains for Hyperphosphorylation and Transcription Factor Binding. *Molecular and Cellular Biology*, **12**, 5363-5372.

Qin, X.Q., Chittenden, T., Livingston, D.M. and Kaelin, W.G. (1992) Identification of a Growth Suppression Domain within the Retinoblastoma Gene-Product. *Genes & Development*, **6**, 953-964.

Raingeaud, J., Whitmarsh, A.J., Barrett, T., Derijard, B. and Davis, R.J. (1996) MKK3- and MKK6-regulated gene expression is mediated by the p38 mitogen-activated protein kinase signal transduction pathway. *Molecular and Cellular Biology*, **16**, 1247-1255.

Rayman, J.B., Takahashi, Y., Indjeian, V.B., Dannenberg, J.H., Catchpole, S., Watson, R.J., Riele, H.T. and Dynlacht, B.D. (2002) E2F mediates cell cycle-dependent transcriptional repression in vivo by recruitment of an HDAC1/mSin3B corepressor complex. *Genes & Development*, **16**, 933-947.

Read, M.A., Whitley, M.Z., Gupta, S., Pierce, J.W., Best, J., Davis, R.J. and Collins, T. (1997) Tumor necrosis factor alpha-induced E-selectin expression is activated by the

nuclear factor-kappa B and c-JUN N-terminal kinase/p38 mitogen-activated protein kinase pathways. *Journal of Biological Chemistry*, **272**, 2753-2761.

Reddy, B.A., Etkin, L.D. and Freemont, P.S. (1992) A Novel Zinc Finger Coiled-Coil Domain in a Family of Nuclear Proteins. *Trends in Biochemical Sciences*, **17**, 344-345.

Reed, S.I. (1992) The Role of P34 Kinases in the G1 to S-Phase Transition. *Annual Review of Cell Biology*, **8**, 529-661.

Renner, C., Baumgartner, R., Noegel, A.A. and Holak, T.A. (1998) Backbone dynamics of the CDK inhibitor p19(INK4d) studied by N-15 NMR relaxation experiments at two field strengths. *Journal of Molecular Biology*, **283**, 221-229.

Reyes, J.C., Barra, J., Muchardt, C., Camus, A., Babinet, C. and Yaniv, M. (1998) Altered control of cellular proliferation in the absence of mammalian brahma (SNF2 alpha). *Embo Journal*, **17**, 6979-6991.

Robertson, K.D., Ait-Si-Ali, S., Yokochi, T., Wade, P.A., Jones, P.L. and Wolffe, A.P. (2000) DNMT1 forms a complex with Rb, E2F1 and HDAC1 and represses transcription from E2F-responsive promoters. *Nature Genetics*, **25**, 338-342.

Ruas, M. and Peters, G. (1998) The p16(INK4a)/CDKN2A tumor suppressor and its relatives. *Biochimica Et Biophysica Acta-Reviews on Cancer*, **1378**, F115-F177.

Russo, A.A., Tong, L., Lee, J.O., Jeffrey, P.D. and Pavletich, N.P. (1998) Structural basis for inhibition of the cyclin-dependent kinase Cdk6 by the tumour suppressor p16(INK4a). *Nature*, **395**, 237-243.

Sasaki, T., Kikuchi, T., Yumoto, N., Yoshimura, N. and Murachi, T. (1984) Comparative Specificity and Kinetic-Studies on Porcine Calpain-I and Calpain-Ii with Naturally-Occurring Peptides and Synthetic Fluorogenic Substrates. *Journal of Biological Chemistry*, **259**, 2489-2494.

Schmidt, E.E., Ichimura, K., Reifenberger, G. and Collins, V.P. (1994) Cdkn2 (P16/Mts1) Gene Deletion or Cdk4 Amplification Occurs in the Majority of Glioblastomas. *Cancer Research*, **54**, 6321-6324.

Schneider, J.W., Gu, W., Zhu, L., Mahdavi, V. and Nadalginard, B. (1994) Reversal of Terminal Differentiation Mediated by P107 in Rb(-/-) Muscle-Cells. *Science*, **264**, 1467-1471.

Schulze, A., Zerfass, K., Spitkovsky, D., Middendorp, S., Berges, J., Helin, K., Jansendurr, P. and Henglein, B. (1995) Cell-Cycle Regulation of the Cyclin-a Gene Promoter Is Mediated by a Variant E2f Site. *Proceedings of the National Academy of Sciences of the United States of America*, **92**, 11264-11268.

Scuderi, R., Palucka, K.A., Pokrovskaja, K., Bjorkholm, M., Wiman, K.G. and Pisa, P. (1996) Cyclin E overexpression in relapsed adult acute lymphoblastic leukemias of B-cell lineage. *Blood*, **87**, 3360-3367.

Sellers, W.R. and Kaelin, W.G. (1997) Role of the retinoblastoma protein in the pathogenesis of human cancer. *Journal of Clinical Oncology*, **15**, 3301-3312.

Sellers, W.R., Rodgers, J.W. and Kaelin, W.G. (1995) A Potent Transrepression Domain in the Retinoblastoma Protein Induces a Cell-Cycle Arrest When Bound to E2f Sites. *Proceedings of the National Academy of Sciences of the United States of America*, **92**, 11544-11548.

Serrano, M. (1997) The tumor suppressor protein p16(INK4a). *Experimental Cell Research*, **237**, 7-13.

Serrano, M., Lin, A.W., McCurrach, M.E., Beach, D. and Lowe, S.W. (1997) Oncogenic ras provokes premature cell senescence associated with accumulation of p53 and p16(INK4a). *Cell*, **88**, 593-602.

Shan, B., Zhu, X.L., Chen, P.L., Durfee, T., Yang, Y.Z., Sharp, D. and Lee, W.H. (1992) Molecular-Cloning of Cellular Genes Encoding Retinoblastoma-Associated Proteins - Identification of a Gene with Properties of the Transcription Factor-E2f. *Molecular and Cellular Biology*, **12**, 5620-5631.

Sherr, C.J. (1993) Mammalian G(1)-Cyclins. *Cell*, **73**, 1059-1065.

Sherr, C.J. (1996) Cancer cell cycles. *Science*, **274**, 1672-1677.

Sherr, C.J. and Roberts, J.M. (1995) Inhibitors of Mammalian G(1) Cyclin-Dependent Kinases. *Genes & Development*, **9**, 1149-1163.

Sherr, C.J. and Roberts, J.M. (1999) CDK inhibitors: positive and negative regulators of G(1)-phase progression. *Genes & Development*, **13**, 1501-1512.

Shih, H.H., Tevosian, S.G. and Yee, A.S. (1998) Regulation of differentiation by HBP1, a target of the retinoblastoma protein. *Molecular and Cellular Biology*, **18**, 4732-4743.

Shimizu, M., Nomura, Y., Suzuki, K., Ichikawa, E., Takeuchi, A., Suzuki, M., Nakamura, T., Nakajima, T. and Oda, K. (1998) Activation of the rat cyclin a promoter by ATF2 and Jun family members and its suppression by ATF4. *Experimental Cell Research*, **239**, 93-103.

Singh, P., Coe, J. and Hong, W.J. (1995) A Role for Retinoblastoma Protein in Potentiating Transcriptional Activation by the Glucocorticoid Receptor. *Nature*, **374**, 562-565.

Spencer, M.J., Croall, D.E. and Tidball, J.G. (1995) Calpains Are Activated in Necrotic Fibers from Mdx Dystrophic Mice. *Journal of Biological Chemistry*, **270**, 10909-10914.

Srinivasan, A., McClellan, A.J., Vartikar, J., Marks, I., Cantalupo, P., Li, Y., Whyte, P., Rundell, K., Brodsky, J.L. and Pipas, J.M. (1997) The amino-terminal transforming region of Simian Virus 40 large T and small t antigens functions as a J domain. *Molecular and Cellular Biology*, **17**, 4761-4773.

Stabach, P.R., Cianci, C.D., Glantz, S.B., Zhang, Z.S. and Morrow, J.S. (1997) Site-directed mutagenesis of alpha II spectrin at codon 1175 modulates its mu-calpain susceptibility. *Biochemistry*, **36**, 57-65.

Sterner, J.M., Dew-Knight, S., Musahl, C., Kornbluth, S. and Horowitz, J.M. (1998) Negative regulation of DNA replication by the retinoblastoma protein is mediated by its association with MCM7. *Molecular and Cellular Biology*, **18**, 2748-2757.

Sterner, J.M., Murata, Y., Kim, H.G., Kennett, S.B., Templeton, D.J. and Horowitz, J.M. (1995) Detection of a Novel Cell-Cycle-Regulated Kinase-Activity That Associates with the Amino-Terminus of the Retinoblastoma Protein in G(2)/M Phases. *Journal of Biological Chemistry*, **270**, 9281-9288.

Stillman, B. (1996) Cell Cycle Control of DNA replication. *Science*, **274**, 1659-1664.

Strelkov, S.V., Herrmann, H., Geisler, N., Wedig, T., Zimbelmann, R., Aebi, U. and Burkhard, P. (2002) Conserved segments 1A and 2B of the intermediate filament dimer: their atomic structures and role in filament assembly. *Embo Journal*, **21**, 1255-1266.

Strober, B.E., Dunaief, J.L., Guha, S. and Goff, S.P. (1996) Functional interactions between the hBRM/hBRG1 transcriptional activators and the pRB family of proteins. *Molecular and Cellular Biology*, **16**, 1576-1583.

Tahara, E. (1995) Genetic Alterations in Human Gastrointestinal Cancers - the Application to Molecular Diagnosis. *Cancer*, **75**, 1410-1417.

Tamami, M., Lindholm, P.F. and Brady, J.N. (1996) The retinoblastoma gene product (Rb) induces binding of a conformationally inactive nuclear factor-kappa B. *Journal of Biological Chemistry*, **271**, 24551-24556.

Tevosian, S.G., Shih, H.H., Mendelson, K.G., Sheppard, K.A., Paulson, K.E. and Yee, A.S. (1997) HBP1: A HMG box transcriptional repressor that is targeted by the retinoblastoma family. *Genes & Development*, **11**, 383-396.

Travis, A., Amsterdam, A., Belanger, C. and Grosschedl, R. (1991) Lef-1, a Gene Encoding a Lymphoid-Specific with Protein, an Hmg Domain, Regulates T-Cell Receptor-Alpha Enhancer Function. *Genes & Development*, **5**, 880-894.

Trouche, D., LeChalony, C., Muchardt, C., Yaniv, M. and Kouzarides, T. (1997) RE and hbrm cooperate to repress the activation functions of E2F1. *Proceedings of the National Academy of Sciences of the United States of America*, **94**, 11268-11273.

Tsai, E.Y., Jain, J., Pesavento, P.A., Rao, A. and Goldfeld, A.E. (1996) Tumor necrosis factor alpha gene regulation in activated T cells involves ATF-2/Jun and NFATp. *Molecular and Cellular Biology*, **16**, 459-467.

Tsutsumi, M., Tsai, Y.C., Gonzalgo, M.L., Nichols, P.W. and Jones, P.A. (1998) Early acquisition of homozygous deletions of p16/p19 during squamous cell carcinogenesis and genetic mosaicism in bladder cancer. *Oncogene*, **17**, 3021-3027.

Vandam, H., Duyndam, M., Rottier, R., Bosch, A., Devriessmits, L., Herrlich, P., Zantema, A., Angel, P. and Vandereb, A.J. (1993) Heterodimer Formation of Cjun and Atf-2 Is Responsible for Induction of C-Jun by the 243-Amino Acid Adenovirus E1a Protein. *Embo Journal*, **12**, 479-487.

Vandam, H., Wilhelm, D., Herr, I., Steffen, A., Herrlich, P. and Angel, P. (1995) Atf-2 Is Preferentially Activated by Stress-Activated Protein-Kinases to Mediate C-Jun Induction in Response to Genotoxic Agents. *Embo Journal*, **14**, 1798-1811.

Verreault, A., Kaufman, P.D., Kobayashi, R. and Stillman, B. (1996) Nucleosome assembly by a complex of CAF-1 and acetylated histones H3/H4. *Cell*, **87**, 95-104.

Verreault, A., Kaufman, P.D., Kobayashi, R. and Stillman, B. (1997) Nucleosomal DNA regulates the core-histone-binding subunit of the human Hat1 acetyltransferase. *Current Biology*, **8**, 96-108.

Vousden, K.H. and Farrell, P.J. (1994) Viruses and Human Cancer. *British Medical Bulletin*, **50**, 560-581.

Wang, W.D., Cote, J., Xue, Y., Zhou, S., Khavari, P.A., Biggar, S.R., Muchardt, C., Kalpana, G.V., Goff, S.P., Yaniv, M., Workman, J.L. and Crabtree, G.R. (1996a) Purification and biochemical heterogeneity of the mammalian SWI-SNF complex. *Embo Journal*, **15**, 5370-5382.

Wang, W.D., Xue, Y.T., Zhou, S., Kuo, A., Cairns, B.R. and Crabtree, G.R. (1996b) Diversity and specialization of mammalian SWI/SNF complexes. *Genes & Development*, **10**, 2117-2130.

Warrell, R.P., Dethe, H., Wang, Z.Y. and Degos, L. (1993) Acute Promyelocytic Leukemia. *New England Journal of Medicine*, **329**, 177-189.

Weinberg, R.A. (1995) The Retinoblastoma Protein and Cell-Cycle Control. *Cell*, **81**, 323-330.

Weintraub, S.J., Chow, K.N.B., Luo, R.X., Zhang, S.H., He, S. and Dean, D.C. (1995) Mechanism of Active Transcriptional Repression by the Retinoblastoma Protein. *Nature*, **375**, 812-815.

Weintraub, S.J. and Dean, D.C. (1992) Interaction of a Common Factor with Atf, Sp1, or Tataa Promoter Elements Is Required for These Sequences to Mediate Transactivation by the Adenoviral Oncogene E1a. *Molecular and Cellular Biology*, **12**, 512-517.

Welch, P.J. and Wang, J.Y.J. (1993) A C-Terminal Protein-Binding Domain in the Retinoblastoma Protein Regulates Nuclear C-Abl Tyrosine Kinase in the Cell-Cycle. *Cell*, **75**, 779-790.

Whyte, P., Williamson, N.M. and Harlow, E. (1989) Cellular Targets for Transformation by the Adenovirus E1a Proteins. *Cell*, **56**, 67-75.

Wiggan, O., Taniguchi-Sidle, A. and Hamel, P.A. (1998) Interaction of the pRB-family proteins with factors containing paired-like homeodomains. *Oncogene*, **16**, 227-236.

Won, K.A. and Reed, S.I. (1996) Activation of cyclin E/CDK2 is coupled to site-specific autophosphorylation and ubiquitin-dependent degradation of cyclin E. *Embo Journal*, **15**, 4182-4193.

Won, K.A., Xiong, Y., Beach, D. and Gilman, M.Z. (1992) Growth-Regulated Expression of D-Type Cyclin Genes in Human-Diploid Fibroblasts. *Proceedings of the National Academy of Sciences of the United States of America*, **89**, 9910-9914.

Woo, M.S.A., Sanchez, I. and Dynlacht, B.D. (1997) p130 and p107 use a conserved domain to inhibit cellular cyclin-dependent kinase activity. *Molecular and Cellular Biology*, **17**, 3566-3579.

Wu, E.W., Clemens, K.E., Heck, D.V. and Munger, K. (1993) The Human Papillomavirus E7 Oncoprotein and the Cellular Transcription Factor E2f Bind to Separate Sites on the Retinoblastoma Tumor Suppressor Protein. *Journal of Virology*, **67**, 2402-2407.

Wu, Z.D., Xie, Y.H., Bucher, N.L.R. and Farmer, S.R. (1995) Conditional Ectopic Expression of C/Ebp-Beta in Nih-3t3 Cells Induces Ppar-Gamma and Stimulates Adipogenesis. *Genes & Development*, **9**, 2350-2363.

Wuarin, J. and Nurse, P. (1996) Regulating S phase: CDKs, licensing and proteolysis. *Cell*, **85**, 785-787.

Yang, X.M., Vogan, K., Gros, P. and Park, M. (1996) Expression of the met receptor tyrosine kinase in muscle progenitor cells in somites and limbs is absent in Splotch mice. *Development*, **122**, 2163-2171.

Yee, A.S., Shih, H.H. and Tevosian, S.G. (1999) New perspectives on retinoblastoma family functions in differentiation. *Pediatric Pathology & Molecular Medicine*, **18**, 275-302.

Zacksenhaus, E., Bremner, R., Phillips, R.A. and Gallie, B.L. (1993) A Bipartite Nuclear-Localization Signal in the Retinoblastoma Gene-Product and Its Importance for Biological-Activity. *Molecular and Cellular Biology*, **13**, 4588-4599.

Zacksenhaus, E., Jiang, Z., Chung, D., Marth, J.D., Phillips, R.A. and Gallie, B.L. (1996) pRb controls proliferation differentiation, and death of skeletal muscle cells and other lineages during embryogenesis. *Genes & Development*, **10**, 3051-3064.

Zhang, H.S., Gavin, M., Dahiya, A., Postigo, A.A., Ma, D.D., Luo, R.X., Harbour, J.W. and Dean, D.C. (2000) Exit from G1 and S phase of the cell cycle is regulated by repressor complexes containing HDAC-Rb-hSWI/SNF and Rb-hSWI/SNF. *Cell*, **101**, 79-89.

Zhang, Y., Iratni, R., ErdjumentBromage, H., Tempst, P. and Reinberg, D. (1997) Histone deacetylases and SAP18, a novel polypeptide, are components of a human Sin3 complex. *Cell*, **89**, 357-364.

Zhang, Y., Ng, H.H., Erdjument-Bromage, H., Tempst, P., Bird, A. and Reinberg, D. (1999) Analysis of the NuRD subunits reveals a histone deacetylase core complex and a connection with DNA methylation. *Genes & Development*, **13**, 1924-1935.

6 Appendix

6.1 Amino acid sequences of different constructs of pRb

6.1.1 Amino acid sequence of full-length of pRb

```
  1 MPPKTPRKTA ATAAAAAAEP PAPPPPPPPE EDPEQDSGPE DLPLVRLEFE ETEEPDFTAL    60
 61 CQKLKIPDHV RERAWLTWEK VSSVDGVLGG YIQKKKELWG ICIFIARVDL DEMSFTLLSY   120
121 RKTYEISVHK FFNLLKEIDT STKVDNAMSR LLKKYDVLFA LFSKLERTCE LIYLTQPSSS   180
181 ISTEINSALV LKVSWITFLL AKGEVLQMED DLVISFQLML CVLDYFIKLS PPMLLKEPYK   240
241 TAVIPINGSP RTPRRGQNRS ARIAKQLEND TRIIEVLCKE HECNIDEVKN VYFKNFIPFM   300
301 NSLGLVTSNG LPEVENLSKR YEEIYLKNKD LDRRLFLDHD KTLQTDSIDS FETQRTPRKS   360
361 NLDEEVNIIP PHTPVRTVMN TIQQLMMILN SASDQPSENL ISYFNNCTVN PKESILKRVK   420
421 DIGYIFKEKF AKAVGQGCVE IGSQRYKLGV RLYYRVMESM LKSEEERLSI QNFSKLLNDN   480
481 IFHMSLLACA LEVVMATYSR STSQNLDSGT DLSFPWILNV LNLKAFDFYK VIESFIKAEG   540
541 NLTREMIKHL ERCEHRIMES LAWLSDSPLF DLIKQSKDRE GPTDHLESAC PLNLPLQNNH   600
601 TAADMYLSPV RSPKKKGSTT RVNSTANAET QATSAFQTQK PLKSTSLSLF YKKVYRLAYL   660
661 RLNTLCERLL SEHPELEHII WTLFQHTLQN EYELMRDRHL DQIMMCSMYG ICKVKNIDLK   720
721 FKIIVTAYKD LPHAVQETFK RVLIKEEEYD SIIVFYNSVF MQRLKTNILQ YASTRPPTLS   780
781 PIPHIPRSPY KFPSSPLRIP GGNIYISPLK SPYKISEGLP TPTKMTPRSR ILVSIGESFG   840
841 TSEKFQKINQ MVCNSDRVLK RSAEGSNPPK PLKKLRFDIE GSDEADGSKH LPGESKFQQK   900
901 LAEMTSTRTR MQKQKMNDSM DTSNKEEK
```

Number of amino acids: 928

Molecular weight: 106394.7

Theoretical pI: 8.52

6.1.2 Amino acid sequence of large-pocket region of pRb

```
                  379 MN TIQQLMMILN SASDQPSENL ISYFNNCTVN PKESILKRVK   420
421 DIGYIFKEKF AKAVGQGCVE IGSQRYKLGV RLYYRVMESM LKSEEERLSI QNFSKLLNDN   480
481 IFHMSLLACA LEVVMATYSR STSQNLDSGT DLSFPWILNV LNLKAFDFYK VIESFIKAEG   540
541 NLTREMIKHL ERCEHRIMES LAWLSDSPLF DLIKQSKDRE GPTDHLESAC PLNLPLQNNH   600
601 TAADMYLSPV RSPKKKGSTT RVNSTANAET QATSAFQTQK PLKSTSLSLF YKKVYRLAYL   660
661 RLNTLCERLL SEHPELEHII WTLFQHTLQN EYELMRDRHL DQIMMCSMYG ICKVKNIDLK   720
721 FKIIVTAYKD LPHAVQETFK RVLIKEEEYD SIIVFYNSVF MQRLKTNILQ YASTRPPTLS   780
781 PIPHIPRSPY KFPSSPLRIP GGNIYISPLK SPYKISEGLP TPTKMTPRSR ILVSIGESFG   840
841 TSEKFQKINQ MVCNSDRVLK RSAEGSNPPK PLKKLRFDIE GSDEADGSKH LPGESKFQQK   900
901 LAEMTSTRTR MQKQKMNDSM DTSNKEEK
```

Number of amino acids: 550

Molecular weight: 63156.9

Theoretical pI: 9.21

6.1.3 Amino acid sequence of small-pocket region of pRb

```
                    379 MN TIQQLMMILN SASDQPSENL ISYFNNCTVN PKESILKRVK   420
421 DIGYIFKEKF AKAVGQGCVE IGSQRYKLGV RLYYRVMESM LKSEEERLSI QNFSKLLNDN   480
481 IFHMSLLACA LEVVMATYSR STSQNLDSGT DLSFPWILNV LNLKAFDFYK VIESFIKAEG   540
541 NLTREMIKHL ERCEHRIMES LAWLSDSPLF DLIKQSKDRE GPTDHLESAC PLNLPLQNNH   600
601 TAADMYLSPV RSPKKKGSTT RVNSTANAET QATSAFQTQK PLKSTSLSLF YKKVYRLAYL   660
661 RLNTLCERLL SEHPELEHII WTLFQHTLQN EYELMRDRHL DQIMMCSMYG ICKVKNIDLK   720
721 FKIIVTAYKD LPHAVQETFK RVLIKEEEYD SIIVFYNSVF MQRLKTNILQ YA 772
```

Number of amino acids: 394

Molecular weight: 45715.9

Theoretical pI: 8.60

6.1.4 Amino acid sequence of A/B-pocket region of pRb

```
                    379 MN TIQQLMMILN SASDQPSENL ISYFNNCTVN PKESILKRVK   420
421 DIGYIFKEKF AKAVGQGCVE IGSQRYKLGV RLYYRVMESM LKSEEERLSI QNFSKLLNDN   480
481 IFHMSLLACA LEVVMATYSR STSQNLDSGT DLSFPWILNV LNLKAFDFYK VIESFIKAEG   540
541 NLTREMIKHL ERCEHRIMES LAWLSDSPLF DLIKQSK... .......... ..........   600
601 .......... .......... .......... .......... ....TSLSLF YKKVYRLAYL   660
661 RLNTLCERLL SEHPELEHII WTLFQHTLQN EYELMRDRHL DQIMMCSMYG ICKVKNIDLK   720
721 FKIIVTAYKD LPHAVQETFK RVLIKEEEYD SIIVFYNSVF MQRLKTNILQ YA 772
```

Number of amino acids: 327

Molecular weight: 38481.8

Theoretical pI: 8.33

6.1.5 Amino acid sequence of A/B pocket of *E. coli* purified recombinant pRb.

```
  1 MRGSHHHHHH GMASMTGGQQ MGRDLYDDDD KDPSSRSAAG TMEFMNTIQQ LMMILNSASD    60
 61 QPSENLISYF NNCTVNPKES ILKRVKDIGY IFKEKFAKAV GQGCVEIGSQ RYKLGVRLYY   120
121 RVMESMLKSE EERLSIQNFS KLLNDNIFHM SLLACALEVV MATYSRSTSQ NLDSGTDLSF   180
181 PWILNVLNLK AFDFYKVIES FIKAEGNLTR EMIKHLERCE HRIMESLAWL SDSPLFDLIK   240
```

```
241 QSKTSLSLFY KKVYRLAYLR LNTLCERLLS EHPELEHIIW TLFQHTLQNE YELMRDRHLD   300
301 QIMMCSMYGI CKVKNIDLKF KIIVTAYKDL PHAVQETFKR VLIKEEEYDS IIVFYNSVFM   360
361 QRLKTNILQY A
```

Number of amino acids: 371

Molecular weight: 43347.1

Theoretical pI: 7.22

6.1.6 Amino acid sequence of A/B pocket of *E. coli* purified pRb after Entirokinase digestion.

```
  1 SAAGTMEFMN TIQQLMMILN SASDQPSENL ISYFNNCTVN PKESILKRVK DIGYIFKEKF    60
 61 AKAVGQGCVE IGSQRYKLGV RLYYRVMESM LKSEEERLSI QNFSKLLNDN IFHMSLLACA   120
121 LEVVMATYSR STSQNLDSGT DLSFPWILNV LNLKAFDFYK VIESFIKAEG NLTREMIKHL   180
181 ERCEHRIMES LAWLSDSPLF DLIKQSKTSL SLFYKKVYRL AYLRLNTLCE RLLSEHPELE   240
241 HIIWTLFQHT LQNEYELMRD RHLDQIMMCS MYGICKVKNI DLKFKIIVTA YKDLPHAVQE   300
301 TFKRVLIKEE EYDSIIVFYN SVFMQRLKTN ILQYA
```

Number of amino acids: 335

Molecular weight: 39276.7

Theoretical pI: 8.04

6.2 Abreviations

(°C)	degree Celsius
(A/B)	small pocket of pRb without loop
(ALB)	small pocket region of pRb
(ALBC)	large pocket region of pRb
(v/v)	volume/volume
(w/v)	weight/volume
µ	micro (10-6)
1D	one-dimensional
aa	amino acid
Ac	acetate
APS	ammonium peroxodisulfate
bp	base pair

cdk	cyclin-dependent kinase
Da	dalton
ddH2O	double-distilled water
DHFR	dihydrofolate reductase
DNase 1	deoxyribonuclease 1
dNTP	Deoxynucleside Triphosphate
DTT	Dithiothreitole
E. coli	Escherichia coli
EDTA	Ethylene Diamine Tetra acetic Acid
EKMax	EntirokinaseMax
FID	free induction decay
g	gram
hr	hour
hrs	hours
HSQC	heteronuclear single quantum coherence
Hz	Hertz
IPTG	isopropyl-β-D-thiogalactopyranoside
M	molar
MCM	minichromosome maintenance protein
MES	(2-(N-morpholino) ethanesulphonic acid)
min	minute
ml	milliliter
mM	millimolar
mV	millivolts
Ni-NTA	nickel-nitrilotriacetic acid
OD	optical density
ORF	open reading frame
PAGE	polyacrylamide gelelectrophoresis
PBST	1% tween 20 in phosphate buffered saline
PCNA	proliferating cell nuclear antigen
PCR	polymerase chain reaction
PEG	polyethylene glycol
POL	DNA polymerase-α
ppm	parts per million

pRb	retinoblastoma protein
RNase 1	ribonuclease 1
SDS	sodium dodecylsulfate
sec	seconds
Sf9 cells	Spodoptera frugiperda cells
TBP	TATA-binding protein
Tris	Tris(hydroxymethyl)aminomethane
β-ME	beta-mercapto- ethanol
PCR	polymerase chain reaction